

https://dspace.org/

A study of vector formulations for distillation processes

Mulopo, Jean Lubilanji

2008-10-23T11:56:09Z
http://hdl.handle.net/10539/5810

Downloaded from a DSpace repository. https://dspace.org/

A STUDY OF VECTOR FORMULATIONS FOR DISTILLATION PROCESSES

by

Jean Lubilanji Mulopo

THESIS SUBMITTED TO THE FACULTY OF ENGINEERING, UNIVERSITY OF THE WITWATERSRAND, JOHANNESBURG, SOUTH AFRICA IN FULFILLMENT OF THE REQUIREMENTS FOR THE DEGREE OF DOCTOR OF PHILOSOPHY

© Jean Mulopo

Johannesburg 2006

Declaration

I declare that this thesis is my own unaided work. It is being submitted for the degree of Doctor of Philosophy at the University of the Witwatersrand, Johannesburg. It has not been submitted before for any degree or examination in any other university.

Jean Lubilanji Mulopo

Abstract

In the last decade Process Synthesis has been an emerging active area of research. Since 1999 at COMPS, we have continuously applied this technique to many studies and recently have carefully started to consider the integration of this technique with others to simplify multilevel process design. In this regard the need for new tools that do not require very accurate data or experimental technique has become an imperative for the initial analysis of systems. This thesis presents some of these results.Process synthesis requires new rapid tools for the assessment and comparison of new technologies (possibilities) in the process development stage.This thesis examines and formulates process synthesis problems in the case of separation processes (separation with mixing , separation with reaction).Using simple generic vectorial tools, the thesis addresses the folowing issue: How the topology and mapping of the process vector field defines patterns that may be used for alternative process synthesis solution and design (structure selection ,stability analysis or controllability etc...) . The tools presented are intended for preliminary process design and feasibility studies and will allow for simple comparisons of various options.The key principle used in the study is the exploitation of the generic vectorial representation of fundamental physical phenomena (separation, mixing , reaction) in the process models as used for process synthesis and analysis.The demonstrated power of this approach is that it allows one to exploit the formal mathematical similarities between the different processing modes. Extensive topological Reactive Column Profile has been generated and analysed, offering new insights for manipulation of process behaviour in process synthesis and design. The significance of the contribution of this research is in offering extended fundamental insigths in creating process synthesis options for reactive-separations systems, creating the essential structural basis for subsequent mathematical optimisation of the performanceof process designs.

Acknowledgments

I would like to express my gratitude to my supervisors Prof. D. Hildebrandt and Prof. D. Glasser for their dedication and guidance throughout the course of this research. Their patient support to my work with seemingly trivial issues has been a great driving force.

I would like to thank Dr. Brendon Hausberger and Dr. Holland for the cooperation and valuable inputs.

Above all my eternal credit goes to my wife Gambie for her support, love and companionship.

Financial support from COMPS, the NRF and the University of the Witwatersrand is gratefully acknowledged.

Table of Contents

Declaration.....ii

Abstract.....iii

Acknowledgments.....iv

List of Tables.....viii

List of Figures.....ix

1 Chapitre 1 Introduction.....1

1.1 Objective of the research.....1

1.2 Thesis Outline.....1

1.2.1 Chapter 2.....2

1.2.2 Chapter 3.....2

1.2.3 Chapter 4.....2

1.2.4 Chapter 5.....3

1.2.5 Chapter 6.....4

1.2.6 Chapter 7.....5

2 Chapter 2 Process Synthesis: Review of the Relationships between Separation Vector Field, Mixing Vector and Analysis of the Resultant Vector field. 6

2.1 Abstract.....6

2.2 Introduction.....6

2.3 The topology of the Separation Vector Field.....8

2.4 The Mixing Vector Field.....10

2.5 Continuous Rectifying Column Equipment.....10

2.6 The Rectifying Batch Equipment.....13

2.6.1 Initial conditions.....14

2.6.2 The parameter α 16

2.6.3 Conclusion.....19

2.7 Column Sections.....20
3 Chapter 3 Batch Experimental Simulation of Distillation Column Profiles: Stripping Section 29
3.1 Abstract.....29
3.2 Introduction.....30
3.3 Theories.....31
3.3.1 Residue Curves.....31
3.4 Experimental Simulation of Rectifying Column Profiles.....34
3.5 Separation and Mixing Vectors.....38
3.6 Experimental simulation of stripping column profiles.....39
3.7 Equipment.....42
3.7.1 Experimental concepts.....42
3.7.2 Experimental Equipment.....45
3.8 Results and Discussion.....47
3.9 Applications.....50
3.10 Conclusions.....52
4 Chapter 4 RRCM Topology: Zero Order Chemical Reaction.....54
4.1 Abstract.....54
4.2 Introduction.....55
4.3 Simple Batch Reactive Distillation 58
4.3.1 Simultaneous Reaction and Separation: Mathematical Preliminaries.....59
4.3.2 Special case for the total number of moles is conserved in the chemical reaction, i.e. 60
4.3.3 Simplification for zero order kinetics.....61
4.3.4 The Separation Vector Field (Residue Curve Map).....62
4.3.5 The Reaction Vector Field.....63
4.4 The RRCM for Zero Order kinetics 64
4.4.1 Singular points of the map.....64
4.4.2 An Interesting Analogy.....66
4.4.3 The Effect of the Stoichiometric Vector on the Topology of the RRCM.....69
4.4.4 Stoichiometric vectors in regions I+ and I-.....71

4.4.5 Stoichiometric vectors in regions II+ and II-....74
4.4.6 Stoichiometric vectors in regions III+ and III-....75
4.4.7 Summary....77
4.4.8 Singular Points....77
4.4.9 Movement of singular points for in regions II+ and II-....78
4.4.10 Movement of singular points for in regions I+ and I-....80
4.4.11 Summary of results on movement of the singular points....81
4.4.12 Effect of the Length of Stoichiometric Vector on the RRCM....82
4.5 Applications to Batch Reactive Distillation Processes 85
4.6 Conclusion....88
5 Chapter 5 RRCM Topology: The Effect of Reversible Chemical Reaction with Nodes....92
5.1 Abstract....92
5.2 Introduction....93
5.3 Process Formulation....96
5.4 Example 1....97
5.4.1 Separation vector field....98
5.4.2 Reaction vector field....99
5.4.3 Process vector field....101
5.4.4 Analytical Analysis....113
5.4.5 Summary of results for example 1....119
5.5 Example 2....119
5.6 Batch Reactive Condensation Experiment....124
5.7 Conclusion....125
6 Chapter 6 Reactive Column Profile Map Topology: Continuous Column with non Reversible Kinetics....128
6.1 Abstract....128
6.2 Introduction....129
6.3 Review of CPM's for systems described by ideal thermodynamic....130
6.4 Preliminary Definitions....133
6.5 Mathematical model of a Reactive Column Section....134

6.6 Reactive Difference Point Composition and Application.....139
6.6.1 Stoichiometric vector.....139
6.6.2 Relationship between CPM and RCPM.....141
6.7 Application.....142
6.8 Discussion.....149
6.9 Conclusion.....151
7 Chapter 7 Conclusion.....155
List of Notation.....x

List of Tables

Table 1: Summary of reactions occurring in each of the 6 defining regions.....71
Table 2: Thermodynamic Data for the Butene (1)-Hexene (2)-Pentene (3) System from ASPEN PLUS.....120
Table 3: General overview of generic vectorial formulae derived and analysed in the thesis.....157

List of Figures

Figure 2.1: Extended Residue Curve Map (RCM) for ideal system 9

Figure 2.2: Continuous rectifying column 10

Figure 2.3: Pinch point curve for an ideal system operating with a total condenser and a distillate (top liquid) composition of XD=[0.35;0.25]. The circled branch represents the valid pinch point curve inside the MBT. The stable branch originates from the high boiling component while the unstable branch originates from the low boiling component. The VLE ideal with constant relative volatilities.....12

Figure 2.4: Rectifying batch vessel 13

Figure 2.5: Theoretical column profiles map for an ideal system with the parameter α=0.85 and distillate material = [0.3 0.4].....16

Figure 2.6: The pinch point curve for a batch system operating with a distillate composition Xd= [0.35; 0.25].The VLE is described by constant relative volatilities. L is the low boiling component, I is the intermediate boiling component and H is the high boiling component. We assume that the volatilities of the components L and H relative to I are equal to 5 and 3 respectively.....17

Figure 2.7: The singular points B1B2B3 for α=1.16 in a batch equipment operating with a distillate material composition of Xd= [0.35; 0.25] and singular points A1A2A3 for r=2.The VLE is described by constant relative volatilities. L is the low boiling component, I is the intermediate boiling component and H is the high boiling component. We assume that the volatilities of the components L and H relative to I are equal to 5 and 3 respectively.....19

Figure 2.8: Distillation column with 4 column sections 21

Figure 2.9: Different shape for the pinch point curve for different Extended in the same region of the composition space (positive space).....24

Figure 2.10: Different shape for the pinch point curve for the difference composition in different region of the composition space in region I and region II 25
Figure 2.11: Crossing distillation boundary for the non ideal system Acetone-Chloroform-Methanol for appropriate choice of parameters XΔ and 26
Figure 3.1: Residue Curve Map (RCM) for the Ethanol/Methanol/Acetone System at 1 atm.....32
Figure 3.2: Rectifying batch vessel.....34
Figure 3.3: (left) the stripping batch vessel (rigth) construction of a stripping profile line for a ternary mixture 40
Figure 3.4: Experimental configurations 45
Figure 3.5: Experimental configurations 47
Figure 3.6: Column stripping profile for s=2.....48
Figure 3.7: Column stripping profile for s=4.....49
Figure 3.8: Column stripping profile in the region of high curvature.....50
Figure 3.9: Experimental combination of stripping and rectifying profiles to emulate the entire distillation column 51
Figure 4.1: Schematic of simple distillation with chemical reaction 58
Figure 4.2: Schematic of the residue curve map extended to the negative space for constant relativity system.....62
Figure 4.3: The reactive residue curve map for zero order kinetics 65
Figure 4.4: Infinite reflux coupled column section configuration.....68
Figure 4.5: Representation of regions of the stoichiometric vector characterizing the RRCM behavior and corresponding component axes.....70
Figure 4.6: RRCM for stoichiometric vector in Region I+.....73
Figure 4.7: RRCM for stoichiometric vector in Region I-.....73
Figure 4.8: stoichiometric vector in Region II+.....74
Figure 4.9: stoichiometric vector in Region II-.....75
Figure 4.10: RRCM for stoichiometric vector in Region III+ 76
Figure 4.11: RRCM for stoichiometric vector in Region III-.....76

Figure 4.12: Qualitative shape of the singular point curve for the stoichiometric vector in Region II+ and II-. The solid arrow corresponds to the movement of singular points along the SPC for the stoichiometric vector in region II+ and increasing value of α. The dashed arrow corresponds to the movement of singular points along the SPC for the stoichiometric vector in region II- and increasing value of α 79

Figure 4.13: Singular points curves (SPC): qualitative shape of the singular point curve for the stoichiometric vector in Region I+ and I-. The solid arrow corresponds to the movement of singular points along the SPC for the stoichiometric vector in region I+ and increasing value of α. The dashed arrow corresponds to the movement of singular points along the SPC for the stoichiometric vector in region I- and increasing value of α 81

Figure 4.14: Movement of Singularities as α change for stoichiometric vector in Region I+ 83

Figure 4.15: Reactive Residue Curve Map (RRCM) for the stoichiometric vector in Region I+ and high value of α. Note that only one node (the stable node) remains outside the MBT. 84

Figure 4.16: Figure 4.14: RRCM with the parameters α=2.3 and = [-0.05 -0.03]. The bold red profile runs directly into the intermediate boiler 85

Figure 4.17: Contour plot of the separation vector S at 1 atm for an ideal system 87

Figure 4.18: Contour plot of the separation vector S+v at 1 atm for an ideal system and v in Region I- 88

Figure 5.1: Ideal system ABC a) Residue Curve Map (left) b) Eigenvalue Map of (right) 98

Figure 5.2: Singular point curve and singular point bifurcation behaviour for different values of parameter α in the range $-\infty \leq \alpha \leq 0$ 102

Figure 5.3: Singular point curve and singular point bifurcation behaviour for different values of parameter α in the range $-\infty \leq \alpha \leq 0$ 103

Figure 5.4: Reactive Residue Curve Map for α=0.22 105

Figure 5.5: Reactive Residue Curve Map for α=0.42 106

Figure 5.6: Residue Curve Map for reactive distillation at the bifurcation point (α~0.355) with the eigenvalue map where unstable region (blue), stable region (red) and saddle region (green).....107
Figure 5.7: Residue Curve Map for reactive distillation; A + B ↔C, Ke=4 109
Figure 5.8: Residue Curve Map for reactive distillation; A + B ↔C, Ke=4 110
Figure 5.9: Enlarged Residue Curve Map for reactive distillation; A + B ↔C, Ke=4 for α=-0.721 111
Figure 5.10: Eigenvalue Map for reactive distillation; A + B ↔C, Ke=4 for α=0.22 115
Figure 5.11: Eigenvalue Map for reactive distillation; A + B ↔C, Ke=4 for α=0.42 116
Figure 5.12: Eigenvalue Map for reactive distillation; A + B ↔C, Ke=4 for α=-0.72....117
Figure 5.13: Singular points curve and bifurcation behavior for different parameter α in the range -∞≤α≤+∞ for the Butene-Hexene-Pentene System 120
Figure 5.14: Residue Curve Map for reactive distillation;.....122
Figure 5.15: Residue Curve Map for reactive distillation;.....123
Figure 5.16: Residue Curve Map for reactive condensation;.....125
Figure 6.1: Extended Residue Curve Map (RCM) for ideal system 131
Figure 6.2: Reactive distillation column with 4 column sections.....134
Figure 6.3: Location of the reactive difference point as the chemical reaction proceeds for reaction A+B→2C.....140
Figure 6.4: Figure 4: Distillation Column with 4 Column Sections (CS).....141
Figure 6.5: Column profile for the first column section for XΔ1 = [0.01; 0.7] 143
Figure 6.6: Column profile for the second column section for XΔ2 = [-0.021; 1.1] 144
Figure 6.7: Reactive column profile for the third column section for XΔ3 = [-0.6 0.52] 146
Figure 6.8: Column profile for the fourth column section for XΔ4 =XB= [0.68;0.08] ..147
Figure 6.9: Reactive column profile for the third column section for XΔ3 = [-1.1 0.02] 148
Figure 6.10: Sequence of column section profiles for the entire distillation column 149

1 Chapitre 1 Introduction

1.1 Objective of the research

Traditionally a transport phenomena based approach has been used for the modelling of equipment such as distillation columns. While these approaches are useful for analyzing unit operations, they are not particularly useful for synthesizing such processes.Previous researchers (for example Doherty and co-workers) have introduced the vector based approach which is geometrical and topological in nature. These approaches have proved to be useful in synthesizing processes. This Thesis contibutes to this work, and in particular looks at the effect of combining vector fields that commonly occur in reactive distillation processes,namely separation, mixing and reaction. In this way the movement of the nodes in the vector map can be predicted and hence the qualitative behavior of the operating profiles of the equipment can be estimated. As a result regions of potentially unstable operation can be avoided and operating policies to achieve desirable performance can be predicted.

1.2 Thesis Outline

To outline the thesis, we provide a detailed summary of the different chapters:

1.2.1 Chapter 2

A typical conceptual synthesis design problem looks for equipments capable of creating a bridge between the inputs and the targeted outputs. In chapter 2 we propose that the potential of such project may be addressed by a simple analysis of vector fields describing the overall process.
The traditional approach has been for chemical engineers to look first at the equipments and then only derive models to describe the phenomena occurring. However this chapter proposes that a different step can be taken if one considers the vector fields describing the process and then derives possible types of corresponding equipments. This chapter is used as an introduction to the thesis.

1.2.2 Chapter 3

In this chapter we re-examine the differential description of the distillation stripping section and using vector concepts show that the removal of material of the bottoms compositions is equivalent to the addition of material of a composition that varies in a mathematically predictable manner with time.
This feed policy is implemented experimentally and it is shown that stripping section profiles can be measured with reasonable accuracy in a batch still. This work verifies and validates experimentally the concept that separation and mixing are opposite vectors phenomena.

1.2.3 Chapter 4

In this chapter, we identify that the processes occurring in batch reactive distillation systems are separation and reaction. We show that these systems can be modelled as a simple linear combination of the two individual vector fields, namely the separation vector field and the reaction vector field. We define a reactive residue curve in an analogous manner to that used for separation processes, namely that a reactive residue curve is the trajectory traced out by the liquid composition in a batch reactive distillation still. The resultant residue curve map has singular points and the movement of these singular points leads to an understanding of the effect of reaction on the feasible products. Surprisingly the most important factor is not the kinetics of the reaction (speed and order of the reaction) but, the direction of the stoichiometric vector. We then show that there are three main types of reactive residue curve maps, and relate them to the direction of the stoichiometric vector. This leads to a very powerful process synthesis tools in that one is in a position to sketch the qualitative behaviour of the reactive residue curve map for a given reaction, and thus for a given stoichiometric vector. One is thus able to easily sketch the reactive residue curve and decide qualitatively on types of control policies to achieve the optimal profiles for the envisaged reactive separation process. In this chapter we demonstrate the idea for the zero order kinetics and ideal ternary component mixture.

1.2.4 Chapter 5

In this chapter we extend the approach presented in chapter 4 to the topological analysis of reactive residue curve maps (RRCMs) of simple batch distillation in which a single reversible chemical reaction with nodes (representing reaction equilibrium points). The approach presented in this chapter provides a visual representation of the RRCM both inside and outside the mass balance triangle (MBT). The results show that the combination of simple distillation and single reversible reaction move

singular points in the composition space. The understanding of the movement of singular points can be used for feasibility analysis and help understand some general design implications related to the change of the topology of the RRCMs. For example the results show how the reaction vector direction is the most determinant factor and that the size of the reaction vector has only a secondary impact on the topology of the reactive residue curve map. Furthermore we show the result of numerical calculations/simulations of the eigenvalues maps of the resultant process. These maps can be used as assessment tools to complete existing methods based on phase diagrams.

1.2.5 Chapter 6

In this chapter we present a new topologically based approach to the analysis and synthesis of continuous countercurrent reactive distillation columns. We extend the definition of Column Profle Map of a Column Section in continuous distillation to a Reactive Column Section (RCS) in a reactive distillation column. A RCS is defined as a section of a reactive distillation column in which there is no addition or removal of material or energy. We introduce the concept of a Reactive Residue Curve Map (RRCM) in which the profiles in the RRCM correspond to the liquid composition profiles in the RCS.

By looking at the singular points in the RRCM, it is demonstrated that for a single chemical reaction with no net change in the total number of models, the bifurcation of the singular points depends on both the initial non reactive difference point as well as the direction of the stoichiometric vector. These two vectors combine to define what we call the Reactive Difference Point Composition. We show that there only certain feasible topologies of the RRCM and these depend only the position of the Reactive Difference Point Composition.

We look at a simple example where the VLE is ideal and show that we can classify regions of Reactive Difference Point Compositions that result in similar topology of the RRCM. Thus by understanding the feasible topologies of the RRCM, one is able to identify profiles in the RRCM that are desirable and hence one is able to synthesis of a continuous counter current reactive distillation column by combining RCS that correspond to the desired profile in the RRCM.

1.2.6 Chapter 7

This chapter concludes the thesis by summarizing the conclusions of all chapters.

2 Chapter 2 Process Synthesis: Review of the Relationships between Separation Vector Field, Mixing Vector and Analysis of the Resultant Vector field.

This chapter is a relook at the work by Doherty et al [1][2][3] and Tapp et al.[4]. This chapter constitutes an introduction to the area of vector field analysis. It is used as an introduction to the thesis.

2.1 Abstract

The approach of using a differential description of distillation column has lately become popular [5]. This approach is used for synthesis of standard column configurations and more recently for novel column configurations as well [6]. In this chapter we review distillation differential equations as introduced by Van Dongen et al [5]. and we reconsider in a vector perspective the link between the equipment configuration and the topology of the distillation vector field.

2.2 Introduction

Hauan *et al.[7]* showed that if the ϕ constant assumption is lifted, the resulting vector describing the distillation process is still a linear combination of the two vector fields

but the scalar term however, would be a matrix allowing for any mixing pattern based on the local value of $\underline{x}$.

A typical conceptual synthesis design problem looks for equipment capable of creating a bridge between the inputs and the targeted outputs [7]. In this review we propose that the solution to this problem may be addressed by a simple analysis of vector fields describing the overall process.

The traditional approach or unit operation has been for chemical engineers to look first at the equipment and then only derive models to describe the phenomena occurring within the equipment. However this chapter shows that a different step can be taken if one considers the vector fields describing the process and then derives possible types of corresponding equipments.

By looking at other alternative configurations corresponding to the same process vector field, one might be able to derive key operational parameters especially at the very early stage of process synthesis. This chapter focuses on the use of vector concepts not only as numerical "platforms" but also as tools for explorations of equipments configurations. The main outcome is that one is now in a position to describe chemical equipments by only looking at vector fields describing the overall process.

This approach can be used for quick scanning of alternatives useful 'routes' for preliminary process synthesis task such as equipments assessment in terms of operability.Hauan *[7]* proposed a simple vector representation of how composition changes occur in chemical reaction processes. They were able to show that chemical processes can be considered as simple combination of elementary phenomena vectors occurring in the system. In this paper we propose an additive idea that chemical equipments, as well, can be described by vectors fields.

If we consider the distillation process as the sum of the separation and mixing vectors, the overall vector field can be described as:

$$\frac{d\underline{x}}{d\zeta} = \underline{S} + \phi\underline{M} \qquad (2.1)$$

Where $\underline{S}$ is the separation vector, $\underline{M}$ is the mixing vector, ϕ is a sizing scalar, $\underline{x}$ is the liquid composition and ζ is a variable related to time or distance along the equipment Thus in summary, the change in composition $\underline{\mathbf{x}}$ during a distillation process is described by a linear combination of a separation vector $\underline{S}$ and the mixing vector $\underline{M}$. The term ϕ in equation (2.1) is a constant scalar and hence affects only the magnitude of the second term and not the direction of the mixing vector.We note that $\underline{S}$ and $\underline{M}$ are in a more mathematical sense vector functions as they appear to have functional dependencies on other external composition variables.

Hauan *[7]* further showed that if the ϕ constant assumption is lifted, the resulting vector describing the distillation process is still a linear combination of the two vector fields but the scalar term however, would be a matrix allowing for any mixing pattern based on the local value of $\underline{x}$. vector field.

Recently Tapp *et al. [7]* showed that the fundamental topology of the resultant vector field is dependent on the topology of the individual vector fields. They were able to show that the term ϕ in front of the mixing term affects the position of the singular points in the composition space when one plots the composition profiles map, but not the type of singular points that one would find. First, we will consider each of the vector fields in turn and in particular their topologies.

2.3 The topology of the Separation Vector Field

The separation vector field $\underline{S} \in R^2$can be represented by the residue curve map. These maps have been well studied by many researchers, including Doherty et al.[1][2]. Tapp et al.[4] extended the residue curve map outside the composition subspace. An

example of an extended residue curve map for a constant relative volatility system is given in Figure 2.1.

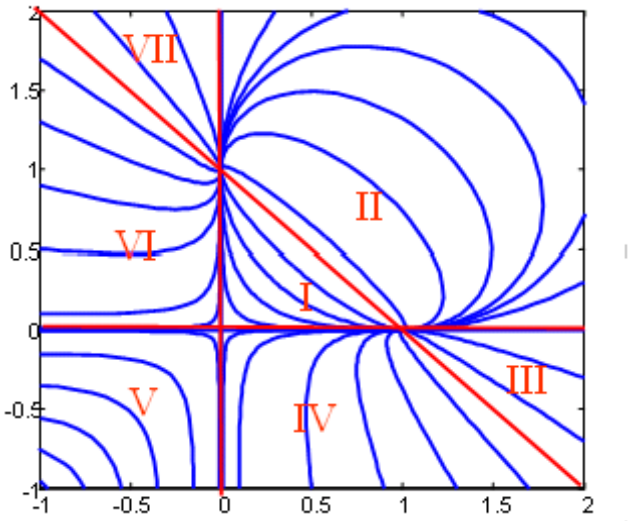


Figure 2.1: Extended Residue Curve Map (RCM) for ideal system

For the purpose of illustration we consider a ternary system, where L refers to the lowest boiling component, H to the highest boiling component and subscript I to the intermediate component.One can see that the entire composition has 3 singular points and that in each region the curves begin at the same node or end at the same node. In addition the curves leave or enter the nodes along the direction of the same eigenvector. Tapp *et al. [4]*were able to divide this extended residue curve map into a number of different regions. For example the positive space is referred as region I. The behaviour in these regions represents all possible profile solutions for a constant relative volatility system.

2.4 The Mixing Vector Field

The mixing vector field $\underline{M}$ is represented by mixing trajectories that are straight lines joining local compositions to the composition of the material being added [7].By manipulating the size and the direction of the mixing linear term, the topology of the resultant vector fields may change when combining the separation and the mixing vector fields. Concretely this means that the curvature of trajectories and position of stationary points of the $\underline{S}$ field may change. In this chapter we consider some of the possible equipment implications for a system with known ideal VLE where only separation and mixing occur.

2.5 Continuous Rectifying Column Equipment

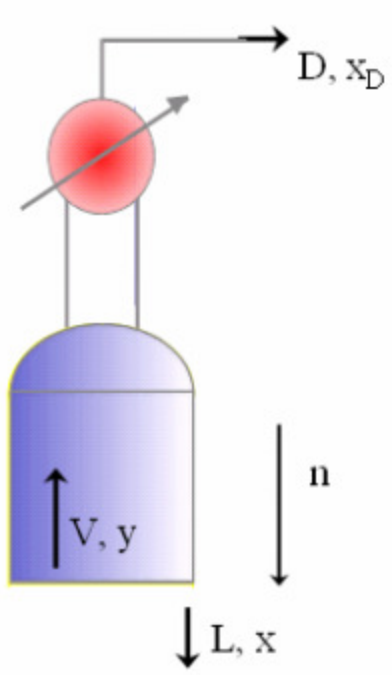


Figure 2.2: Continuous rectifying column

Let us consider the general process vector equation represented by:

$$\frac{d\underline{x}}{d\eta} = \underline{\rho}_{column} = \underline{S} + (1-\alpha)\underline{M} \qquad (2.2)$$

Where the separation vector $\underline{S}$ equal to the term $(\underline{x} - \underline{y}^*)$ and the vector $\underline{M}$ is the mixing vector. Let us also suppose that one applied constraint such that the term $\alpha \in [0,1]$ and that the initial condition for the vector equation (2.2) is set equal to the composition of the distillate material from the total condenser

One can see that the process vector $\underline{\rho}_{column}$ describes the distillation equipment shown in Figure (2.2) under the assumptions of constant molar overflow, ideal equilibrium stages and steady state. The mixing vector $\underline{M}$ equal to the term $(\underline{x}_D - \underline{x})$ where $\underline{x}_D$ defines the composition of the distillate material.

In Figure 2.2, D is the distillate flow collected at the total condenser, $\underline{x}$ is the liquid mole fraction, $\underline{y}^*$ is the vapour mole fraction in equilibrium with the liquid $\underline{x}$ .One can see that the parameter α is equal to the ratio $\frac{L}{V}$ where V,L are respectively the vapour and liquid flow rates in the equipment.The constraint for this equipment is that the distillate material composition and the initial point are the same and the only free parameter that can be varied is the parameter α or equivalently L/V ratio. We see that the singular points of the process field for a fixed distillate material $\underline{x}_D$, move on a curve called pinch point curve and defined by:

$$\frac{(x_1 - y_1^*(x))}{(x_2 - y_2^*(x))} = \frac{(x_{D1} - x_1)}{(x_{D2} - x_2)} \qquad (2.3)$$

The pinch point curve for a distillate (top liquid) composition of x_D = [0.35; 0.25] is shown in Figure 2.3.The pinch points represent the limits of the feasible compositions of the distillation process. The pinch point curve in Figure 2.3 shows also how far the stable node H can move inside the MBT for all possible values of the parameter α. We have been able to identify three parameters in the process vector equation 2.2 that describe the column equipment: the parameter α, the initial integration material

composition x_o and the mixing material composition x_D. We realize that for the above equipment the initial material x_o is equal to the distillate material composition x_D and that the parameter α is constrained to the range $\alpha = [0,1]$. In other words in this equipment one has the possibility to change the size of the mixing vector via the parameter α and not its direction. What Figure 2.3 tell us also is that because one can not change the direction of the mixing vector, the location of the pinch point curve is fixed and one does not have the freedom to choose which one of the singular points of the S field one want to move in and out the MBT.

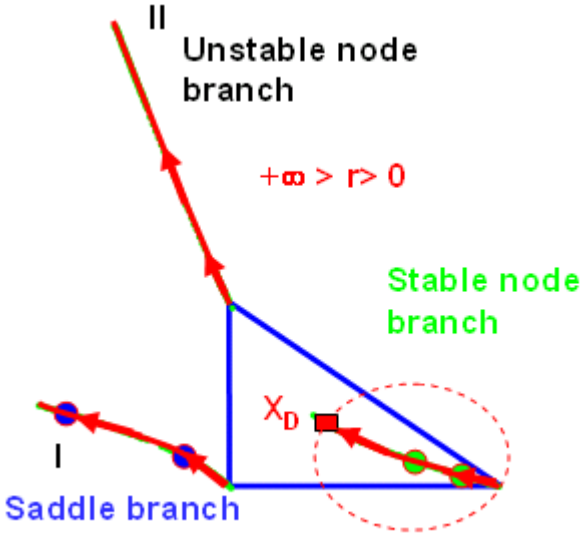


Figure 2.3: Pinch point curve for an ideal system operating with a total condenser and a distillate (top liquid) composition of XD=[0.35;0.25]. The circled branch represents the valid pinch point curve inside the MBT. The stable branch originates from the high boiling component while the unstable branch originates from the low boiling component. The VLE is ideal with constant relative volatilities.

We now address the question of whether there are other types of equipment that could be described by a similar differential equation (Equation 2.1), i.e. by a linear

combination of a separation and mixing vector. We consider two other pieces of equipments that have similar description as the distillation column and look at potential similarities and differences.

2.6 The Rectifying Batch Equipment

The equipment described below (Figure 2.4) could be described also by the same vector equation:

$$\frac{d\underline{x}}{d\xi} = \underline{\rho}_{rectifying-batch} = \underline{S} + (1-\alpha)\underline{M} \qquad (2.4)$$

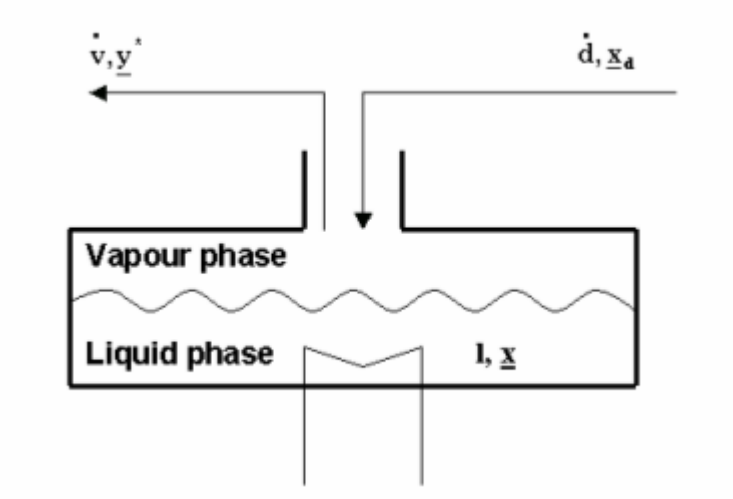


Figure 2.4: Rectifying batch vessel

In equation 2.4 $\underline{S}$ is the separation vector equal to the term $(\underline{x} - \underline{y}^*)$ and $\underline{M}$ is the mixing vector equal to the term $(\underline{x}_d - \underline{x})$, $\underline{y}^*$ is the composition of the leaving vapour in equilibrium with the liquid residue of composition $\underline{x}$ in the still and $\underline{x}_d$ is

the composition of the material being mixed to the liquid. One can see that the process vector $\rho_{rectifying-batch}$ describing the liquid composition in the batch apparatus is a combination of a separation vector and a mixing vector. The integration variable ξ is related to the time t and the parameter α is defined by the ratio $\alpha = \frac{\dot{l}}{\dot{v}}$ where $\dot{l}$ and $\dot{v}$ are respectively the liquid and the vapour removal rate in the batch equipment.If we set $\alpha = \frac{\dot{l}}{\dot{v}} = \frac{L}{V}$ we can see that $\rho_{column} = \rho_{rectifyin\ \ batch}$

2.6.1 Initial conditions

However there are two possibilities for the initial conditions as the batch starting composition $\underline{\mathbf{x}}|_{\mathbf{t=0}}$ can be set equal or different to the added material composition $\underline{\mathbf{x}}_{\mathbf{d}}$. We will consider each case separately:

- If $\underline{x}|_{t=0} = \underline{x}_d = \underline{x}_D$ and if $\alpha = \frac{\dot{l}}{\dot{v}} = \frac{L}{V}$, the batch profile will follow the distillation column profile. Tapp et al. [8] experimentally confirmed this point. They showed that there is a good agreement between the results given by the ASPEN PLUS® simulation of a multistage distillation column using the Wilson model and the results obtained by running a batch distillation vessel where they set the initial material composition equal to the top stage composition $\underline{x}_D$ in the ASPEN PLUS® simulation.

- If $\underline{x}|_{t=0} \neq \underline{x}_d (\underline{x}_d = \underline{x}_D)$ the batch profile moves in a different direction than the distillation column. One can generate a map for fixed distillate material composition $\underline{x}_d$ but different initial conditions $\underline{x}|_{t=0}$ This map has been referred

as the column profile map (CPM) [4]. It represents all attainable profiles for fixed material composition $\underline{x}_d$. These profiles pinch at a unique node in the composition space of mole fractions (Figure 2.5). These profiles are used in complex column configurations, such as divided wall or Petlyuk columns. The use of these profiles allows for a wide range of possible operations than that achieved with the previous column equipment. In Figure 2.5 if we set α= 0.85 and the composition of the distillate material $\underline{x}_d$ = [0.3 0.4] we can populate the space with profiles and one can see that the new column profile map is a

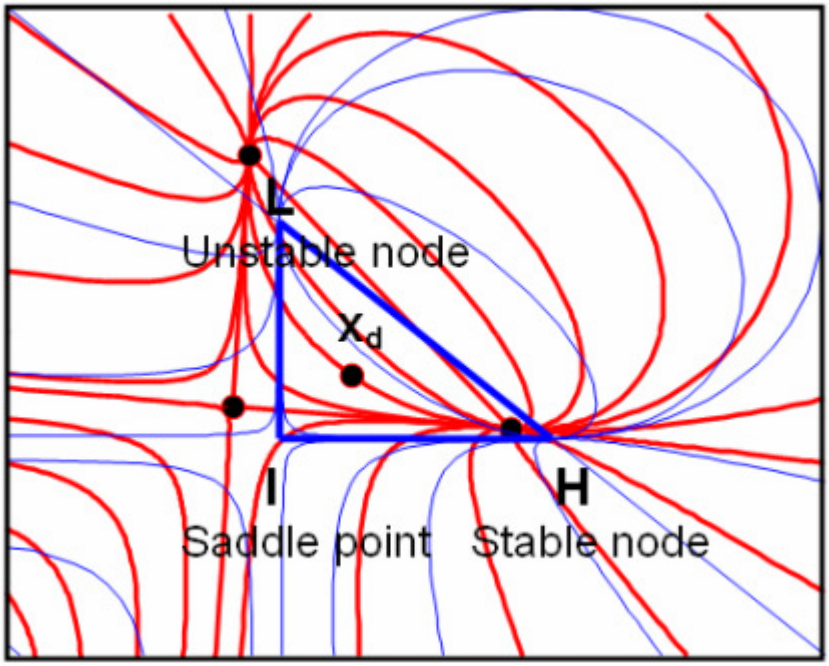


Figure 2.5: Theoretical column profiles map for an ideal system with the parameter α=0.85 and distillate material $\underline{x}_d$ = [0.3 0.4]

The advantage of using any initial material composition in the batch still is that one has now the possibility to follow a variety of compositional paths. However, even in

this case, the distillate material composition $\underline{x}_d$ is not changing and the parameter α is kept constant when plotting the column profile map as shown in Figure (2.5). However in batch equipment the term α can take a broader range of values namely $\alpha \in [0,+\infty[$. Let us look at the implication of this.

2.6.2 The parameter α

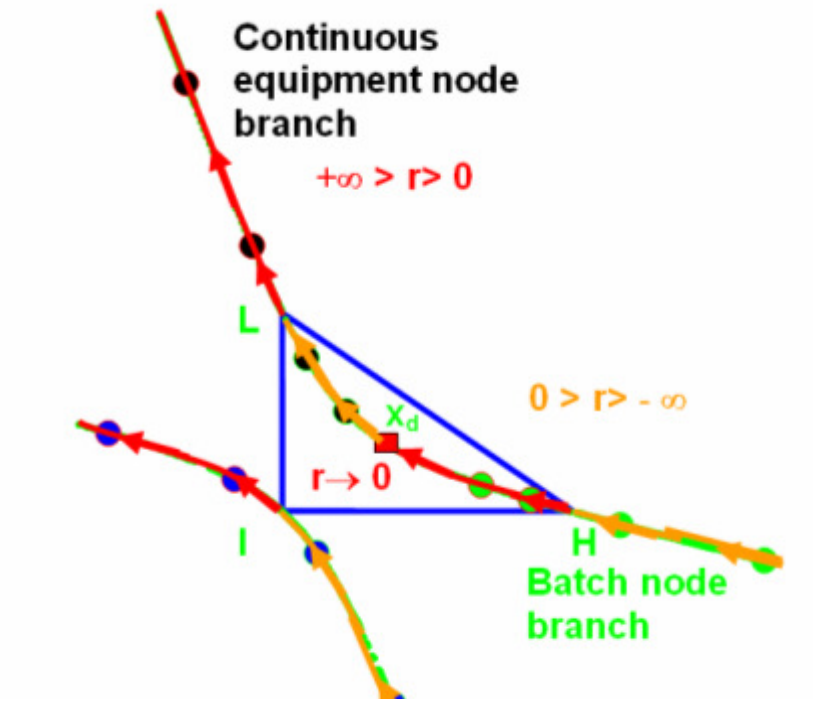


Figure 2.6: The pinch point curve for a batch system operating with a distillate composition Xd= [0.35; 0.25].The VLE is ideal and described by constant relative volatilities. L is the low boiling component, I is the intermediate boiling component and H is the high boiling component. We assume that the volatilities of the components L and H relative to I are equal to 5 and 3 respectively

As pointed out earlier, the variable α has a wide range of operation namely $\alpha \in [0,+\infty[$ whereas continuous column equipment as described in the previous case is limited to operating range of $\alpha = [0,1]$. Thus a batch apparatus as described in Figure 2.6 can access not only column profiles found in distillation column equipment but also some profiles that are not achievable by continuous column equipment. The value of the parameter α is physically meaningful between [0,+1] i.e. when the liquid

feed rate is positive and smaller than the vapour rate in continuous equipment. However in batch still the liquid feed rate can exceed the vapour rate and in this case the mass content of the batch vessel increase and ultimately go to infinity. This batch situation corresponds to α between $[0, +\infty[$. For the continuous case this case remains constrained to the reflux ratio between $[-1, 0]$ as even though the distillate material is being added (the distillate flow rate D is negative), the addition rate of distillate (-D) cannot exceed the liquid down flow L ($D=-L \rightarrow r=-1$).

We can see in Figure 2.6 that the singular points which are the possible limit products of the separation process could only move on the red branches of the pinch point curve for the column equipment and that for the batch equipment the entire pinch point curve (yellow and red branches) is valid path for the singular points. This means that the batch still can reach zone untouched by the standard column and allow one to achieve compositions beyond the conventional operation "zone" as defined for the column equipment. This has the advantage that column profiles previously thought impossible in the column equipment are now feasible. For example because of the structure of the pinch point curve in Figure 2.6 one can now move the unstable node inside the MBT for values of the parameter $\alpha > 1$.

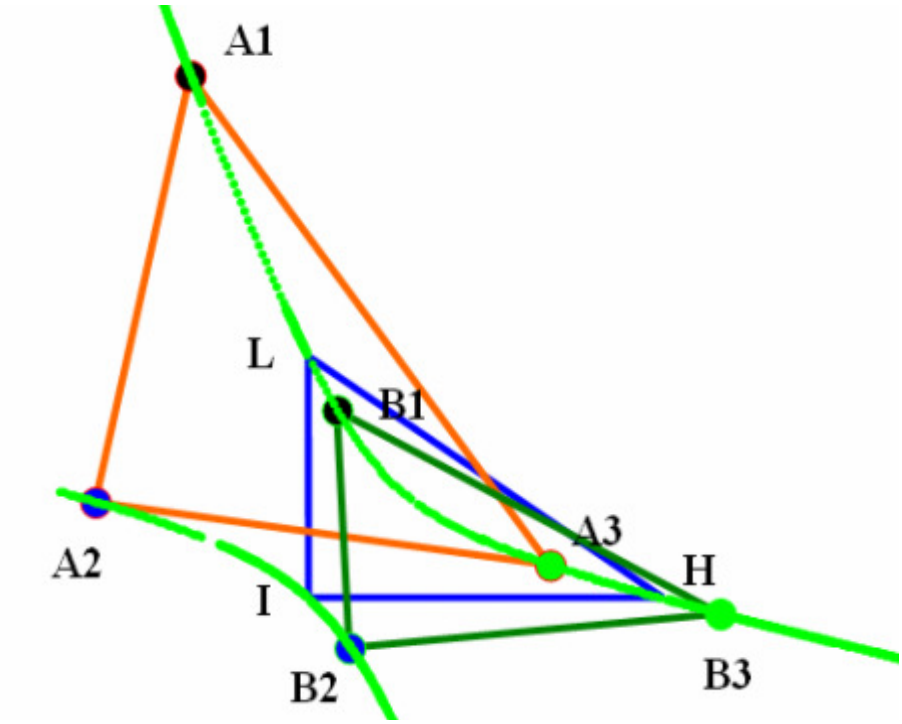


Figure 2.7: The singular points B1B2B3 for α=1.16 in a batch equipment operating with a distillate material composition of Xd= [0.35; 0.25] and singular points A1A2A3 for α=2 .The VLE is ideal and described by constant relative volatilities. L is the low boiling component, I is the intermediate boiling component and H is the high boiling component. We assume that the volatilities of the components L and H relative to I are equal to 5 and 3 respectively

2.6.3 Conclusion

From the vector process equation $\underline{p} = \underline{S} + (1-\alpha)\underline{M}$, we have considered two different types of equipments by modifying the range of the parameter α and/or the initial condition for the integration of the vector equation. These different constraints affect the topology of the resultant vector field and lead to very different range of operating regions and behaviors. By looking at the pinch point curve we have been able to show

that new composition profiles can be reached in a batch still that was thought impossible in standard column equipment. However a further analysis reveals that because the distillate material composition is fixed in either cases ($\underline{x}_d$ or $\underline{x}_D$) the position of the pinch point curve could not be changed and that the singular points of the $\underline{S}$ field were constrained to move on a fixed pinch curve. Next we look at different kind of equipment with the same general process vector but which offer the possibility to change the position of the pinch point curve and therefore introduce an even more flexibility in the resultant topology with regard to the movement of nodes when combining the separation and mixing vectors.
constant relative volatility system.

2.7 Column Sections

We have found equipments that operate and give not only conventional rectifying profiles but also other solutions. We ask now if a relationship between profiles where initial condition and mixing point are not the same can be related to a more conventional distillation column.
In this order we consider a column section (Figure 2.8). A column section has been defined as a length of column between points of addition or removal of material or heat [4]

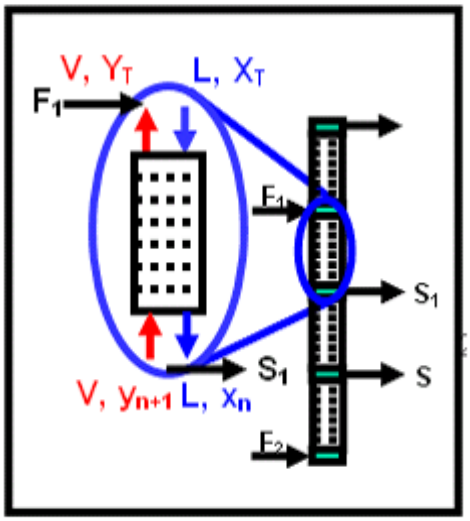


Figure 2.8: Distillation column with 4 column sections

The column section shown above can also be described by a linear combination of the mixing vector $\underline{M}$ equal to the term $(\underline{x}_{\Delta} - \underline{x})$ and the vector separation vector $\underline{S} = (\underline{x} - \underline{y}^{*})$ and the equation describing this equipmemt will be:

$$\frac{d\underline{x}}{d\eta} = \underline{S} + (1-\alpha)\underline{M} \qquad (2.5)$$

The integration variable η is related to the length of the column section and $\alpha = \frac{r_{\Delta}}{r_{\Delta}+1}$. The term $r_{\Delta} = \frac{L}{\Delta}$ and $\Delta = V - L$ is defined as the molar flow rate of material in the column section (difference of molar flow rate of streams flowing out

and molar flow rate of streams flowing in) and $x_{\Delta} = \frac{VY_T - LX_T}{V - L}$ is the composition difference point in the column section. In this case the parameter α has a wide range of values namely $-\infty < \alpha < +\infty$.

The initial composition is set equal to the top composition $\underline{X}_T$ and the difference composition $\underline{x}_{\Delta}$ is not restricted to compositions inside the mass balance triangle.

One can see that the vector equation of the column section is a more general form from which one can deduce the previous continuous equipment by allowing specific constraints. For example if $V - L = D$ and $\underline{x}_{\Delta} = \underline{x}_D$ the parameter α reduces to $\alpha = \frac{L}{V}$ and for the initial condition $\underline{X}_T = \underline{x}_D$, one retrieves the continuous column equipment.

In the previous two equipments, the mixing material compositions were not allowed to change. When difference point equation (Equation 2.5) is concerned however, the direction of the mixing vector is related to quantities such as the composition difference point in the column section. This quantity is not restricted to positive space, and has not an upper bound as well: mole fractions may exceed the value of 1. Therefore, we are not limited in the types of linear terms that can be added to alter the $\underline{S}$ trajectory space since the composition difference $\underline{x}_{\Delta}$ and the initial material composition $\underline{x}_T$ are vectors of state variables which may not be bounded within the MBT. We are also not only removing restrictions in the values of the composition difference point, but also in the parameter α as $-\infty < \alpha < +\infty$.We notice that the parameter α is a function of the term Δ = V-L. This term can be considered to be the equivalent molar flow rate of material in the column section. Hence if Δ is negative, the net molar flow of material in the column is downwards, in the direction of the liquid flow, while if Δ is positive the net molar flow rate in the column is upwards in the direction of the vapour stream. The net molar flowrate remains constant in a column section and only changes when Δ is changed, such as by feed addition, side

stream withdrawal or phase change. The sign of this term is very important. If the term is positive, it means that there is a net flow of component i up the column, or in the direction of the vapour. If the term is negative, then conversely, there is a net flowrate of component i downwards, or in the direction of the liquid flow. Let us for a minute consider the more traditional rectifying column section. In a rectifying column section, Δ is positive while in a stripping column section, Δ is negative.

Tapp et al.[4] have observed in the column section equipment that interesting features of the topology may, and do; occur when the composition difference point can be located inside or outside the MBT.

The most important feature in term of the topological behaviour for the column section equipments is that the composition difference point can change and move from one region of the composition space to another via addition of feed streams or removal of side streams . Depending on the position of $\underline{x}_{\Delta}$, the pinch point curve will connect very different singular points and shows very different shape (Figures 2.9 and 2.10).

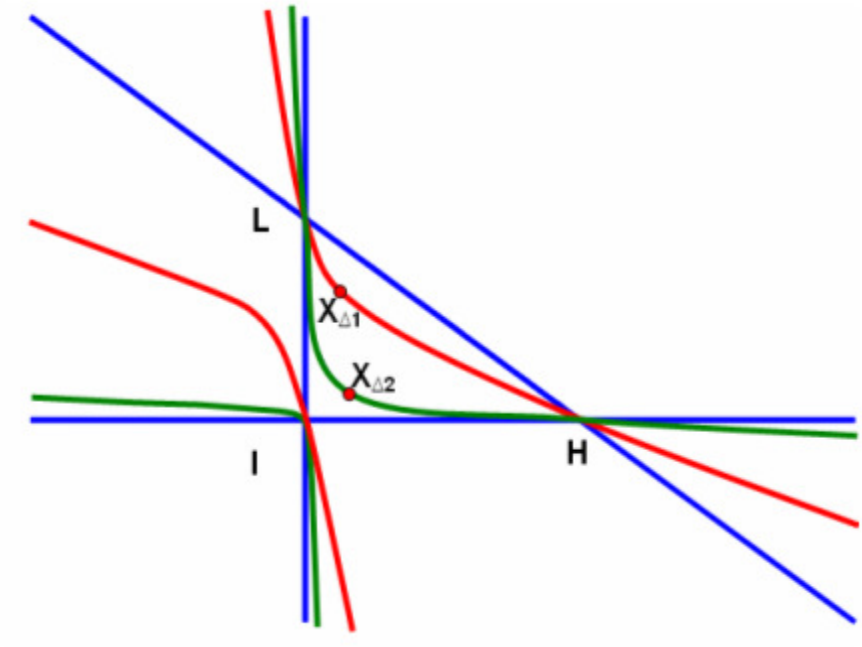


Figure 2.9: Different shape for the pinch point curve for different Extended in the same region of the composition space (positive space)

- If the difference composition $\underline{x}_{\Delta}$ changes but remains in the same region of the composition space as defined in Figure 2.1, the pinch point curve will connect the same singular points but will change the curvature as shown in Figure 2.9. This is still an advantage as one has the possibility to move the singular points at any point inside the MBT in Figure 2.9.

- If the difference composition $\underline{x}_{\Delta}$ changes and moves from one region to another region of the composition space as defined in Figure 2.1, the pinch point curve will connect different singular points. This is also an advantage in a design point of view as one has the possibility now to choose which of the singular points he want

to move in or out the MBT. For example in Figure 2.10 for $\underline{x}_{\Delta 2}$, the pinch point curve is a continuous elliptic curve. This means that no singular points can be moved inside the MBT while for $\underline{x}_{\Delta 1}$, two of the singular points can be moved inside the MBT (the stable and the unstable node).

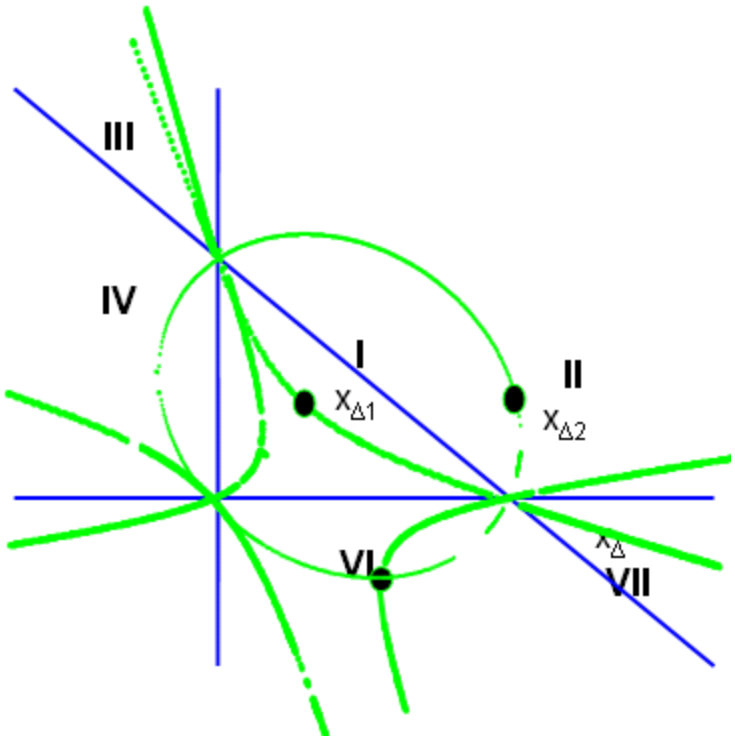


Figure 2.10: Different shape for the pinch point curve for the difference composition in different region of the composition space in region I and region II

An important application of the above mentioned behaviors is that for non-ideal Thermodynamics for example, column profiles can be made to move into regions previously thought impossible with an appropriate choice of X_Δ and R_Δ. For example

distillation boundaries can be crossed (Figure 2.11) and this could not be achieved with the two previous equipments [4].

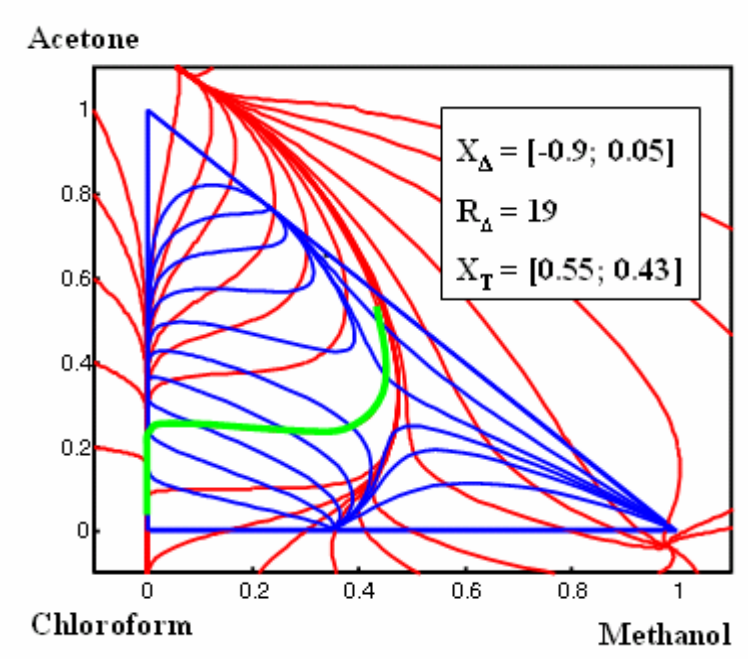


Figure 2.11: Crossing distillation boundary for the non ideal system Acetone-Chloroform-Methanol for appropriate choice of parameters XΔ and R_Δ

We bring an additive idea to the concept developed by Hauan [7] that the distillation process can be considered as a linear combination of the separation and mixing vectors. We show that different combinations of these individual vectors bring new topological scenarios. By choosing "different" combination of the separation and mixing vectors, one can move differently the nodes of the $\underline{S}$ field and get very special behaviors.

Next we look at the combination of the separation and mixing vector to simulate experimentally distillation stripping profiles.

Bibliography

1: Doherty,M.F.,Perkins,J.D., " On the Dynamics of distillation processes-I, the simple distillation of multicomponent non-reacting homogeneous liquid mixtures",Chemical Engineering Science, 1978,33,pp 281-301

2: Doherty,M.F.,Perkins,J.D., "On the dynamics of distillation processes-II, The Simple Distillation of Model Solutions",Chemical Engineering Science, 1978,33,pp 569-578

3: Doherty,M.F.,Malone,J.D.,"Conceptual design of distillation systems", 2001,McGraw Hill,New York

4: Tapp,M.,Holland,S.T.,Glasser,D.,Hildebrandt,D.,"Column Profile Maps Part A: Derivation and interpretation", Industrial and Engineering Chemistry Research,2004,43,pp 364-374

5: Van Dongen,D.B., Doherty,M.F., "Design and Synthesis of Homogeneous Azeotropic Distillations 1Problem Formulations for a single column", Industrial Engineering chemistry Fundamental,1985,24,pp 454-463

6: Holland,S.T.,Tapp,M.,Glasser,D.,Hildebrandt,D.,"Novel separation system design using 'moving triangles", Computers and Chemical Engineering,2004,29,pp 181-189

7: Hauan,S.,"On the behaviour of reactive distillation systems" PhD Thesis, Norvwegian University of Science and Technology, Trondheim, 1998

8: Tapp,M.,Glasser,D.,Hildebrandt,D., "Experimental simulation of distillation column concentration profiles using batch apparatus" Chemical Engineering Science,2003,58, pp 479-486

3 Chapter 3 Batch Experimental Simulation of Distillation Column Profiles: Stripping Section

This chapter was published in Chemical Engineering Science, 28 (5), (2005), 829-837 under the title: experimental simulation of distillation concentration column profiles: column stripping section.

3.1 Abstract

It has been shown that distillation column rectifying profiles can be measured experimentally in a batch boiling apparatus using a combination of equilibrium boiling, vapour removal and the addition of material of the distillate composition [1]. The problem with using this concept for stripping profiles is that in order to follow the concentration profiles one needs to remove material of the bottoms composition while retaining equilibrium boiling conditions. This cannot be effectively implemented as the bottoms composition is not produced in the apparatus and that the removal of this material would not be possible under equilibrium conditions.

In this paper we re-examine the differential description of the distillation stripping section and using vector concepts show that the removal of material of the bottoms compositions is equivalent to the addition of material of a composition that varies in a mathematically predictable manner with time.

This feed policy has been implemented experimentally and it is shown that

stripping section profiles can be measured with reasonable accuracy in a batch still. This work verifies and validates experimentally the concept that separation and mixing are opposite vectors phenomena [2] and also offers an opportunity to combine computer software and experimental simulation to simplify troublesome calculations and help reducing computational time.

3.2 Introduction

Distillation column concentration profiles can be used to assist the design engineer in designing complex distillation columns [3]. However, to be able to determine the feasibility of a required separation in a distillation column, one need to determine the column profiles for both the rectifying and stripping sections. In traditional distillation design the general short-cut technique has been to determine the liquid composition profiles from the rectifying section calculated from the distillate down the length of the column and the liquid composition profiles for the stripping section calculated from the bottoms up the column. A separation is considered to be feasible if these liquid profiles intersect. Current techniques to determine these profiles use simulator packages or require laboratory-scale plot plants. These 2 methods raise major concerns among the engineers.

The time consuming and the lack of insights into solutions do not always allow the designer to rely completely on computing methods. A combination of computer packages and simple experimental techniques can be a simplification. On the other hand the costs associated with pilot plants and the poor extrapolation to full scale has lead designers to not consider this alternative.

The simulation of these profiles can be substantially simplified through the implementation of quick and simple experimental techniques. The implementation of the experimental simulation for the distillation rectifying profiles has been presented [1]. In this paper we present a new concept to support the computer simulation of

column profiles for the stripping section.We transform the stripping batch process into an equivalent rectifying batch process where the composition of the feed material $\underline{x}_d$ is now a time dependent variable. We use a vector interpretation of the traditional rectifying and stripping differential equations for a continuous single distillation column. This approach allows for the basic mechanisms to be clearly understood when looking for equivalence between continuous and batch distillation equations. Understanding these mechanisms enable the formulation of simple experimental policies for the distillation stripping section. The technique developed could be used as a complementary aspect of the computer programming methods.

3.3 Theories

Similar to the rectifying section [1] the development and comparison of the continuous distillation and batch distillation equations are essential for the implementation of experimental techniques. The following will present the theory behind both rectifying and stripping profiles.

3.3.1 Residue Curves

Doherty *et al [4][5]* developed the geometric distillation design approach by reviving the concept of residues curves. Schreinemakers *et al.[6]* first defined residue curves as trajectories of residue compositions during a simple batch evaporation of a given mixture. He established the relationship between the vapour-liquid equilibrium of a mixture and the behaviour of evaporation residue curves for ternary mixtures. An overall components and material balance over the simple evaporation batch leads to the following residue curve equation:

$$\frac{d\underline{x}}{d\xi} = \underline{x} - \underline{y}^* \qquad (3.1)$$

where $\underline{y}^*$ is the vector composition of the vapour in phase equilibrium with $\underline{x}$, $\underline{x}$ is the vector composition of the liquid mixture and ξ is a scalar quantity non-linearly related to time.

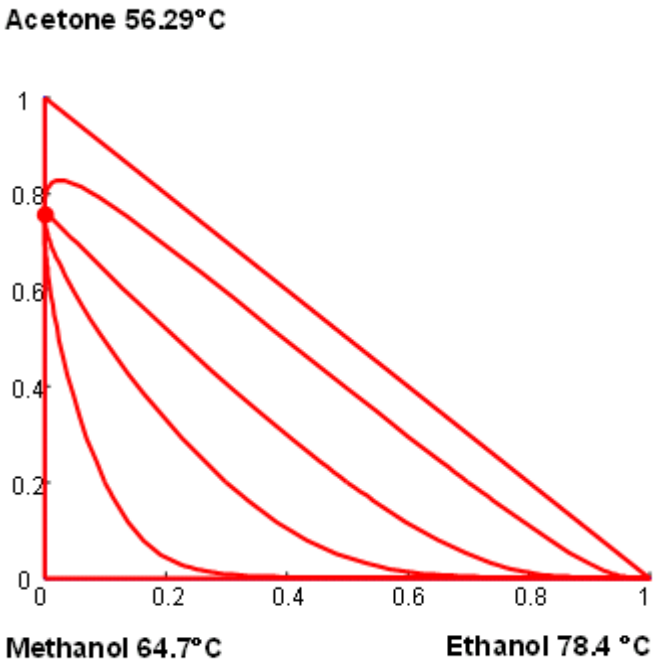


Figure 3.1: Residue Curve Map (RCM) for the Ethanol/Methanol/Acetone System at 1 atm

Doherty et al.[4][5] further showed that by starting with different compositions of liquid in the still the interior of the composition space can be filled with residue curves to form a Residue Curves Map(RCM). The Residue Curve Map (RCM) for the Ethanol/Acetone/Methanol system at 1 atm is shown in Figure 3.1, as the experimental measurements will be done using this system. All the composition profiles leave from the low boiling binary azeotrope between the pure components acetone and methanol, move toward the intermediate boiling components (methanol

or acetone) and end at the high boiling pure component (Ethanol). One can see in Figure 3.1 that there are different zones corresponding to different "shapes" for residue curves. For instance regions around the methanol and acetone apex are zones of high curvature in the shape of residue curves while the region close to binary edge ethanol-acetone is a zone of "flat" residue curves. Depending in which region the experiment is conducted; the experimental simulation of composition profiles can be quick or very slow; extended on a large portion or limited to few points. The explanation of such behaviour could be attributed to the local behaviour of the separation vector defined by the vector $\underline{S} = \underline{x} - \underline{y}^*$, i.e. for starting material close to the binary azeotrope, the separation vector $\underline{S}$ is very small and one should expect the experimental simulation to be slow around this point.Residue curves maps proved to be useful tools for the prediction of attainable product compositions in distillation columns, qualitative prediction of composition changes in distillation columns, feasibility of columns sequences, and entrainer selection for azeotropic distillation [4][5].

Residue curves have been also considered as column profiles for an infinite reflux column [7]. For distillation operating at finite reflux the composition profiles differ slightly compared to the residues curves under the same isobaric conditions[8]. The rectifying section of a distillation column of distillate composition $\underline{x}_D$ is described by the following first-order ordinary differential equation:

$$\frac{d\underline{x}}{dh} = \frac{r+1}{r}(\underline{x} - \underline{y}^*) + \frac{1}{r}(\underline{x}_D - \underline{x}) \qquad (3.2)$$

The initial condition is $\underline{x}\big|_1 = \underline{x}_D$, and h is the number of stages in the rectifying section and is counted top down in the column.

The stripping section of bottom composition $\underline{x}_B$ is described by the following first-order ordinary differential equation:

$$\frac{d\underline{x}}{dh'} = \frac{s}{s+1}(\underline{y}^{*} - \underline{x}) + \frac{1}{s+1}(\underline{x}_B - \underline{x}) \qquad (3.3)$$

The initial condition is $\underline{x}\big|_1 = \underline{x}_B$, and h' is the number of stages in the stripping section and is counted down up in the column

r and s are respectively the reflux ratio and the reboil ratio.

The equations (3.2) and (3.3) have been derived by Van Dongen et al.[9]

3.4 Experimental Simulation of Rectifying Column Profiles

Tapp et al.[1] showed that Doherty's rectifying differential equation in a distillation column could be approximated by a time dependent differential batch equation using a rectifying batch still.

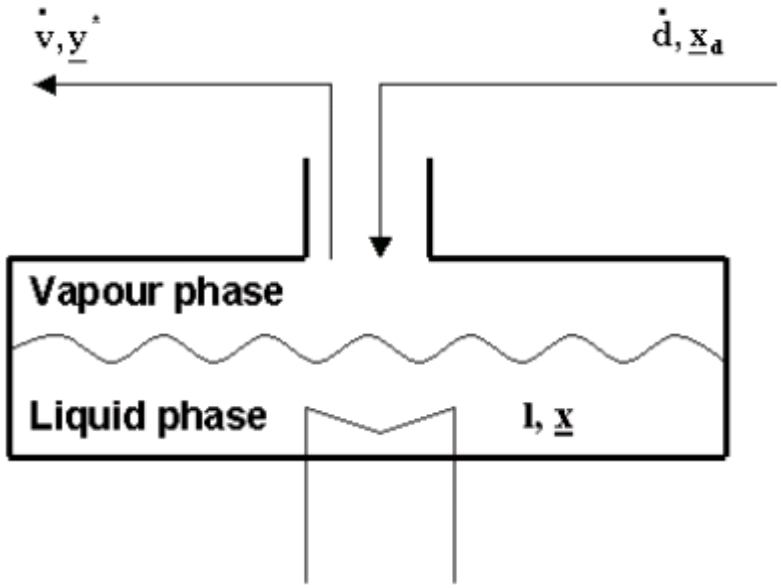


Figure 3.2: Rectifying batch vessel

Consider a simple boiling unit as shown in Figure 3.2 where the leaving vapour of composition $\underline{y}^*$ is in equilibrium with the liquid residue of composition $\underline{x}$ in the still and material of composition $\underline{x}_d$ is added to the liquid.

The differential equation describing this batch apparatus is:

$$\frac{d\underline{x}}{\frac{\dot{v}}{l}dt} = \frac{d\underline{x}}{d\xi} = \underline{\rho}_{rectifying\ \ batch} = (\underline{x} - \underline{y}^*) + \frac{\dot{d}}{\dot{v}}(\underline{x}_d - \underline{x}) \qquad (3.4)$$

$\dot{v}$ is the molar flow rate of vapour being removed

$\dot{d}$ is the molar flow rate of feed material

l is the molar liquid hold-up in the still

In equation (3.4) the vector $\underline{x} - \underline{y}^*$ represents the separation vector and it is this vector that is tangent to the residue curve at point $\underline{x}$ and the vector $(\underline{x}_d - \underline{x})$ can be thought of as a mixing vector where material of composition $\underline{x}_d$ is mixed into the process. Thus the process vector describing the rectifying column profile is a linear combination of the separation vector and the mixing vector.

Description: a) to approximate equation (3.4), material of distillate composition $\underline{x}_d = \underline{x}_D$ is added at discrete time intervals to the batch vessel during the boiling process and $\underline{x}_D$ is the top stage composition in the continuous column.

Equation (3.2) (column rectifying profile) and equation (3.4) (batch rectifying profile) are equivalent in the composition space of mole fractions only if one set:

$$\frac{D}{V} = \frac{\dot{d}}{\dot{v}} = \frac{1}{r+1} \qquad (3.5)$$

One notes that the above condition is set in order to get the same combination of separation and mixing vector as in the continuous distillation column as D and V are respectively the distillate and the vapour flow rates in the continuous distillation column and r is the reflux ratio.

One can consider that:

$$\frac{\partial l}{\partial t} = -\dot{v} \qquad (3.6)$$

where $\frac{\partial l}{\partial t}$ is the rate of boil off of liquid during a period when no feed material is added.

One deduces that $\dot{d} = \frac{\frac{-\partial l}{\partial t}}{r+1}$ (3.7)

Thus, in order to follow compositions profile of continuous columns in batch apparatus, one needs to use the addition policy described by equation (3.7).

However $\dot{v}$ is set by the heat addition rate to the liquid and the latent heat of the material in the still. For small composition changes, the change in latent heat is negligible. One can see that $\dot{v}$ is a measured and not a controlled variable and that what one controls is the ratio of vapour losses to liquid addition.

There are two possibilities for the initial conditions as the feed material composition $\underline{x}_F$ to the batch still can be set equal or different to the distillate material composition $\underline{x}_d$. We will discuss each case separately:

- If $\underline{x}_F = \underline{x}_d = \underline{x}_D$ and if the conditions defined by equation (3.7) are met, the batch profile will follow the distillation column profile.

  Tapp et al.[1] experimentally confirmed this point. They showed that there is a good agreement between the results given by the ASPEN PLUS® simulation of a multistage distillation column using the Wilson model and the results obtained by running a batch distillation vessel where they set the initial material composition $\underline{x}_F$ equal to the top stage composition in the continuous column $\underline{x}_D$. However the batch still offers some operating regions not possible to achieve in a continuous rectifying section as the scaling factor $\frac{\dot{d}}{\dot{v}}$ before the mixing term can take a broader range of values namely $\frac{\dot{d}}{\dot{v}} \in [0, \infty[$.

- If $\underline{x}_F \neq \underline{x}_d (\underline{x}_d = \underline{x}_D)$, the batch profile moves in a different direction than the distillation column. One can generate a map for fixed distillate material composition $\underline{x}_d$ but different feed material composition $\underline{x}_F$ to the batch still. This map has been referred as the column profile map (CPM) [10]. It represents all attainable profiles for fixed distillate composition $\underline{x}_d$. These profiles pinch at a unique node in the composition space of mole fractions. These profiles are used in complex column configurations, such as divided wall or Petlyuk columns. The use

of these profiles allows for a wide range of possible operations than that achieved with standard rectifying profiles.

Advantages:

1. For its application the method of Tapp et al. requires very little amount of material
2. Provides an effective tool for the study of mixtures with non available thermodynamic data
3. Simplifies expensive full scale experiments and reduces dramatically the computational time.

Limitations:

A practical limitation of this method lies in its "discrete" nature and that the boiling "period" is optional. The choice of the "extent of movement" along the separation vector before adding material of distillate composition affects the experimental results.

Applications:

1. In azeotropic mixtures, product compositions often depend on the location of the feed composition in the composition space of mole fractions. The method of Tapp et al. offers a quick way to check the feasibility of a desired separation. For instance Wahnschafft et al [7] showed that one can cross distillation boundaries in a single rectifying (stripping) section of a distillation column. This is possible if the distillation boundary is curved and that the distillate composition lies close and on the convex side of it and that the distillation column operates over a certain range of reflux ratio. Simple rectifying batch experiments can be performed to determine the range of reflux ratio over which the rectifying profiles flip over the distillation boundary.

2. One can find also an application in the use of "operation leaves" concept introduced by Castillo et al.[11]. Operation leaves for the rectifying section defines the whole range of possible rectifying profiles for all constant reflux ratios with respect to a given distillate material. But in most of the cases, distillation column use side condensers, reboilers or remove side streams. In these cases the reflux ratio is not constant along the column and one can use the method of Tapp et al.[1] to assess quickly the effect of the change of the reflux ratio on the operation leaves.

3.5 Separation and Mixing Vectors

If one considers equations (3.2) and (3.4), one can see that the distillation column is described by the simultaneous or sequential occurrence of separation and mixing. Hauan[2] considers each phenomenon as a vector in composition space and assumes that the two individual phenomena are independent of each other. To explain the idea beyond this paper let us consider a hold-up L of composition $\underline{x}$. One can remove material V of composition $\underline{y}^*$ and the separation vector $\underline{S}$ describing the process can be defined by: $\frac{d\underline{x}}{dt} = \underline{S} = \frac{V}{L}(\underline{x} - \underline{y}^*)$

But one can alternatively choose to add material of flow rate L' and composition $\underline{x}_d$ to the same hold up defined previously. The mixing vector $\underline{M}$ describing this process is given by: $\frac{d\underline{x}}{dt} = \underline{M} = \frac{L'}{L}(\underline{x}_d - \underline{x})$

It can be seen that the separation and mixing vectors are "flows" applied to the same point $\underline{x}$ and that it is possible to evaluate parameters L' and/or $\underline{x}_d$ such that $\underline{S} = \underline{M}$. This is the key idea we will use in the following to show experimentally that mixing and separation are opposite vectors [2]. One can potentially replace a difficult separation vector by a mixing vector.

3.6 Experimental simulation of stripping column profiles

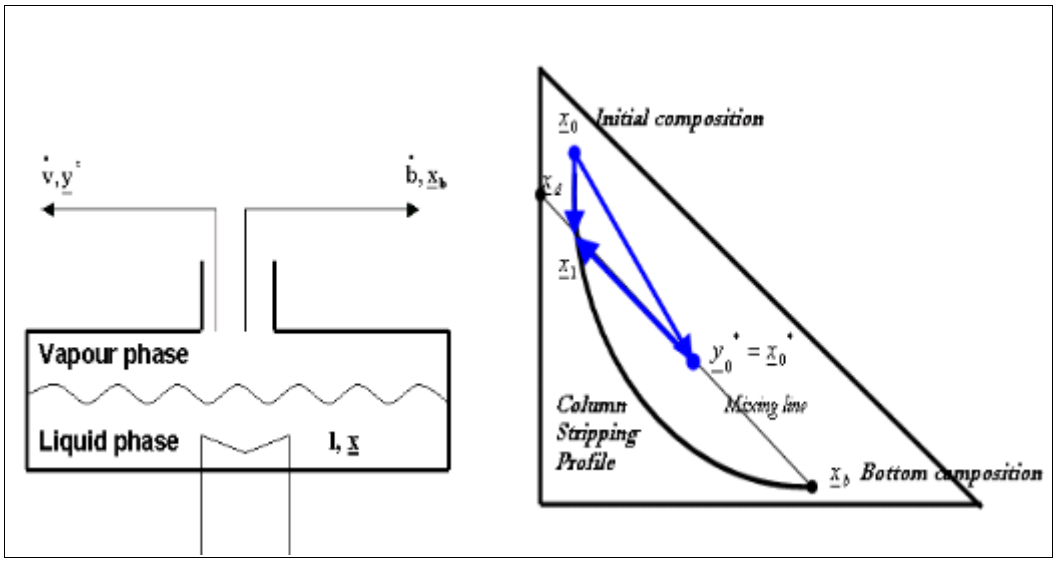


Figure 3.3: (left) the stripping batch vessel (rigth) construction of a stripping profile line for a ternary mixture

Consider a simple boiling unit as shown in Figure 3.3 (left) where the leaving vapour of composition $\underline{y}^*$ is in equilibrium with the liquid residue of composition $\underline{x}$ in the still and material of composition $\underline{x}_b$ is removed from the liquid.

The overall mole balance gives:

$$-\frac{dl}{dt} = -\dot{b} - \dot{v} \qquad (3.8)$$

A component balance yields:

$$-\frac{d(lx_i)}{dt} = -bx_{bi} - \dot{v}y_i^* \qquad i = 1...c \qquad (3.9)$$

With $\sum_{i=1}^{c} y_i = 1$ and $\sum_{i=1}^{c} x_i = 1$

$\dot{v}$ is the molar flow rate of vapour

$\dot{b}$ is the molar flow rate of removed material

l is the molar liquid hold-up in the still

Combining (3.8) and (3.9) we get:

$$(-\dot{b} - \dot{v})x_i - l\frac{dx_i}{dt} = -\dot{b}x_{bi} - \dot{v}y_i^* \qquad (3.10)$$

Hence in vector notation:

$$\frac{d\underline{x}}{\dot{v}dt/l} = \underline{\rho}_{strippingbatch} = (\underline{y}^* - \underline{x}) + \frac{\dot{b}}{\dot{v}}(\underline{x}_b - \underline{x}) \qquad (3.11)$$

Again equation (3.11) can be thought of as a linear combination of a vector mixing term $(\underline{x}_b - \underline{x})$ and a vector separation term $(\underline{y}^* - \underline{x})$.

Equation (3.11) is similar to the Equation (3.3). The only difference between the two equations is that the batch integration variable is the time while in the Doherty equation it is a variable representing stages. If the results are plotted in composition space of mole fractions where time or stages do not appear explicitly the two equations are identical.

We now ask if one can use equation 3.11 in a batch apparatus to experimentally follow distillation column profiles generated by equation 3.3.

The separation term in equation 3.3 has a "negative sign" compared to the residue curve equation, thus the profiles represented by this equation should normally be simulated using a batch condensing apparatus as the "separation parts" in the two processes are equivalent.

In fact simple condensation is a process where a vapour of quantity V and composition $\underline{y}$ is condensed and the equilibrium liquid of composition $\underline{x}^*$ is removed as it is formed at a molar rate $\dot{C}$ [12]. The differential equation describing simple condensation is given by:

$$\frac{d\underline{y}}{d\xi} = (\underline{y} - \underline{x}^*) \qquad (3.12)$$

Equation 3.12 describes vapour residue curves that, although similar, do not coincide with the liquid residue curves. However the boiling process offers more technical advantages than the condensing process, as it is much simple to control the main process variables in liquid phase than in vapour phases as the molar density of a liquid is very much higher than that of a vapour.

If one looks at the batch differential equation 3.11, one can see that to follow profiles derived from equation 3.3 one need to remove material of the bottom composition $\underline{x}_b$ from the batch while retaining equilibrium boiling conditions. But although the vector equations agree we do have problem of how to implement this in terms of equipment. We address this problem by using a rectifying batch apparatus where we add feed material of variable composition.

3.7 Equipment

3.7.1 Experimental concepts

If one considers the rectifying and stripping batch equations (3.4) and (3.11), one can see that the separation processes are linear combinations of the separation vectors and mixing vectors. The net separation processes vectors $\underline{\rho}_{rectifying-batch}$ and $\underline{\rho}_{strippingbatch}$ are defined as tangents to the respective column profiles at point $\underline{x}$.

Geometrically the equation $\frac{d\underline{x}}{\dot{v}dt/l} = \underline{\rho}_{rectifying-batch}$ means that the profile trajectory through the point $\underline{x}$ has a tangent that is collinear with the net vector $\underline{\rho}_{rectifying-batch}$ evaluated at this point.

We now ask under what conditions the two equations (equation 3.4 and equation 3.11) are equivalent:

To answer this question we need to find an appropriate mixing policy with the rectifying batch equation to keep the net distillation vector $\underline{\rho}_{rectifying-batch}$ at any time tangent to the profile defined by the stripping equation.

In Figure 3.3b, material of composition $\underline{x}_o$ on the stripping profile is boiled off and results in a vapour of composition $\underline{y}_o^*$ in equilibrium with $\underline{x}_o$. Material $\underline{y}_o^*$ lies on the tangent on the residue curve through $\underline{x}_o$. We consider that the vapour $\underline{y}_o^*$ is totally condensed and results in a liquid of composition $\underline{x}_o^* = \underline{y}_o^*$. The vector of points $\underline{x}_o$ and $\underline{x}_o^*$ represents the separation vector. The vector of points $\underline{x}_o^*$ nd $\underline{x}_b$ represents the direction of the mixing line. The next point $\underline{x}_1$ on the column profile is found by mixing back with material of composition $\underline{x}_d$ such that the vector of points

$\underline{x}_o$ and $\underline{x}_1$ is tangent to the column profile. A series of many similar steps yields a column profile beginning at point $\underline{x}_o$ and running towards the product $\underline{x}_b$. In this particular figure the mixing material $\underline{x}_d$ is located on a binary edge. But this is not a necessary condition as the mixing point can lie anywhere on the mixing line defined by the vector of points $\underline{x}_o^*$ and $\underline{x}_b$ Thus to get the same distillation vectors $\underline{\rho}_{rectifyingbatch} = \underline{\rho}_{stripping-batch}$ in magnitude and direction, we can set from equations 3.4 and 3.11 that:

$$\frac{\dot{b}}{\dot{v}}(\underline{x} - \underline{x}_b) = \frac{\dot{d}}{\dot{v}}(\underline{x}_d - \underline{x}) \qquad (3.13)$$

We must get both the magnitude and direction the same in order to satisfy equation (3.13):

a) *Magnitude*

In order for magnitudes to be the same we require:

$$\frac{\dot{b}}{\dot{v}}\frac{|\underline{x} - \underline{x}_b|}{|\underline{x}_d - \underline{x}|} = \frac{\dot{d}}{\dot{v}} \qquad (3.14)$$

We set $\frac{\dot{b}}{\dot{v}} = \frac{B}{V} = \frac{1}{s}$ in order for batch apparatus to behave as continuous stripping column.

Where s is the reboil ratio, B is the bottom product flow rate in the column, and V is the vapour flow rate in the column.

In equation (3.14) the quantity $\frac{\dot{b}}{\dot{v}} = \frac{1}{s}$ is assumed to be known and fixed whereas variables d and $\underline{x}_d$ are unknown quantities. Hence there are two independent equations but 3 unknowns for a ternary mixture ($\dot{d}$ and 2 components of vector $\underline{x}_d$). Hence there is one degree of freedom that has to be freely specified.

In the time interval when there is no feed addition $\dot{v} = \frac{-\partial l}{\partial t}$ in the batch apparatus, thus equation (3.14) becomes:

$$\frac{1}{s}\frac{|\underline{x} - \underline{x}_b|}{|\underline{x}_d - \underline{x}|} = \frac{\dot{d}}{\partial l / \partial t} \qquad (3.15)$$

We can determine $\frac{-\partial l}{\partial t}$ from the rate of change of level of the liquid in the batch apparatus and having chosen $\underline{x}_d$ we can calculate the flow rate $\dot{d}$ for a required reboil ratio s.

b) *Direction:*

The expression (3.15) implies that the three points $\underline{x}, \underline{x}_d, \underline{x}_b$ form a straight line.However there are two special choices of interest:

- The mixing material composition $\underline{x}_d$ is a binary mixture: this means that we freely set for a certain component $j : \underline{x}_d(j) = 0$ and equation (3.15) is used to determine $\dot{d}$ and the remaining elements of vector $\underline{x}_d$.
- One can specify $\frac{\dot{v}}{\dot{b}} = \frac{\dot{v}}{\dot{d}}$ and use equation (3.14) to determine the corresponding feed composition $\underline{x}_d$.

3.7.2 Experimental Equipment

The experimental apparatus (Figure 3.4) consists of a graduated still immersed in a water bath. The still contains boiling stones that serve as nucleation sites. The still is connected to a bubbler to maintain a constant pressure in the still. The exit gases from the bubbler are passed through a condenser. A magnetic stirrer is used to ensure effective mixing inside the still for a good approach to VLE. The water bath temperature is continuously changed to ensure that the liquid residue is kept boiling at reasonable rate. A HP 5840 Gas Chromatograph GC with a flame ionisation detector

is used for the analysis of the liquid samples. A personal computer interprets results from the GC using an in-house BET and a hyper plot data analysis packages. MATLAB software is used to compute a candidate starting composition $\underline{x}_{t=0}$. A sample with this composition is then prepared.

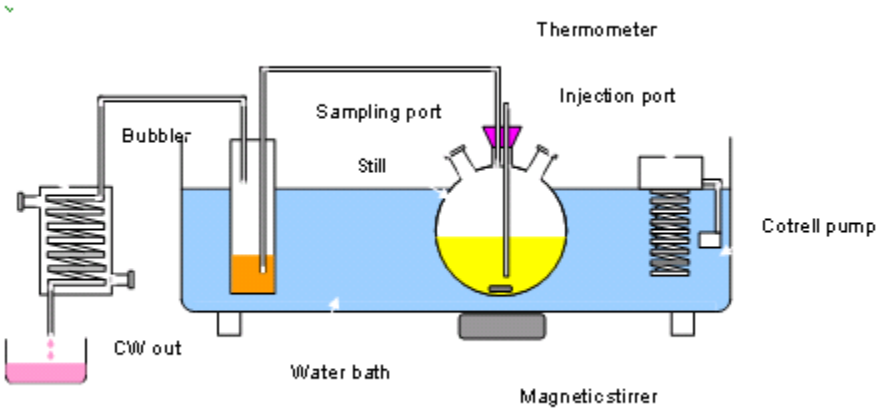


Figure 3.4: Experimental configurations

However the starting material composition does not need to be necessarily computed as it can be determined directly using graphical "insights" and boiling experiment. Let us suppose that one experimentally simulates a simple residue curve through an arbitrary point $\underline{x}_O$ (Chronis *et al. [13]*) and calls $\underline{x}_P$ the point of contact between this residue curve and the tangent to it through a given bottom product $\underline{x}_b$ (Figure 3.5). The point $\underline{x}_P$ is a pinch point. It may be seen that there is only one stripping

profile joining the points $\underline{x}_b$ and $\underline{x}_P$. One can measure the separation vector at the pinch point by a simple boiling exercise and using the fact that at this point $\frac{d\underline{x}}{d\xi} = 0 = \frac{s}{s+1}(\underline{y}_P^* - \underline{x}_P) + \frac{1}{s+1}(\underline{x}_b - \underline{x}_P)$, one can calculate the corresponding reboil ratio. One is now able to simulate experimentally the stripping profile through the product composition $\underline{x}_b$ by using initial material of composition $\underline{x}_P$ in the batch still and the calculated reboil ratio s. The exercise can be repeated for different residue curves to determine stripping profiles for different reboil ratio. However the point $\underline{x}_P$ is an unstable node and one should expect the experiment to be very unstable as for small deviations in compositions, one can simulates a completely different profile.

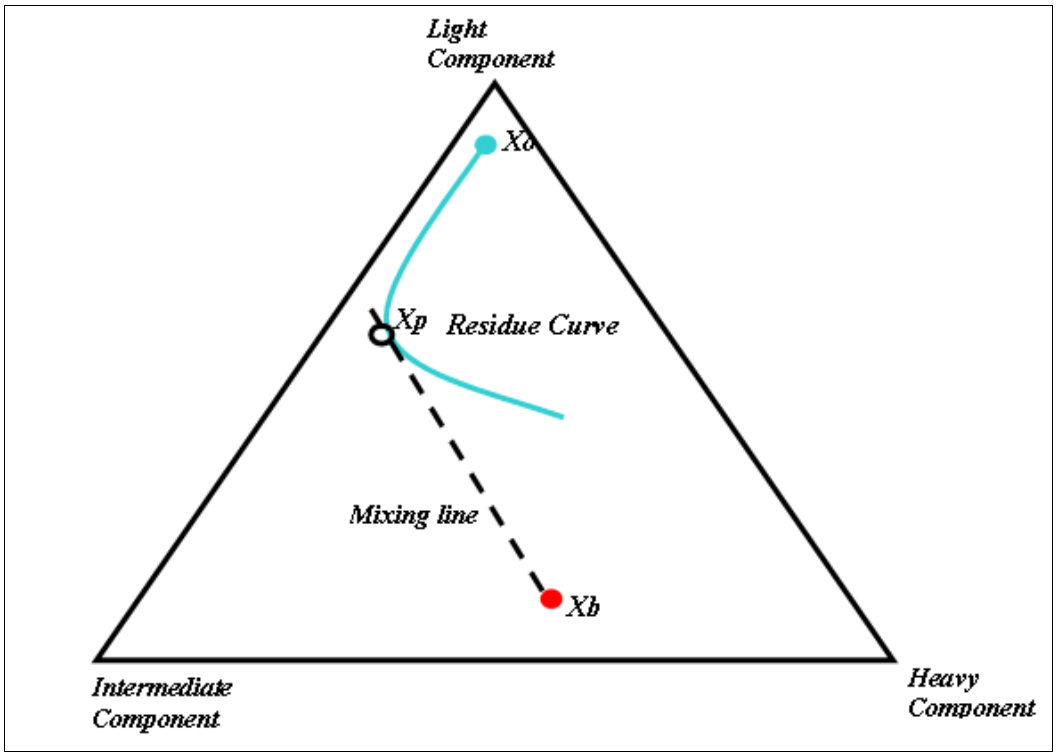


Figure 3.5: Experimental configurations

3.8 Results and Discussion

The methanol/ethanol/acetone system was studied. Results were compared for different reboil ratios. The experimental results were compared to the theoretical curves generated in MATLAB with thermodynamic data obtained from ASPEN PLUS and using the Wilson Model. Bottom compositions $\underline{x}_b$ were specified as: acetone 5 mol%, ethanol 80 mol% and methanol 15 mol % and acetone 0.45 mol%, ethanol 16 mol% and methanol 83.55 mol % respectively. The results for a reboil ratio s=2 and s=4 are presented. One can see that the experimental data points follow the theoretical curves well with a variance less than 3% (Figures 3.6, 3.7, 3.8)

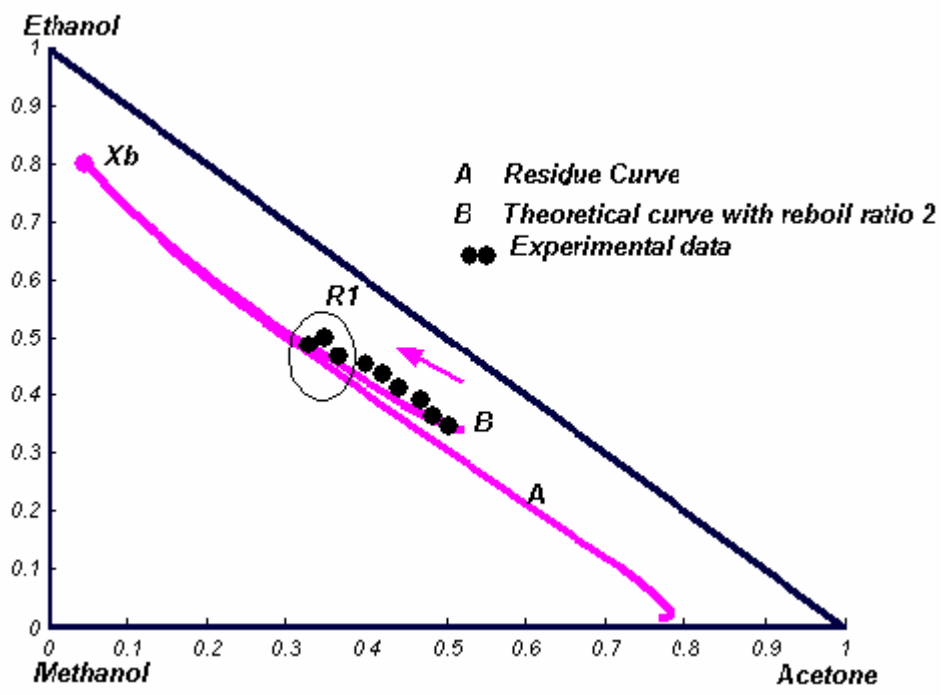


Figure 3.6: Column stripping profile for s=2

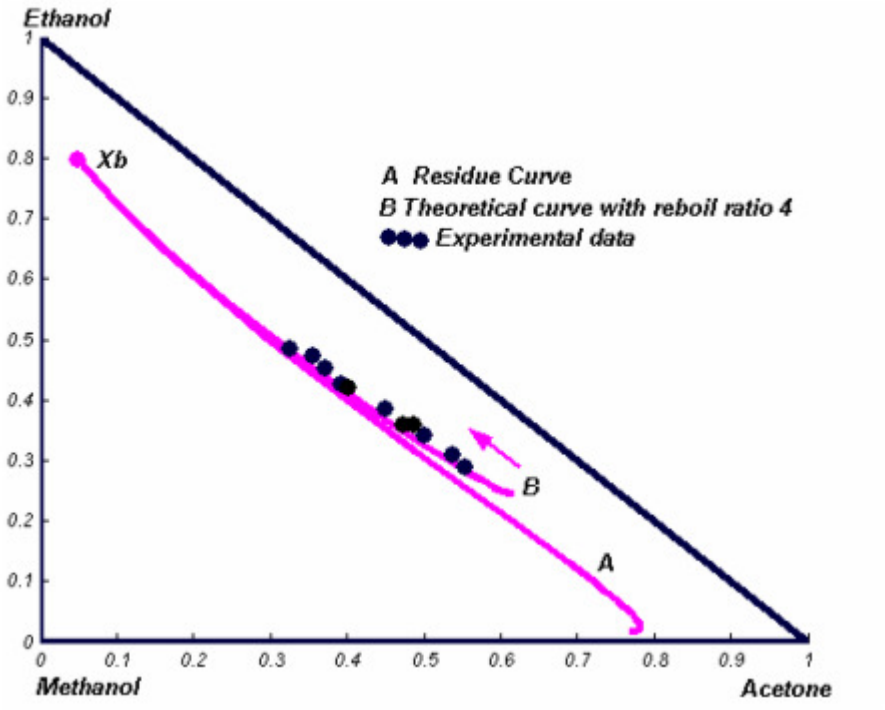


Figure 3.7: Column stripping profile for s=4

However one must consider that:

- The experiment needs to be aborted after a long run. This is because the feed material composition $\underline{x}_d$ moves far away from the composition $\underline{x}$ and the ratio $\frac{\dot{d}}{\dot{v}}$ becomes very small (Region R1 in Figure 3.6).
- Experimental points deviate from the theoretical curve if the time interval between feed material additions increases. In this case $\underline{x}_t$ is no longer close to $\underline{x}_{t+1}$ and the difference equation followed by the experiment is not a good approximation of the theoretical first-order differential equation.
- Deviation is observed in region of high curvature due to the local behavior of the separation and the mixing vectors (Region R2 in Figure 3.8).

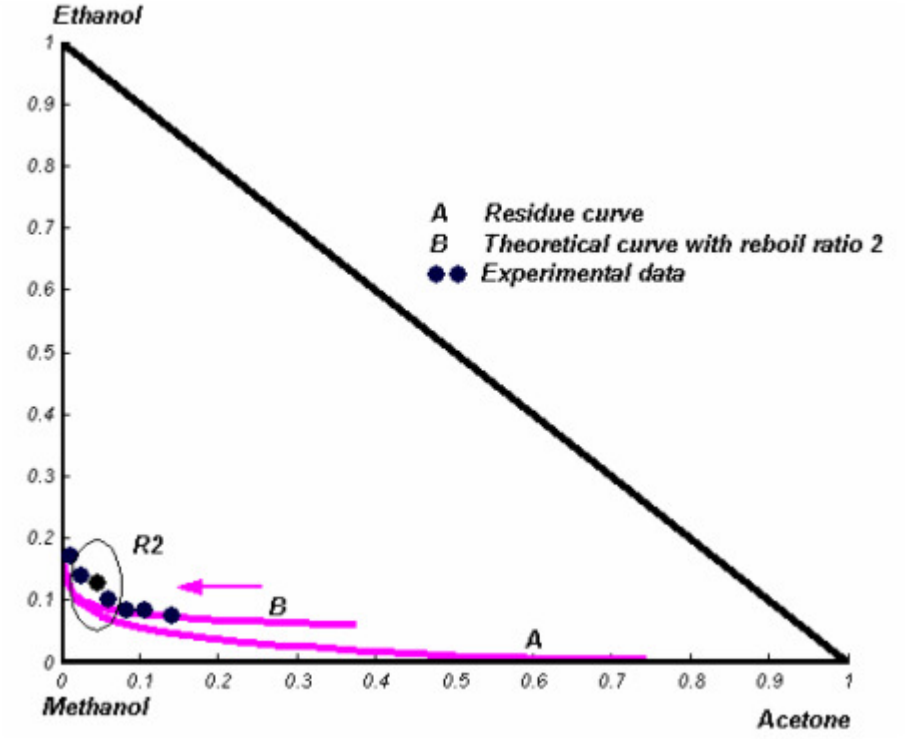


Figure 3.8: Column stripping profile in the region of high curvature

3.9 Applications

Usually when designing a distillation column, one sets the composition of the desired component in each product stream. For instance, one can set the compositions x_{B1} and x_{D1} of the heavy component 1 respectively in the bottom stream and in the distillate stream. We will show how one can use experimental simulation of column profiles to support distillation column design. Let us suppose that the vector of feed composition $\underline{x}_F$, the feed state q, the reboil ratio s and the product stream flow rates D and B are known assuming constant molar overflow. One can calculate the reflux ratio r and

using the overall component balance one can also calculate the distillate composition assuming that the light component in the bottoms is very small ($X_{B2} \approx 1 - X_{B1}$).Thus if one fills the batch still with material of distillate composition $\underline{x}_D$, one can experimentally simulates the rectifying column profile corresponding to the calculated reflux r. Let us suppose also that one ends the column profile measurement at the pinch point $\underline{x}_P$. From various points $\underline{x}_0$ close to the pinch point $\underline{x}_P$, one can use the method developed above and simulate experimentally stripping profiles until they intersect the desired bottom composition of component1.Stripping profiles that move away from the desired composition of 1 are infeasible profiles (Figure 3.9).

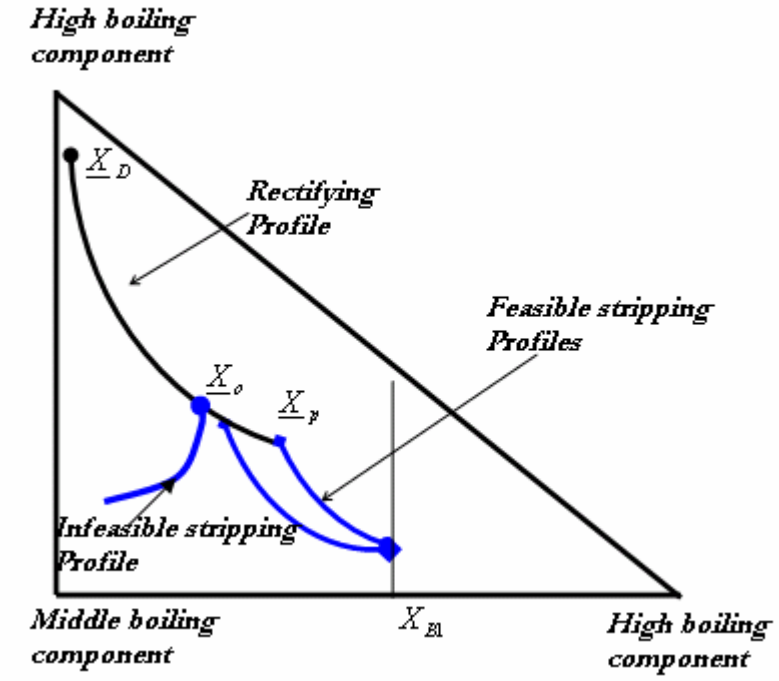


Figure 3.9: Experimental combination of stripping and rectifying profiles to emulate the entire distillation column

3.10 Conclusions

An experimental technique to support computer simulation of distillation column stripping profiles has been presented. The data generated could be used for preliminary design. Column profiles at different reboil ratios have been measured for the methanol/ethanol/acetone system and the experimental data points obtained follow the theoretical curves fairly well. The standard deviation error of concentration measurements in all case is less than 0.03, which is within the G.C error. More importantly, we have validated experimentally the concept that mixing and separation are opposite vectors phenomena [2].

Bibliography

1: Tapp,M.,Glasser,D.,Hildebrandt,D., "Experimental simulation of distillation column concentration profiles using batch apparatus" Chemical Engineering Science,2003,58, pp 479-486

2: Hauan,S.,"On the behaviour of reactive distillation systems" PhD Thesis, Norvwegian University of Science and Technology, Trondheim, 1998

3: Doherty,M.F.,Malone,J.D.,"Conceptual design of distillation systems", 2001,McGraw Hill,New York

4: Doherty,M.F.,Perkins,J.D., " On the Dynamics of distillation processes-I, the simple distillation of multicomponent non-reacting homogeneous liquid mixtures",Chemical Engineering Science, 1978,33,pp 281-301

5: Doherty,M.F.,Perkins,J.D., "On the dynamics of distillation processes-II, The Simple Distillation of Model Solutions",Chemical Engineering Science, 1978,33,pp 569-578

6: Schreinemakers,F.A.H.,, "Einege bemerkungen uber dampfdrucke Ternarer gemische", Z.Phys.Chem,1902,43,pp671-685

7: Wahnschafft,O.M.,Koelher,j.w.,Blass,A.,Westerberg,A.W.,, "The product of composition regions of single feed azeotropic distillation", Industrial and Engineering Chemistry Research,1992,pp 2345-2362

8: Fien,G.,Liu,Y.,, "Heuristic synthesis and shortcut design of separation processes using Residue Curve Maps", Industrial and Engineering Chemistry Research,1994,33,pp364-374

9: Van Dongen,D.B.,Doherty,M.F. "Design and synthesis of homogneous azeotropic distillations 1.Problem Formulation for a single column", Ind.Eng.Chem.Fundam,1985,24,pp 454-463

10:Tapp,M.,Holland,S.T.,Glasser,D.,Hildebrandt,D.,"Column Profile Maps Part A: Derivation and interpretation", Industrial and Engineering Chemistry Research,2004,43,pp 364-374

11: Castillo,F.,Thong,D., "Homogeneous azeotropic distillation I.Design procedure for single-feed columns at non total reflux", Industrial and Enginering Chemistry Research,1998,37,pp 987-997

12: Kiva,V.N.,Hilmen.E.K.,Skogestad,S., "Azeotropic Phase Equilibrium Diagrams:a Survey", Chemical Engineering Science,2003,58,pp 1903-1953

13: Chronis,T.,Glasser,D.,Hildebrandt,D., "A simple, reasonable accurate method for measuring Residue Curves and the associated VLE", In R.Dayton(Ed.),Distillation Absorption1997, Ind.Chem.Eng.,1,pp 187-196

4 Chapter 4 RRCM Topology: Zero Order Chemical Reaction

Preliminary versions of this chapter presented at the AIChE Annual Meeting 2004, , Austin, Texas, USA and the World Congress of Chemical Engineering, 2005, UK under the title: topological analysis of simple distillation accompanied by single chemical reaction. This paper is currently submitted to the chemical engineering journal and is under review

4.1 Abstract

A batch reactive distillation process can be described as a linear combination of the separation and reaction vector fields. The resulting vector field, for a reactive distillation batch process, is described by a Reactive Residue Curve Map (RRCM). We use the concept of "Moving Triangles" [1] to explain the behaviour resulting from the combination of the separation and reaction vector fields. The analysis is illustrated for a constant relativity system with zero order reaction. We conclude that a zero order reaction vector field does not introduce new singularities to the reactive residue curve map. However the reaction moves the existing singularities of the residue curve map in the composition space. By changing the stoichiometric vector direction, behaviour that previously was outside the Mass Balance Triangle can be shifted inside the Mass Balance Triangle and separation previously considered as non-attainable can be achieved [2].

4.2 Introduction

Combining distillation and reaction in a single unit is aimed at developing a cost effective process. The main goal is to establish whether a desired set of products can be achieved by using a combination of these two processes. In the last two decades, much research has been devoted to this problem and some effective techniques for design and modelling have emerged as key steps in the development of reactive distillation. Many of these techniques are computer oriented such as the equilibrium and non equilibrium simulation stage models [3] or the mixed integer non linear programming model (MINLP) to determine the optimum number of equilibrium stages, feed tray location and reflux by combining tray-by-tray model, kinetics rate based expressions and cost estimation [4] or the mixed integer non linear-bilevel method to design reactive distillation columns by minimizing the Gibbs free energy on each tray and the total annualised cost [5]. These techniques use commercial simulation packages and numerical optimization techniques. These methods may be quite effective but they do not always allow the user to obtain insights into the solutions.

Residue curve map for feasibility analysis of reactive distillation has been also considered under the assumptions of chemical equilibrium and using the transformed mole fractions [6][7]. Using this novel composition transformation, they were able to transform the equation of a staged reactive distillation column into a common equation of non-reactive distillation column, allowing the use of "traditional" shortcut design techniques. They were also able to observe that reactive azeotropes can occur even for ideal mixtures and that non-reactive azeotropes can disappear when chemical reaction is combined with distillation.

Okasinski et al [8] further investigated the influence of the chemical equilibrium constants on the existence and location of reactive azeotropes. Venimadhavan et al.[9] considered the use of residue curves in the case of kinetically controlled reactions. For

a particular heating control policy on a given reactive batch still, they were able to derive an autonomous differential equation describing the evolution of the composition in the batch apparatus. They showed that this differential equation was a function of the Damkholer number Da. They further carried out a singularity analysis using the Damkholer number as the bifurcation parameter and were able to show the effect of Da on the trajectory of the residues curves:

1. For Da =0, the residue curve profiles end at the stable node (pure component or non reactive azeotrope).
2. For Da=∞, the residue curve profiles end at a stable node (pure component or reactive azeotrope).

Thiel et al.[10] investigated residue curves for heterogeneously catalyzed reactive distillation and showed that the location of singular points in the residue curve map is a function of the Damkholer number and the operating pressure.

Hoffmaster et al.[11] give a powerful analysis of the qualitative effect of reaction distribution on the behaviours of distillation column sectional profiles using well-known techniques for non-reactive distillation. They were able to show how chemical reactions affect column profiles inside a distillation column and they provide also a stability analysis to predict pinch points for reactive profiles.

Recently Tapp et al.[1] extended the concept of the residue curve to the entire composition space (positive and negative space). They were able to show that the mathematics of the differential equation describing the non reactive residue curve is not bound by any physically relevant initial conditions and that it is possible to evaluate this differential equation for any initial values inside or outside the MBT. In this case one is able to fill not only the realistic composition space but also the entire space surrounding the MBT with residue curves. An example of such a map will be shown and discussed later in this paper. The extended ideal residue curve map for a 3-component system with either ideal thermodynamics or constant relative volatility has only three singularities: a stable node, an unstable node and a saddle point. We

refer the reader to the work by Doherty et al.[12][13][14] for more details on singular points in ideal multi-component mixtures. Tapp et al.[1] further showed that the extended residue curves map could be divided into different regions. These regions represent sub-spaces of profiles solution with the same topological behaviour.
Tapp et al.[1] extended this concept to the simultaneous combination of separation and mixing as is found in a Column Section. They were able to show that by adding a mixing term $\phi(\underline{x}_d - \underline{x})$ to the separation vector, where ϕ is a scaling factor and $\underline{x}_d$ is the composition of the product from the Column Section, one is able to move singularities of the Residue Curve Map (RCM) in the composition space. By integrating the net distillation differential equation for common values of ϕ and $\underline{x}_d$ but different initial conditions, they showed that one obtained a map called Column Profile Map (CPM) that was a simple transform of the residue curves map. Thus although the behaviour of a section of a distillation column can appear quite complex, when viewed in this way, the behaviour can be seen as a result of different parts of the residue curve map moving in and out of the MBT. The important result from this is that if certain behaviour is required, it allows the designer to choose the parameters that can be used to achieve this behaviour. It also allows for quick scanning of the map so that the designer can identify any potential unstable behaviour.
In this chapter, we extend these ideas to reactive distillation systems. We identify that the processes occurring in batch reactive distillation systems are separation and reaction. We show that these systems can be modelled as a simple linear combination of the two individual vector fields, namely the separation vector field and the reaction vector field. We define a reactive residue curve in an analogous manner to that used for separation processes, namely that a reactive residue curve is the trajectory traced out by the liquid composition in a batch reactive distillation still. The resultant residue curve map has singular points and the movement of these singular points leads to an understanding of the effect of reaction on the feasible products. Surprisingly the most important factor is not the kinetics of the reaction (speed and order of the reaction)

but, as also outlined by [2] the direction of the stoichiometric vector. We then show that there are three main types of reactive residue curve maps, and relate them to the direction of the stoichiometric vector. This leads to a very powerful process synthesis tools in that one is in a position to sketch the qualitative behaviour of the reactive residue curve map for a given reaction, and thus for a given stoichiometric vector. One is thus able to easily sketch the reactive residue curve and decide qualitatively on types of control policies to achieve the optimal profiles for the envisaged reactive separation process. In this chapter we demonstrate the idea for the zero order kinetics and ideal ternary component mixture.

4.3 Simple Batch Reactive Distillation

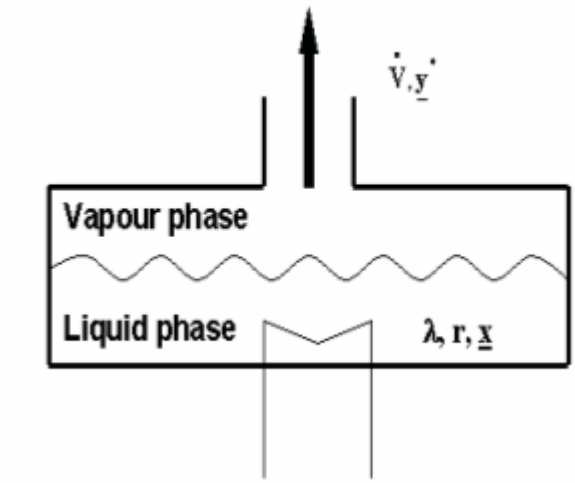


Figure 4.1: Schematic of simple distillation with chemical reaction

Let us consider a simple boiling unit as shown in Figure 4.1 where the vapour is being drawn off at a rate $\dot{V}$ and the composition of the vapour, $\underline{y^*} = (y_1^*, y_2^*, \ldots y_n^*)$, is in equilibrium with the liquid residue of composition $\underline{x^*} = (x_1^*, x_2^*, \ldots x_n^*)$ in the still. Heat is supplied to the still to maintain boiling. The amount of liquid in the still is λ and changes with time. In addition a simple chemical reaction takes place in the still and the reaction is described by the stoichiometry and reaction rate. The following assumptions are made:

- There is a single chemical reaction occurring and this proceeds in the liquid phase only
- The liquid in the still is homogeneous.
- The molar density of the mixture is constant.
- Reaction rate constants for the purpose of simplicity are temperature independent. This constraint however can be relaxed.
- Constant relative volatility. Again this assumption is made to simplify the analysis and this constraint can be relaxed.

4.3.1 Simultaneous Reaction and Separation: Mathematical Preliminaries

Consider a reaction described by $\sum_{i=1}^{n} \nu_i A_i = 0$, where A_i are the species and υ_i the stoichiometric coefficients. The rate of reaction is described by r and the mole fraction of species A_i in the liquid is x_i, n is the number of components and υ_i is the stoichiometric coefficient of component i. If $\upsilon_i < 0$, component i is a reactant while if $\upsilon_i > 0$, component i is a product. $\upsilon_T = \sum \upsilon_i$ and represents the total molar change of the chemical reaction. The vector equation describing the process is given by:

$$\frac{d\underline{x}}{d\xi} = (\underline{x} - \underline{y}^*) + (\underline{\upsilon} - \underline{x}\upsilon_T)\frac{r}{\rho}\frac{\lambda}{\dot{V}} \qquad (4.1)$$

Where $\dot{V}$ is the molar flow rate of escaping vapour, λ is the molar liquid hold-up in the still, ρ is the molar density , ξ is a non-linear transformation of the real time with $\frac{\dot{V}dt}{\lambda} = d\xi$. The vector $\underline{\upsilon^*} = (\upsilon_1^*, \upsilon_2^*, ...\upsilon_n^*)$ defines the stoichiometry of the reaction.

4.3.2 Special case for the total number of moles is conserved in the chemical reaction, i.e. $v_T = 0$

In this case $v_T = 0$ and equation (4.1) reduces to:

$$\frac{d\underline{x}}{d\xi} = (\underline{x} - \underline{y}^*) + \alpha.\underline{v} \qquad (4.2)$$

Where $\alpha = \frac{r}{\rho}\frac{\lambda}{\dot{V}}$

We also note that this simplification is not as restrictive as it first appears. In cases where the moles are not conserved in the reaction, the equation could be written in terms of mass fractions rather than mole fractions and the resulting equation would look very similar to that of equation 4.2 above. The ideas and theory outlined in this chapter would still apply, although the plots would be in mass fraction space rather than mole fraction space. We have made this simplification so that we can work in the mole fraction space, which is more familiar as it is used in residue curve maps.
We note that on relooking at equation 4.2, that the right hand side of the equation is the sum of two vector fields, namely the separation vector $\underline{S(x)} = (\underline{x} - \underline{y}^*)$ and the reaction or stoichiometric vector $\underline{\upsilon}$. We further note that we can write the right hand side as a linear combination of the two vector fields, that is:

$$\frac{d\underline{x}}{d\xi} = \underline{S}(\underline{x}) + \alpha\underline{\upsilon} \qquad (4.3)$$

4.3.3 Simplification for zero order kinetics

For the special case of zero order kinetics, the term $r = k_o$ is a constant and does not depend on $\underline{x}$. We are also assuming that the rate constant k_o is not a strong function of temperature or the temperature range in the experiment is small. If in addition the vapour is removed at a rate such that $\frac{\lambda}{\dot{V}}$ is constant, the term α in equation 4.3 is a constant. In this case α is a scalar and hence affects only the magnitude of the second term and not the direction of the reaction vector.

Again these simplifications are made to understand the basic concept of reactive distillation being a linear combination of two vector fields. If the zero order assumption is lifted, then the resulting vector describing the reactive distillation process is still a linear combination of the two vector fields. The scalar term however would vary with the value of $\underline{x}$. As it will be shown in this chapter, the fundamental topology of the reactive residue curve is dependent on the topology of the vector fields. The term α affects the position of the singular points in the map but not the type of singular point that one would find. Hence this assumption is used to simplify the analysis at this stage but is not necessary and the resulting theory still applies when it is lifted.

By using a constant α policy, the batch reactive distillation process undergoes autonomous dynamic behaviour. One can see that the parameter α is equivalent to the Damkholer number , which is the ratio of the characteristic reaction rate to the characteristic escaping total flux as $\alpha = \frac{k_0}{\rho}\frac{\lambda}{\dot{V}}$. This parameter can be used for the characterization of reaction kinetics effect [15].

It should be noted that the term $\alpha\underline{\upsilon}$ is collinear to the stoichiometric or reaction vector $\underline{\upsilon}$ and that the value of α affects the magnitude of this term but not the direction. The implication of this will be discussed later in this paper.

Thus in summary, the change in composition $\underline{x}$ during a reactive distillation process is described by a linear combination of a separation vector $\underline{S} = (\underline{x} - \underline{y}^*)$ and the reaction or stoichiometric vector $\underline{\upsilon}$. We will consider each of the vector fields in turn and in particular the topology of the fields.

4.3.4 The Separation Vector Field (Residue Curve Map)

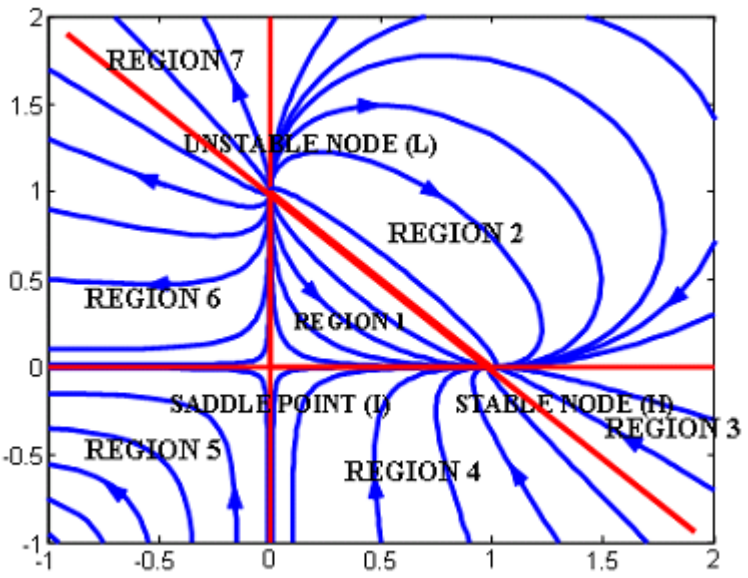


Figure 4.2: Schematic of the residue curve map extended to the negative space for constant relativity system.

The separation vector field $\underline{S}$ can be represented by the residue curve map. These maps have been well studied by many researchers, including [12][13][14].
Tapp *et al.*, [1] extended the residue curve map outside the composition subspace. An example of a residue curve map for a constant relative volatility system is given in Figure 4.2 above.
For the purpose of illustration we consider a ternary system, where L refers to the lowest boiling component, H to the highest boiling component and subscript I to the intermediate component. We note that there are 7 regions indicated in Figure 4.2. In each region the curves begin at the same node or end at the same node. In addition the curves leave or enter the nodes along the direction of the same eigenvector.
In the remainder of the paper we will use the separation vector field and therefore the residue curve map described in Figure 4.2 above. Again the theory described in this paper applies generally and the constraint of constant relative volatility can be lifted.

4.3.5 The Reaction Vector Field

The reaction vector field $\underline{v}$ is represented by reaction trajectories that are straight lines [2].
If the zero order constraint is lifted, this would not change the direction of the vectors. Lifting this constraint would however change the magnitude of the reaction vectors. If the reaction was made reversible for example, this would introduce stationary points into the reaction vector map. These would usually not be isolated but be a line or curve of stationary points. In this case the direction of the arrows would swap around at the stationary point [2].

4.4 The RRCM for Zero Order kinetics

Mathematically the differential equation (equation 4.2) can be integrated in the entire (x_1,x_2) space, where x_3=1-x_1-x_2, for different initial conditions (in the negative or positive space) and fixed values of parameters α and $\underline{\upsilon}$ to generate the Reactive Residue Curve Map (RRCM). Such a map is shown in Figure 4.3. The MBT, that is the region where the mole fractions of all the components are positive, is marked as the blue lines that make up the triangle. The trajectories are drawn in light red lines. We will discuss various points that become apparent on examining Figure 4. 3.

4.4.1 Singular points of the map

The analysis of equation 4.2 reveals that none of the pure component vertices are singular points. In fact the vectors $\underline{x}$= [1, 0], $\underline{x}$= [0, 1] and $\underline{x}$= [0, 0] do not make the right-hand side of the differential equation (4.2) equal to zero. Consequently for constant relativity systems, the edges of the MBT are transformed but maintain their straightness to form a transformed triangle. Thus the lines in Figure 4.3 given in black, which join the singular points in the reactive residue curve map, remain straight lines. In more complex thermodynamics, these lines become curved [1].
It can be seen that there are two singular points in the MBT, namely a saddle point node (point A) and a stable node (point B). The movement of these two singular points into the MBT, with the unstable node moving out of the space, results in the topology that we see in Figure 4.3. The movement of the singular points in and out of the MBT is very important as this determines the topology of the portion of the reactive residue curve map in the MBT.

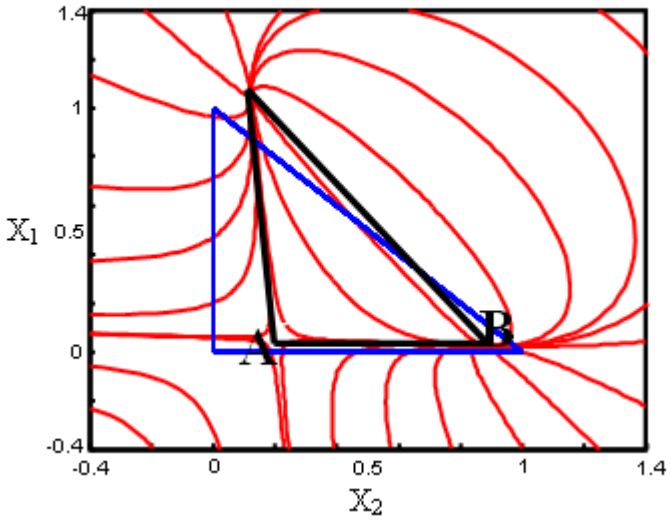


Figure 4.3: The reactive residue curve map for zero order kinetics

We also note that the black lines, namely the lines from the transformed MBT, act as boundaries and divide the space into various regions. We see that if we start reactive residue curves from neighbouring points to point A on Figure 4.3, the curves could move in very different directions. Thus the region around this boundary exhibits bifurcations and a system with an initial point in this region would appear to be unstable. The region around the saddle point would also show complex behaviour as can be seen from Figure 4.3. Thus by understanding how the singular points move and in particular which singular points move into the MBT one can predict the behaviour of the Reactive Residue Curve Map (RRCM).

In summary, the map shown in Figure 4.3 is the Reactive Residue Curve Map (RRCM). A RRCM is then a transform of the Residue Curve Map (RCM) presented in Figure 4.2. All the singularities of the RCM are present but have been shifted in the

composition space. All 3 singular points are still present, although not all of the singular points lie in the MBT

4.4.2 An Interesting Analogy

Consider two Columns Sections that are joined in parallel as shown in Figure 4.4. The two Column Sections share a condenser and hence have the same liquid composition flowing into the two Column Sections. The Column Sections also share a reboiler, so that the vapour entering the Column Sections at the bottom also has the same concentration.

The mathematical modelling of the above-coupled system has been done at the infinite reflux case [16], i.e. $V_1 = L_1$ and $V_2 = L_2$. If the liquid composition $\underline{X}_T$ entering the top of the column 1 or 2 is not equal to the vapour composition $\underline{Y}_T$ leaving the top of that column, the equation describing the liquid composition in the columns becomes:

$$\frac{d\underline{x}}{d\xi} = (\underline{x} - \underline{y}^*) + \underline{X}_\Delta = \underline{S} + \underline{X}_\Delta \quad \text{(LHS column)} \qquad (4a)$$

and

$$\frac{d\underline{x}}{d\xi} = (\underline{x} - \underline{y}^*) - \underline{X}_\Delta = \underline{S} \quad -\underline{X}_\Delta \qquad \text{(RHS column)} \qquad (4b)$$

Where the term has been referred to as the difference vector and

$$\sum X_{\Delta,i} = \sum (Y_i^T - X_i^T) = \sum Y_i^T - \sum X_i^T = 0 \qquad (4c)$$

Equations (4.4a and 4.4b) describe the infinite reflux coupled Column section configuration shown in Figure 4. Holland *et al*. [16] found that the behaviour of the Column Sections profiles depended on the vector $\underline{X}_\Delta$. They showed that there were 6

different regions of the difference vector $\underline{X}_\Delta$ corresponding to 6 different qualitative topologies of the Column Profile Map. It can be shown that in order for equation (4.4c) to be satisfied, not all the components in the Column Section move in the same direction, and hence the requirement that $\sum X_{\Delta i} = 0$ can be met.

We can see that for the case where $\upsilon_T = \sum \upsilon_i$, equations (4.2) and (4.4a) or (4.4b) have the same form. This leads to an interesting analogy. We can consider the set of possible composition profiles of a Column Section in the system as shown in Figure 4.4 for a given $\underline{X}_\Delta$ but varying initial concentrations. We call this set of profiles the Column Profile Map. We can also consider the RRCM for a system where $\alpha \underline{\upsilon} = \underline{X}_\Delta$. We can see that because of the identical mathematics between equation (4.4) for the column and equation (4.2) for the batch reactive distillation still, the two maps would be identical. *Thus we would find that the Column Profile Map is identical to the RRCM, even though the processes or equipment that equation (4.2) and (4.4a) are describing appear to be very different phenomena and unit operations.*

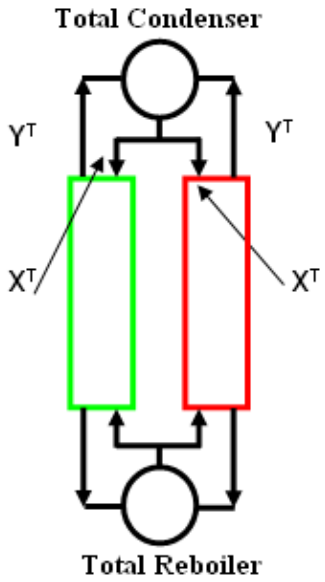


Figure 4.4: Infinite reflux coupled column section configuration

This arises from the fact that the equipment can be described by a linear combination of vector fields. The Column Profile is a described as a linear combination of a separation vector field $\underline{S}$ and a vector field described by the difference vector $\underline{X}_{\Delta}$. The batch reactive distillation still on the other hand is described by a linear combination of the separation vector field $\underline{S}$ and a reaction vector map, which we can consider to be $\alpha\underline{v}$ in this case. When the reaction vector field is the same as the difference vector field, we can see that the vector field resulting from the linear combination must be the same. Hence the interesting and perhaps surprising result is that the two maps are identical.This is the strength of the vector approach in that the analysis of the vector fields allows insights and interpretations that may be more difficult to come by from other approaches.

4.4.3 The Effect of the Stoichiometric Vector on the Topology of the RRCM

We can extend the results of Holland *et al.* [16] and say that, for a ternary system where all the 3 components, namely the heavy H, the light L and the intermediate I, are involved in a zero order single chemical reaction, one can relate the type of chemical reactions and the topology of the RRCM.

In Figure 4.5, we use a spatial representation of all possible variants of stoichiometric vector as introduced by Hauan *et al [2]*. We define a system of three axes. Each axis divides the space into sub-regions of opposite signs with regard to the stoichiometric coefficient of the component represented by that particular axis. Let us call $\underline{\upsilon} = (\upsilon_1, \upsilon_2, ...\upsilon_n)$ and $\underline{\upsilon^*} = (\upsilon_1^*, \upsilon_2^*, ...\upsilon_n^*)$ two stoichiometric vectors. We say that the two vectors belong to the same stoichiometric region if their respective stoichiometric coefficients all have the same sign. When one of the components changes the sign, we move into a different stoichiometric region. Using this approach and for a ternary mixture where all the 3 components are involved in a chemical reaction, we find six different regions of the stoichiometric vectors. In Figure 4.5, one can see that if one considers all three components, there are 6 sub-regions corresponding to 6 different sets of stoichiometric vector. In each region, i.e. region I^+, each component will have a defined sign. The combination of signs for all the three components gives an indication on the type of the single chemical reaction occurring in this region.

The stoichiometric vector (+1, +1, -2) lies in region I^+, and this stoichiometric vector corresponds to the reaction $2I \rightarrow H+L$. Similarly the stoichiometric vector (-1, -1, +2) lies in region I^-, and this stoichiometric vector corresponds to the reaction $H+L \rightarrow 2I$. We call the space represented in Figure 4.5, the space of stoichiometric sub-regions (SSR). This representation is a powerful concept. It addresses two concerns:

1. The diagram allows one to determine the number of possible regions for the stoichiometric vector for a defined number of reacting components.

2. The diagram allows one to interpret the stoichiometric vector in terms of an actual chemical reaction stoichiometry (Table 1)

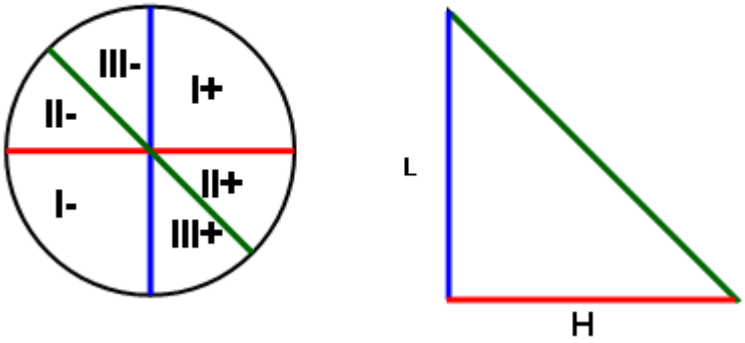


Figure 4.5: Representation of regions of the stoichiometric vector characterizing the RRCM behavior and corresponding component axes

This allows for easy classification of the behaviour of reactive batch separation when using the stoichiometric vector as the variable parameter. A similar map can be derived for multicomponent mixtures.

Direction	*Reaction*
Region I+	*2I→L+H*
Region I-	*L+H→2I*
Region II+	*L+I→2H*
Region II-	*2H→L+I*
Region III+	*2L→I+H*
Region III-	*I+H→2L*

Table 1: Summary of reactions occurring in each of the 6 defining regions

RRCM produced with stoichiometric vectors in different SSR's are qualitatively different. Because of this, a particular direction of a stoichiometric vector may offer advantages or disadvantages for a reactive separation process. This will be examined in more detail below.

4.4.4 Stoichiometric vectors in regions I^+ and I^-

Reactions with stoichiometry 2I → L+H or L+H → 2I would be reactions that have stoichiometric vectors $\underline{v}$= *(1, 1, -2)* or $\underline{\boldsymbol{v}}$= *(-1, -1, 2).* These vectors lie in Region I^+ or I^- respectively.The RRCMs for these two cases are shown in Figure 4.6 and 4.7 respectively. For stoichiometric vectors lying in region I^+ or I^-, we can see that all singular points (unstable node, stable node, saddle point) move outside the MBT. *This is very interesting behaviour as it implies that there are no singular points in the mass balance space, i.e. in the region of positive mole fractions.*

Let us consider what this means from the experimental point of view: as the experiment proceeded, the still would get richer in some components, poorer in others but as time increased the contents of the still would not reach a steady state, no matter

what the initial starting composition was. This behaviour is somewhat counterintuitive and we do not fully understand the implications.

One can also see from Figure 4.6, that there are three different regions, namely region 1, region 4 and region 2, of the original RCM as described in Figure 4.2 that have been moved inside the MBT. This means that for a stoichiometric vector in region I^+, a region of bifurcation near the light-intermediate axis is moved into the MBT. Thus the liquid composition in the still would be very sensitive to initial conditions in this region. Conversely, it can be seen that for a stoichiometric vector in region I^-, a line of bifurcation is moved into the MBT near the intermediate-heavy axis. However all the profiles move towards the stable node and so these profiles are not sensitive to the initial condition.

This shifting of singularities of the RCM in and out of the MBT can be used to introduce desirable behavior into the MBT. For example in both Figures 4.6 and 4.7 there are profiles that move into the intermediate corner. Hence the intermediate component, which was an unstable node in the RCM, now has profiles moving directly into it. One might therefore be able to produce pure intermediate by using a profile that runs into the intermediate corner.

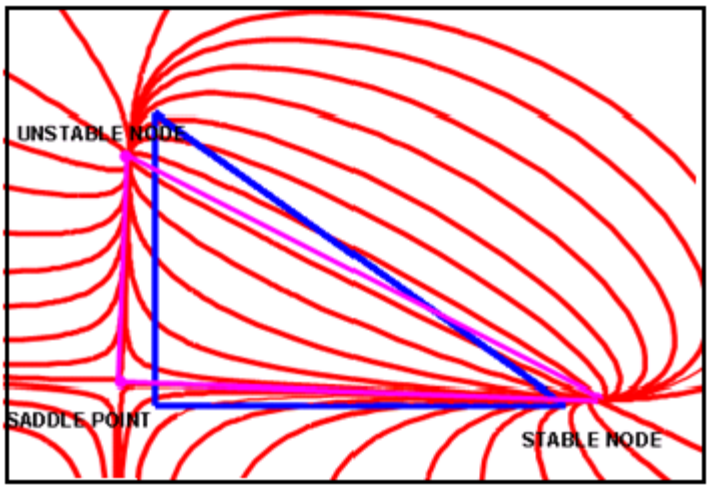


Figure 4.6: RRCM for stoichiometric vector in Region I+

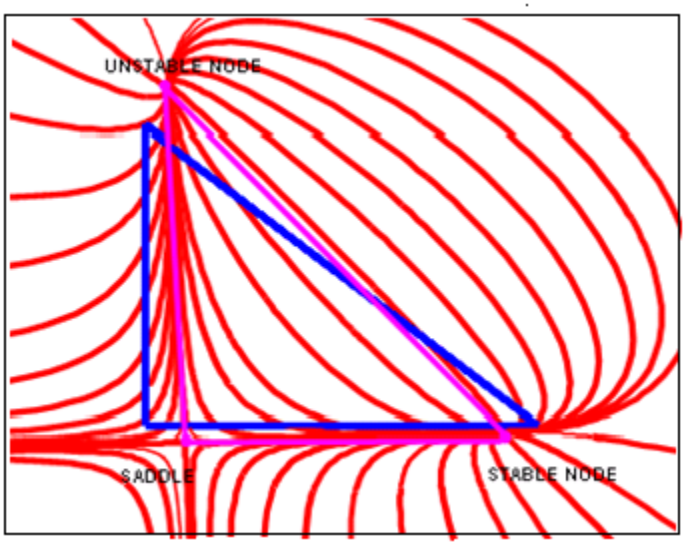


Figure 4.7: RRCM for stoichiometric vector in Region I-

4.4.5 Stoichiometric vectors in regions II^+ and II^-

Reactions with stoichiometry L+I→2H or 2H→ I+L would be reactions that have stoichiometric vectors $\underline{\upsilon} = (2, -1, -1)$ or $\underline{\upsilon} = (-2, 1, 1)$. These vectors lie in Region II^+ or II^-.The RRCMs for these two stoichiometric vectors are shown in Figure 4.8 and 4.9. For stoichiometric vectors lying in region II^+, we can see that two of the singular points (the unstable node and saddle point) move inside the MBT, while the stable node moves outside the MBT (Figure 4.7a). Doherty and co-workers [6][7] referred to these nodes as Reactive Azeotropes. One of the implications of the above map is that if one starts the batch experiment with initial mixture compositions in the unstable region A, one might end up at completely different points. Reactive batch operating near region A would be very sensitive to initial conditions in the still. Furthermore, because of the unstable node moving into the region, the behavior of the

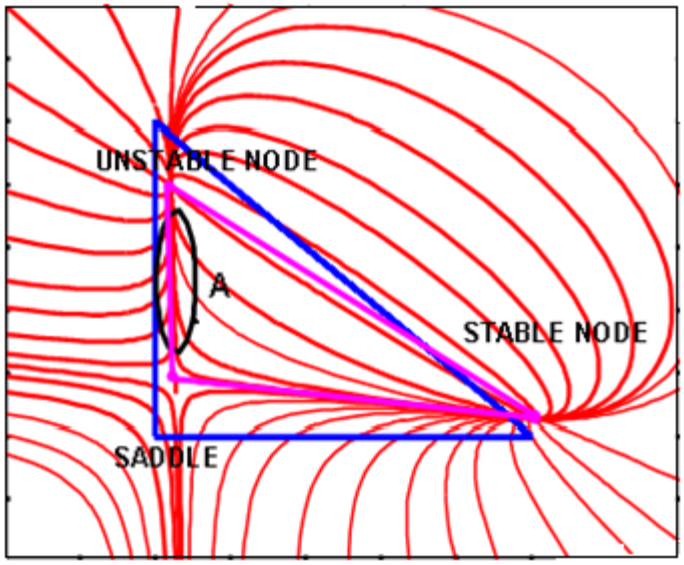


Figure 4.8: stoichiometric vector in Region II+

still would be unstable at, or in the vicinity, of this node.

For stoichiometric vectors lying in region II-, all of the singular points (stable node, unstable node, and saddle point) move outside the MBT (Figure 4.9). However the behaviour that remains in the MBT is not the same as in the case seen for regions I+ and I-. In this case, no bifurcation lines are moved into the mass balance space and thus there are no instabilities with respect to initial concentration in the profiles. Furthermore, according to the classification of Doherty and co-workers, no reactive azeotropes would exist in this system.

4.4.6 Stoichiometric vectors in regions III^+ and III^-

An example of a reaction with a stoichiometric vector that lies in region III^+ is the reaction 2L→I+H which is described by the stoichiometric vector $\underline{\boldsymbol{\nu}}$= *(1, -2, 1)*.

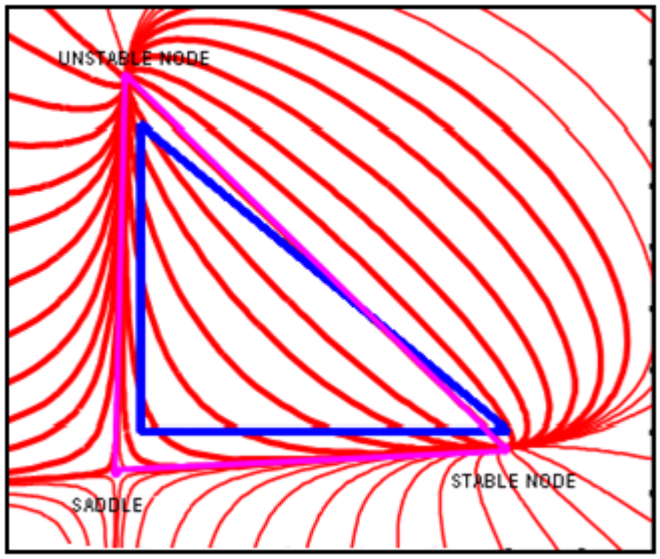


Figure 4.9: stoichiometric vector in Region II-

Similarly the reaction I+H→ 2L is described by the stoichiometric vector $\underline{\nu}$= *(-1, 2,*

-*1)* which lies in region III$^-$. The RRCMs for these two cases are shown in Figures 4.10 and 4.11. For stoichiometric vectors lying in region III$^+$, we can see from Figure 4.10 that again two of the singular points move inside the MBT. However in this case, the stable node and the saddle point move into the space while the unstable node moves outside the MBT. Thus a line of bifurcation is introduced in the region near the light-intermediate axis. However as the stable node is moved into the space, all the profiles starting on the left hand side of the bifurcation line all end at the stable node. Thus experimentally one would see that there is a well-defined singular point, which corresponds to what our intuition would lead us to believe. We can thus see in this case that we have both a stable and saddle reactive azeotrope in the space. For stoichiometric vectors lying in region III$^-$, we can see that all of the singular points (stable node, unstable node and saddle point) move outside the MBT (Figure 4.11). This means that there are no regions of bifurcation in the MBT and there are also no singular points.

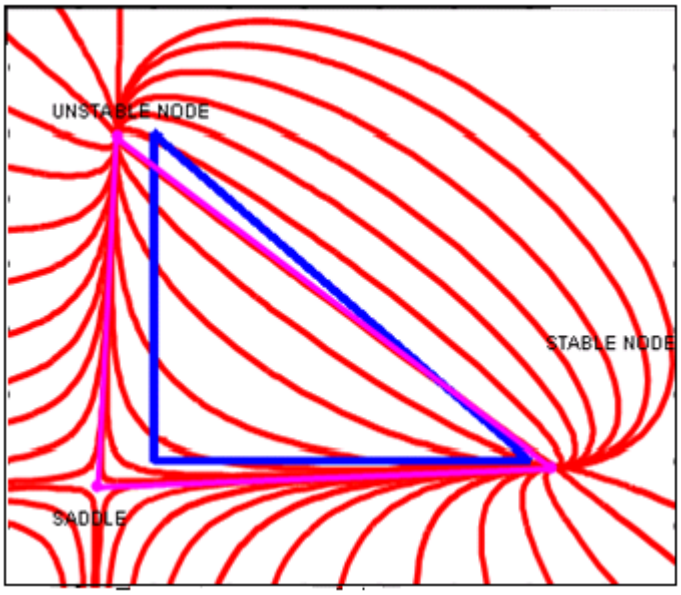


Figure 4.11: RRCM for stoichiometric vector in Region III-

4.4.7 Summary

In conclusion we can see that the zero order reaction vector field does not introduce new singularities (nodes or saddles) into the RRCM. The number of singularities remains the same as in the separation vector field or equivalently RCM. Furthermore the combination of the reaction vector field and the separation vector field moves the singularities of the non-RRCM (RCM) in the composition space. The type and location of singularities in the MBT depends on the stoichiometric vector direction. We are able to move regions of the RCM that previously lay out of the MBT into the MBT. A consequence of this is that composition profiles can be made to move in directions that would not have occurred in the distillation only process. Thus reactive residue curves can be made to move in directions that would not be possible in residue curves by an appropriate choice of the direction of the stoichiometric vector. We now consider the nodes or singularities of the RRCM in more detail.

4.4.8 Singular Points

Singular points determine the limits of the batch reactive trajectories and hence the topology of the RRCM. An interesting analysis of the stability of singular points both in reactive residue curve map and the more general case of pinch points is described by Hauan *et al* [2].In this section, we look at the movement of the singular points when the value of the parameter α is changed. The path or curve traced out by the nodes is called the singular point curves (SPC). This curve can be mathematically determined by solving where the differential equation (4.2) is zero, that is:

$$\frac{d\underline{x}}{d\xi} = (\underline{x} - \underline{y}^*) + \alpha\underline{\upsilon} = 0 \qquad (4.5)$$

Hauan *et al.[2]* sketch the SPC in the positive space by hand. In this section we will show that by extending Hauan's analysis to the negative space, one is able to sketch

the topology of the reactive residue curve maps. Hoffmaster *et al*.[11] provide also an analysis of the pinch points curve inside and outside the positive space.

Equation (4.5) defines a curve in two dimensional spaces (x_1, x_2) and the shape of this curve is in the case of zero order kinetics and constant relative volatility a function of stoichiometry and the parameter α only.Changing the stoichiometric vector $\underline{\upsilon}$ shifts the SPC. Remembering that the singularities of the RRCMs move on these curves; this means that the topology of the RRCM is determined by the shape and position of the SPC.

Another important point is that if one chooses two reaction vectors such that they remain collinear, for example $\underline{\upsilon}$ and $\alpha\underline{\upsilon}$; the position and shape of the SPC will not change. Thus the SPC and hence the topology of the RCM is fixed by the direction of the stoichiometric vector and not by the size of the stoichiometric vector.

We will now show how the direction of the stoichiometric vector affects the location and shape of the SPC and consequently the product compositions that can be reached by simple batch distillation accompanied by a zero order chemical reaction

4.4.9 Movement of singular points for $\underline{\nu}$ in regions II^+ and II^-

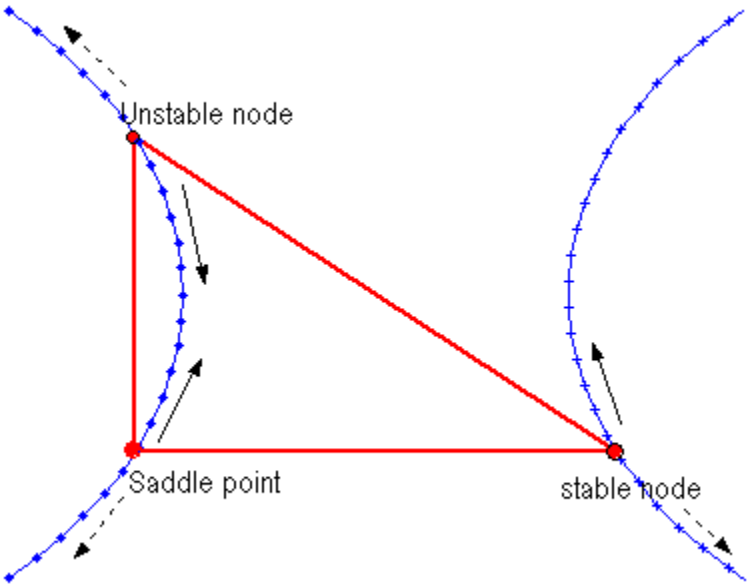


Figure 4.12: Qualitative shape of the singular point curve for the stoichiometric vector in Region II+ and II-. The solid arrow corresponds to the movement of singular points along the SPC for the stoichiometric vector in region II+ and increasing value of α. The dashed arrow corresponds to the movement of singular points along the SPC for the stoichiometric vector in region II- and increasing value of α

The singular point curves (SPC) for stoichiometric vector $\underline{\nu}$ in regions II^+ and II^- are shown in Figure 4.12. In Figure 4.12 the arrows indicate directions that the nodes shift with increasing alpha. The SPC has a branch of the curve running through the stable node , and a second branch that runs through the unstable node and the saddle point . Thus one can see that the unstable node and saddle point move into the MBT for stoichiometric vectors in region II^+ and the singular points move further into the region as the value of the parameter increases. The stable node moves out of the region in such a way that the boundary that corresponds to the intermediate-heavy

axis in the RCM moves into the space. When the stoichiometric vector $\underline{\nu}$ is in the region II^- however, all the singular points shift outside the MBT. Furthermore, none of the boundaries that existed in the RCM move into the MBT.

4.4.10 Movement of singular points for $\underline{\nu}$ in regions I^+ and I^-

The SPC for the stoichiometric vector $\underline{\nu}$ is in regions I+ and I- is shown in Figure 4.13 and the directions that the nodes shift with increasing alpha . In this case the SPC has one branch running through all the singular points (unstable node, stable node, and the saddle point). The singular points do not move inside the MBT for the stoichiometric vector $\underline{\nu}$ in either region I+ or I- . Thus there are no singular points in the MBT in this case which means that there will be no reactive azeotropes for this type of reaction. We can also see that a stoichiometric vector in Region I- will move the boundary that corresponded to the light intermediate axis in the RCM into the MBT thus introducing region of unstable behaviour into the real space. Again one can see that the unstable node can only move in region 2 or 6, the saddle point in region 4 and 6 and the stable node in region 2 and 4 of the extended RCM defined in Figure 4.2.

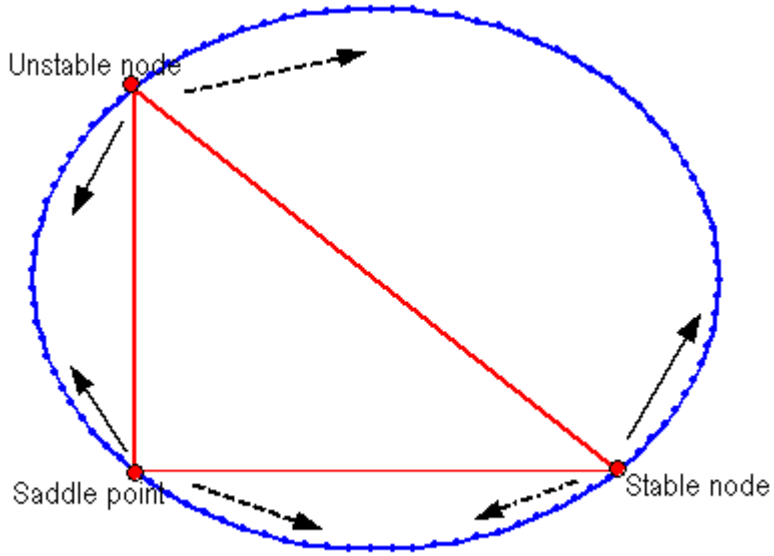


Figure 4.13: Singular points curves (SPC): qualitative shape of the singular point curve for the stoichiometric vector in Region I+ and I-. The solid arrow corresponds to the movement of singular points along the SPC for the stoichiometric vector in region I+ and increasing value of α. The dashed arrow corresponds to the movement of singular points along the SPC for the stoichiometric vector in region I- and increasing value of α

4.4.11 Summary of results on movement of the singular points

The overall behaviour or the topology of the RRCMs is determined by the singular point curves (SPC). The direction of the stoichiometric vector determines the location of the singular point curves. In particular the singular point curve passes through the singular points of the RCMs and the way that the SPC connects the singular points affects the topology of the RRCMs. Different stoichiometric vectors in the same region of the stoichiometric space will only change the curvatures of the SPC but the overall pattern remains the same in that the same singular points are

connected by the SPC. The SPC show different behaviour depending on the direction of the stoichiometric vector. SPC describe the path that the singular points of the RRCM trace out. The topology of the RRCM changes depending on how the singular points shift in the composition space.

Thus the number and type of singular points in a given system, known as reactive azeotropes, is determined by the direction of the stoichiometric vector. The movement of regions of unstable behaviour into the real composition space is also determined by movement of the singular points and hence the stability of the system to initial concentration is determined by the reaction stoichiometry.

4.4.12 Effect of the Length of Stoichiometric Vector on the RRCM

We next look at the question of how the length of the stoichiometric vector or the value of the parameter α in the differential equation 4.2 affects the RRCM. The shape of the SPC depends on the direction of the stoichiometric vector $\underline{\upsilon}$ and the dimensionless parameter α parameterizes the curve. Thus changing either the value of α or the magnitude of the stoichiometric vector moves the singular points on the SPC as shown in Figure 4.14

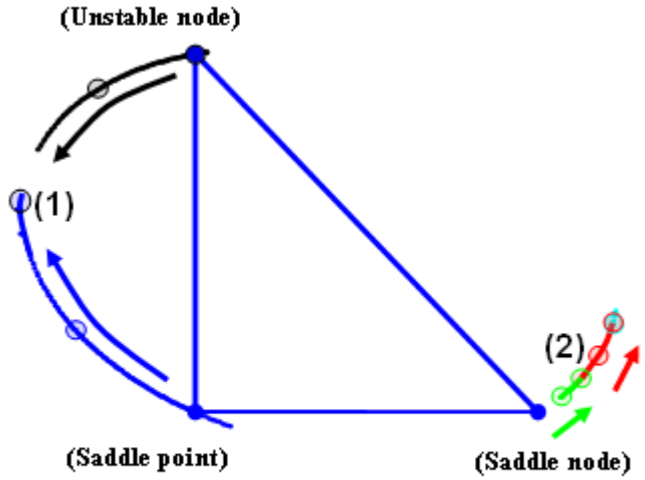


Figure 4.14: Movement of Singularities as α change for stoichiometric vector in Region I+

In Figure 4.14, all the singular points move outside the MBT. One can see that the topology of the RRCM does not change as α change. The position of the singular points, or equivalently the location of singular points in the RRCM, moves along the SPC.

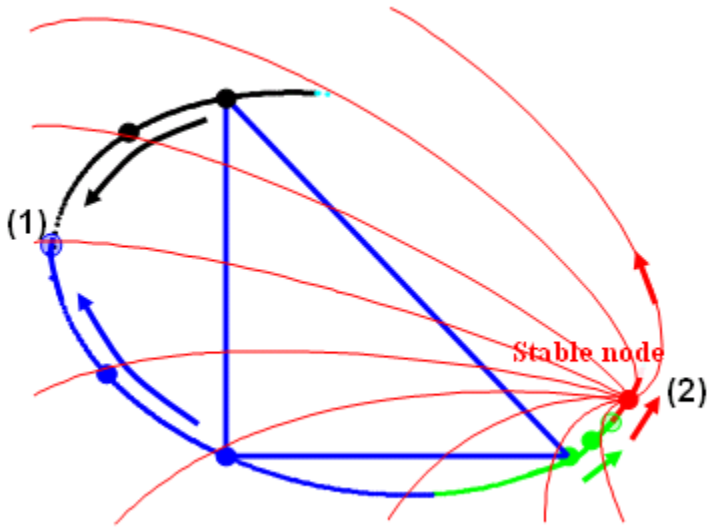


Figure 4.15: Reactive Residue Curve Map (RRCM) for the stoichiometric vector in Region I+ and high value of α. Note that only one node (the stable node) remains outside the MBT.

At a high enough value of α, two of the singular points will merge (point 1 in Figure 4.15) and only one node will remain outside the MBT (point 2 in Figure 4.15). These values of α would be important to identify, as an increased value of α will change the topology. Tapp *et al*., 2004 looked at this topological change for Column Profile Maps and identified the critical value of the scalar parameter. Figure 4.15 shows the RRCM for the stoichiometric vector lying in region I+; the unstable node and the saddle point disappear and only remains the stable node outside the MBT.

4.5 Applications to Batch Reactive Distillation Processes

1. Intermediate boiler in ideal systems

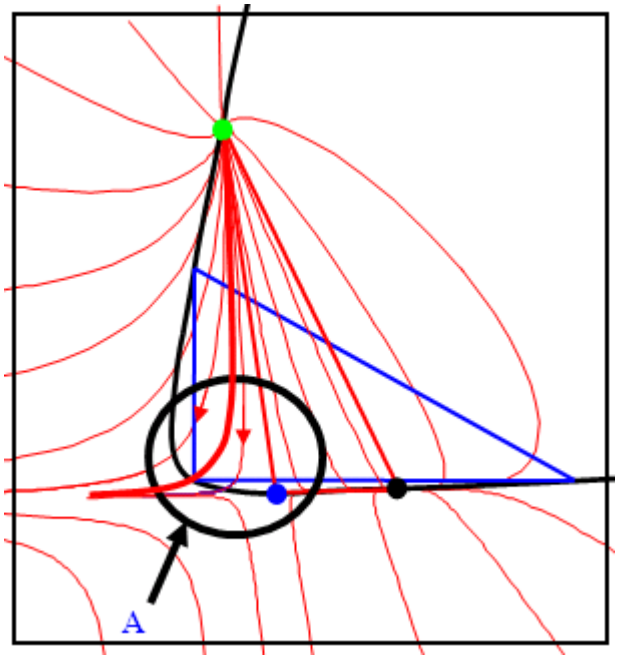


Figure 4.16: Figure 4.14: RRCM with the parameters α=2.3 and = [-0.05 -0.03]. The bold red profile runs directly into the intermediate boiler

One is in principle able to transform the topology of the reactive residue curve map as one can influence the kind of singularity occurring via the size α of the reaction vector and can shift the singular points curves via the stoichiometric vector direction such that the positions of the singularities suits his design. This example is a problem to sample the intermediate boiler in ideal systems as demonstrated by Tapp et al. (2004). As the node is described as a saddle point; conventional design techniques require an infinite number of stages for 100% purity. The objective is to generate a profile that

runs straight into the corner. This can be performed by transforming the system such, that the resulting singularities offer a reactive residue curve map that achieves the desired separation. The bold line in Figure 4.16 represents the one profile that runs directly into the corner.

2. Contour of the process vector

Insights into the effect of reaction on a batch reactive separation process can be deduced by plotting contours of the vector of the net process vector as defined in equation 4.2. This form of projection was introduced by Hauan *et al*., 1998. Figure 4.17 shows contour plots of the magnitude of the separation vector and it can be seen that around the pure component singular points the magnitude of the vector goes to zero. In Figure 4.18 we have plotted contours of the magnitude of the process vector length for a reactive distillation batch process as defined by equation 4.2. We have used a zero order chemical reaction with the stoichiometric vector lying in region I^+ and a value of $\alpha=1$. From our previous arguments, we showed that in this case all three singular points would lie outside the MBT and we can see this in Figure 4.18 that the contours get smaller at the three singular points, which indeed lie outside the MBT. However this means that the magnitude of the contours inside the MBT are higher than those found in Figure 4.17 and thus we can conclude that the magnitude of the process vector is increased by reaction in this case.
This would happen in all the cases where singular points moved out of the MBT and this could offer potential advantages in the design and operation of reactive distillation systems.

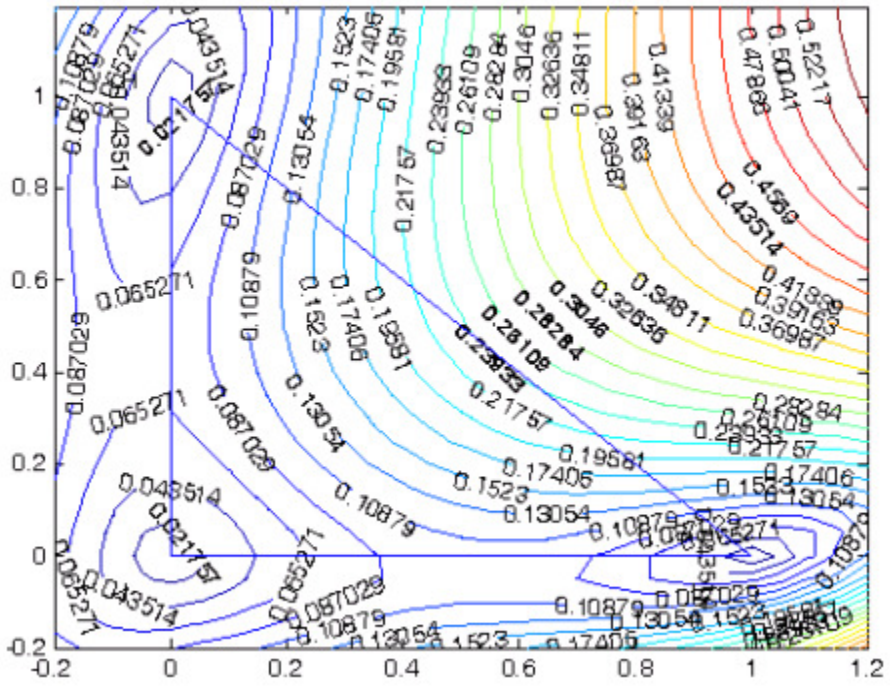


Figure 4.17: Contour plot of the separation vector S at 1 atm for an ideal system

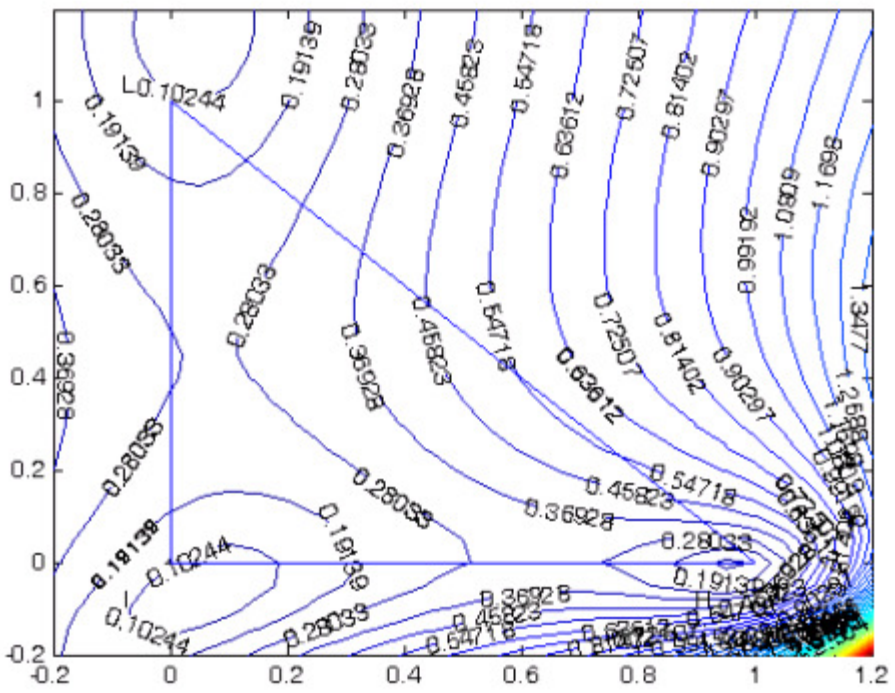


Figure 4.18: Contour plot of the separation vector S+v at 1 atm for an ideal system and v in Region I-

4.6 Conclusion

We have looked at reactive distillation as a combination of two vector fields, namely the separation vector field and the reaction vector field. We considered the zero order reaction where we assume that the total number of moles in the chemical reaction is conserved. In this case the reaction vector $\underline{r}$ and the stoichiometric vector $\underline{\upsilon}$ have the

same direction. We also consider a simple separation vector $\underline{S}$ defined for a constant relative volatility system.

We have shown that for common operating parameters (the parameter α and the stoichiometric vector $\underline{\upsilon}$) and different starting compositions one can generate a map of all possible profiles achievable in a simple reactive distillation batch apparatus, which we call the reactive residue curve map. By extending this map to the negative space we were able to show that parts of the residue cure map are shifted in and out of the mass balance triangle.

The addition of the reaction vector field to the separation vector moved the existing singular points in the RCM and we showed that the RRCM is a transform of the RCM. The effect of the direction of the reaction vector on the location of singular points of the resultant RRCM was analysed and it was shown to be a key parameter in defining the topology. The size of the reaction vector only affected the movement of the singular points on the singular point curves and thus did not affect the topology. From this we can conclude that the reaction kinetics, as long as the kinetics do not introduce singular points into the reaction vector map, will not significantly affect our analysis and conclusions.

One might use this shifting of singularities of the RCM to introduce not only desirable system behaviour in MBT space but also to identify what conditions can avoid the possibility of singular points in the MBT. This shifting of composition profiles can be used also to determine regions of instability for the reactive batch still. By choosing appropriate parameters ($\alpha, \underline{\upsilon}$), one can shift the stable regions in or out the operating region and avoid regions of instability.

By looking at the topology of RRCM as a shift of the topology of the RCM, we believe that we have introduced a very powerful analysis tool to the understanding of reactive distillation systems.

It is also interesting to ask what the effect of introducing singular points into the reaction vector map will be on the topology of the RRCM. Answering this question will be the subject of the next chapter.

Bibliography

1. Tapp, M., Holland, S. T., Hildebrandt, D., Glasser, D.,"Column Profile Maps Part A: Derivation and interpretation" Industrial and Engineering Chemistry Research, 2004, **43**(2), pp 364-374
2. Hauan, S., Westerberg, A.W, Lien, K.L.,"Phenomena-based analysis of fixed points in reactive separation systems" Chemical Engineering Science, 2000, **55** (6)**,** pp. 1053-1075
3. Baur, R., Higler, A.P., Taylor, R., Krishna, R.,"Comparison of equilibrium stage and nonequilibrium stage models for reactive distillation" Chemical Engineering Journal, 2000, **76** (1), pp. 33-47
4. Ciric, A.R, GU, D.," Synthesis of non equilibrium reactive distillation processes by MINLP optimization" AICHE Journal, 1994, **40** (9)**,** pp.1479-1487
5. Gumus, Z.H, Ciric, A.R," Reactive distillation column design with vapour/liquid/liquid equilibria" Computers and chemical engineering, 1997, **21**(1), S983-S988
6. Ung, S., Doherty, M.F," Vapor-liquid phase equilibrium in systems with chemical reactions" Chemical Engineering Science, 1995, **50** (1), pp.23-48
7. Barbosa, D., Doherty.M.F,"The simple distillation of homogeneous reacting mixtures" Chemical Engineering Science, 1988, **43** (3), pp.541-550
8. Okasinski, M., Doherty.M.F," Thermodynamic behaviour of reactive azeotropes" AICHE Journal, 1997, **43** (9), pp.2227-2238

9. Venimadhavan, G., Buzad, G., and Doherty, M.F.,"Effects of kinetics on residue curve maps for reactive distillation." AICHE Journal, 1994, **40** (11), pp. 1814-1824

10. Thiel, C., Sundmacher, K., Hoffmann, U.," Residue curve maps for heterogeneously catalyzed reactive distillation of fuel ethers MTBE and TAME" Chemical Engineering Science, 1997, **52** (6), pp.993-1005

11. Hoffmaster, W. R., Hauan, S.," Difference points in reactive and extractive cascades III-Properties of column section profiles with arbitrary reaction distribution" Chemical Engineering Science, 2004, **59** (17), pp. 3671-3693

12. Doherty, M.F., Perkins, J.D.,"On the Dynamics of Distillation Processes-I, the Simple Distillation of Multicomponent Non-Reacting, Homogeneous Liquid Mixtures" Chemical Engineering Science, 1978, **33** (3), pp 281-301

13. Doherty, M.F., Perkins, J.D.," On the Dynamics of Distillation Processes-II., The Simple Distillation of Model Solutions" Chemical Engineering Science, 1978, **33** (5), pp 569-578

14. Doherty, M.F., Perkins, J.D.,"On the Dynamics of Distillation Processes-III-The topological structure of ternary residue curve maps", Chemical Engineering Science, 1979, **34** (12), pp 1401-1414

15. Damkohler, G.," Stromungs and warmeubergangsprobleme in chemischer technik und forschung", Chem.Ing.Tech, 1939, **12**, pp.469-480

16. Holland, S.T., Tapp, M., Glasser, D., Hildebrandt, D., Hausberger, D.,"Novel separation system design using "moving triangles" Computers and chemical engineering, 2004, **29** (1), pp.181-189

17. Hauan, S., Lien, K.L.,"A phenomena based design approach to reactive distillation" Chemical Engineering Research & Design, Transactions of the Institute of Chemical Engineers, 1998, **76**(A), pp.396-407

5 Chapter 5 RRCM Topology: The Effect of Reversible Chemical Reaction with Nodes

Preliminary versions of this chapter presented at the AIChE Annual Meeting 2004, , Austin, Texas, USA and the World Congress of Chemical Engineering, 2005, UK under the title: topological analysis of simple distillation accompanied by single chemical reaction.

5.1 Abstract

In chapter 4 we considered the reactive distillation process as a linear combination of the separation and reaction vector fields. The objective of chapter 4 was to analyze the behavior of reactive residue curve maps (RRCMs) for a combination of a simple reaction vector field without nodes (irreversible chemical reactions) and an ideal separation vector field (with standard pure component nodes). In this work we extend the approach to the topological analysis of reactive residue curve maps (RRCMs) of simple batch reactive distillation in which the reaction vector field has nodes (corresponding to equilibrium points) has been incorporated. The approach presented in this paper provides a visual representation of the RRCM both inside and outside the mass balance triangle (MBT). The approach is based on the extension of the work of Doherty *et al.[1][2]*, Hauan *et al.[3][4][5]*, and Huang *et al.[6]* based on reactive distillation and reactive membrane separation. The results show that the combination of simple distillation and a single reversible reaction move singular points in the composition space in very complex

way resulting in very different topologies. The understanding of the movement of singular points can be used for feasibility analysis and help understand some general design implications related to the change of the topology of the RRCMs. The results show how the reaction vector direction is the most determinant factor and that the size of the reaction vector (precise kinetics relationships) has only a secondary impact on the topology of the reactive residue curve map. Furthermore we show the result of numerical calculations/simulations of the eigenvalues maps of the resultant process. These maps can be used as assessment tools to complete existing methods based on phase diagrams

5.2 Introduction

Attempts to extend the residue curve mapping technique to reactive distillation processes began in the late 1980's when Doherty *et al.[1][2]* defined residue curve maps in terms of transformed molar compositions for multicomponents systems undergoing multiple equilibrium reactions. They used the term reactive azeotropes to refer to the singular points occurring in such systems at point where the reaction and separation were simultaneously zero or had a net zero effect.
Venimadhavan *et al.[7]* introduced the concept of reactive autonomous differential equations as shortcut tool to model the dynamic behavior of the liquid phase composition in a simple reactive batch using a constant heating policy input. The simplicity of this first order differential approximation that describes the transition from the non reactive residue curve map to the limiting case of chemical equilibrium makes it the preferred model for preliminary analysis. Tapp et al.[9] considered the topology of the Residue Curve Map (RCM) in the full space (i.e. Including negative mole fractions) where the sum of mole fractions is unity. The accessible part of this map is that which lies in the Mass Balance Triangle (MBT), that is the region where

all the moles fractions are positive. They introduced the concept of a Column Profile Map (CPM) which is a plot of the liquid profiles in all column sections with a given nett molar flow rate Δ and nett molar flowrate of the individual components defined by Δx_{Δ}. The CPM is a linear combination of the separation vector field (or RCM) and the mixing vector field. More importantly they showed that the topology of the CPM is the same as that seen in the RCM but the part of the map that is accessible in the MBT changes in a well defined way. This transformation (i.e. The CPM) could be thougth of simplistically as the MBT moving across the RCM (or visa versa). The map one would see through the MBT would be very different as one changed the parameters Δ and x_{Δ} and the topology inside this triangle would appear to change in very complex ways. However standing back and looking at the full space made an understanding of the observed behavior much simpler.

Tapp et al.[9] further showed that the separation vector field (or equivalently RCM) of ternary systems described by ideal thermodynamics have three nodes corresponding to each of the pure components. Non-ideal thermodynamics may introduce extra nodes into the space. If these nodes are on boundaries of the Mass Balance Triangle, we call them binary azeotropes and those that occur in the inside the MBT are known as ternary azeotropes.

In chapter 4 we considered batch reactive distillation processes. We showed that these processes can be described by a linear combination of the separation vector and reaction vector field . We redefined Reactive Residue Curve Map (RRCMs) as the plot of all possible liquid profiles in a reactive batch still for given rates of vapor removal to the liquid holdup in the batch still. The behavior of the RRCMs for non-equilibrium chemical reaction (irreversible reactions) was analyzed and it was shown that RRCMs are merely the transform of the non reactive RCM. For example, for the case of ternary ideal system with a single irreversible chemical reaction, we were able to show that for a particular orientation of the stoichiometric vector one could move two of the equilibrium points (the unstable node and saddle point or the stable node

and the saddle point) inside the MBT introducing a bifurcation inside the MBT. We further showed that one could choose a different orientation of the stoichiometric vector such that all the equilibrium points (unstable node, stable node, saddle point) moved out of the MBT and that no bifurcation line would exist in the MBT.

The results showed a strong analogy with the results previously found in a system of coupled column maps by Holland et al. [10]. However, if these systems are described by vector equations, the similarity in behavior can be seen to arise in that both systems are linear combinations of a separation vector field and a second vector field of constant direction. From this it can be seen that the combined vector and topology approach is very powerful.

This chapter is an extension of chapter 4 in that it considers batch reactive processes where the reaction that occurs is reversible. The main difference between an irreversible and reversible vector field is that a reversible reaction vector field introduces a continuous curve of nodes in the reaction vector field map. In all the other situations previously looked at, such as separation and mixing vector fields, the nodes were isolated and the number of nodes was finite.

We will show that the introduction of the continuous curve of nodes in the reversible reaction vector field causes a change in the way singular points in the combined reactive-separation map move in the composition space compared to the case where there are no nodes in the reaction vector map. Furthermore the topological transformations of the separation vector field in the reactive distillation system, (i.e. a linear combination of reaction and separation) are more complex than in the case of say distillation systems (i.e. a linear combination of a separation vector field and mixing vector field) or even reactive distillation with a non-reversible reaction. We believe that this analysis will give a better understanding of reactive distillation processes by allowing a systematic evaluation of the relationship between kinetic parameters, operating conditions and bifurcations seen in the liquid.

5.3 Process Formulation

Let us consider a liquid in a batch still with N components where the mole fractions in the still are described by $\underline{x} = [x_1,...,x_N]$. The liquid molar holdup is λ at it is at its equilibrium boiling temperature. The vapour in the still is in equilibrium with the liquid, the mole fraction in the vapour is $\underline{y}^* = [y_1,....y_N]$ and it is removed at a flow rate $\dot{V}$. We will consider a single chemical reaction described by the reaction stoichiometric vector $\underline{\upsilon} = [\upsilon_1,..., \upsilon_N]$ taking place in the liquid phase, the rate being described by R.

The unsteady state mole balance in the liquid phase gives:

$$\frac{d\underline{x}}{d\xi} = \underline{p} = (\underline{x} - \underline{y}^*) + \alpha(\underline{\upsilon} - \underline{x}\upsilon_T)\mathrm{R} \qquad (5.1a)$$

where $\alpha = \dfrac{\lambda}{\rho \dot{V}}$ (5.1b)

$\upsilon_T = \sum \upsilon_i$ is the summation of υ_i and represents the total molar change of the chemical reaction, ρ is the molar density of the liquid and is assumed to be constant, ξ is a non-linear transformation of the real time t with $\dfrac{\dot{V}}{\lambda} dt = d\xi$

The ratio $\dfrac{\lambda}{\dot{V}}$ depends on the heating policy of the process. If the heating input to the batch still is such that the ratio $\dfrac{\lambda}{\dot{V}} = \dfrac{\lambda_0}{\dot{V}_0}$ is a constant; then the parameter α defined in equation (5.1b) is also a constant and equation (5.1a) can be seen to be a linear combination of two vector fields:

$$\frac{d\underline{x}}{d\xi} = \underline{p} = \underline{S} + \alpha\underline{r} \qquad (5.2)$$

Where $\underline{S} = \underline{x} - \underline{y}^*$ is the separation vector field and $\underline{r} = (\underline{\upsilon} - \underline{x}\upsilon_T)R$ is the reaction vector field.We will now consider Equation 5.2 and look at the topological relationships between the vector field S and r and the linear combination of them as described by the vector p in two examples.

5.4 Example 1

The first example deals with a hypothetical ideal case.We look at the ideal vapour-liquid system of ABC in which a simple reaction A + B ↔C occurs in the liquid phase. The molar reaction rate $R(x)$ is given by: $R(x) = k_f (x_A x_B - \frac{x_C}{K_{eq}})$

We assume that the chemical equilibrium constant is $K_{eq} = 4$ and the rate constant k_f is independent of temperature. The VLE is described by constant relative volatilities. Furthermore A is the low boiling component, B is the intermediate boiling component and C is the high boiling component. We assume that the volatilities of the components A and B relative to C are equal to 5 and 3 respectively

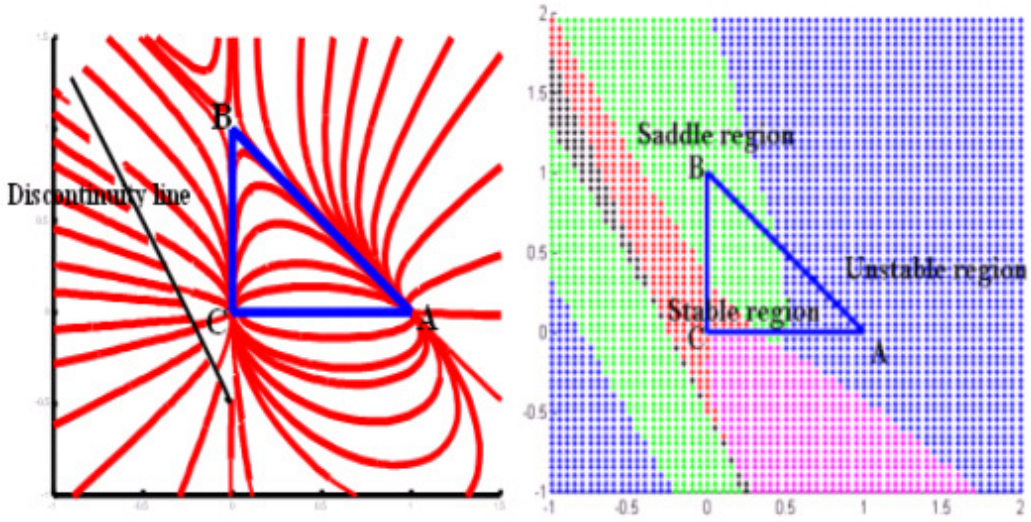


Figure 5.1: Ideal system ABC a) Residue Curve Map (left) b) Eigenvalue Map of $\underline{S}$ (right)

5.4.1 Separation vector field

The $\underline{S}$ field of the ABC system consists only of the **three pure component nodes**.

For x_1 and x_2 ranging from $-\infty \leq \alpha \leq \infty$ no other singular points can be found (Figure 5.1a)

The eigenvalues can also be calculated, see Figure 5.1b. The Figure 5.1b shows the nature of the singularities occurring at the pure components nodes A, B, C. It is interesting to see that the entire space is divided in regions of similar behaviour with regard to the kind of singularities occurring. We refer to these regions as the stable region, the unstable region and the saddle region. The eigenvalue map represented in Figure 5.1b is particular to the separation vector field, and if one adds a chemical reaction to the separation vector field the eigenvalue map will change. The way the

eigenvalue map changes is related to the movement and bifurcation of singular points. We will analyze this kind of map later in this work.

We also notice by looking at Figure 5.1a that there is a region in the phase diagram where the profiles are discontinuous. This region corresponds to the border region of the saddle and the stable singularities on the eigenvalue map. We will show that this region can not be moved by adding a reaction vector field to the separation vector field and that this gives a limitation on what areas of the composition space can be moved inside the positive space

5.4.2 Reaction vector field

To understand the topology of the reaction vector field let us consider a batch still in which only a single reversible reaction occurs.

The general vector equation of the batch reactor, as developed by Hauan *et al.[3]* is then defined by:

$$\frac{d\underline{x}}{d\xi} = \underline{r} = (\underline{\upsilon} - \underline{x}\upsilon_T)\mathrm{R} \qquad (5.3)$$

It follows that the factors affecting a chemical reaction vector $\underline{r}$ can be classified into two groups:

- The scaling effect included in the chemical rate R
- The rotational effect induced by the vector of stoichiometric coefficients $\underline{\upsilon}$

The integration of equation (5.3) for different initial conditions defines a set of reaction profiles in the composition space. The integration of this equation results in a set of straight lines whose slope is defined by the stoichiometry of the reaction

system. We will call the result of this integration a reaction profile map and will examine its behaviour.

Hauan *et al.[3]* showed that the reaction profiles are linear; and that the reaction vector and reaction profiles are collinear at any point.

They further applied a steady state analysis to equation (5.4) and were able to give information on the key parameters affecting the behaviour of the reaction vector. They showed that at singular points of the equation (5.3) the vector equation reduces to zero: $(\underline{\upsilon} - \underline{x}\upsilon_T)\mathrm{R} = 0$ and they were able to deduce two limiting cases:

- The condition $R = 0$ defines a specific line of nodes called the chemical equilibrium line which is an important structural element. Their analysis reveals that at the chemical equilibrium line the size of all reaction vectors is null and as expected the directions of reaction vectors change from one side to the other of the chemical equilibrium line. This observation although evident from a kinetics perspective was a powerful result as in vector interpretation, reaction vectors are "flows" moving in defined direction. This work will show that the most important factor is not the change of the **size** of reaction vectors along reaction paths but the change of **direction** of reaction vectors along these paths. The reaction vectors change the direction at the chemical reaction equilibrium line (surface), and despite the fact that this line introduces a set of equilibrium nodes; it will be demonstrated that it also introduces an overall "limitation" in the movement of some of the singular points of the resultant vector process.
- The quantity $(\underline{\upsilon} - \underline{x}\upsilon_T)$ is a vector and affects the orientation of the reaction vector $\underline{r}$. It follows that the condition $(\underline{\upsilon} - \underline{x}\upsilon_T) = 0$ defines a specific point in the composition space. They referred to this point as the "pole" node. In all cases they deduced that the reaction profiles are straight lines collinear to the reaction vectors, bound by the chemical equilibrium line and going though the pole node and in the

case where the total number of moles is conserved in the chemical reaction, the pole node goes to infinity.

5.4.3 Process vector field

As outlined earlier, the process vector equation $\underline{p}$ can be simply formulated as a linear combination of the separation vector field $\underline{S}$ and the reaction vector field $\underline{r}$:

$$\frac{d\underline{x}}{d\xi} = \underline{p} = \underline{S} + \alpha\underline{r} \qquad (5.4)$$

In the case of the simultaneous combination of separation and mixing, as is found in a Distillation Column Section, it has been showed that the pinch point curve can be constructed graphically by finding the points on the residue curves with their tangent passing through the composition $\underline{X}_D$ of the product from the column section [11]. For the dynamic systems defined by the equation 5.4, the singular point curve is defined by $\underline{p} = 0$ and follows the condition:

$$\underline{S} + \alpha\underline{r} = 0 \qquad (5.5)$$

This equation shows that the pinch point or singular point curve defined by $\underline{S}$ is tangent to the reactions lines defined by $\underline{r}$ at singular points.

The singular point curve for this system is plotted in Figure (5.2) (for $0 \le \alpha \le \infty$) and in Figure (5.3) (for $-\infty \le \alpha \le 0$) together with the chemical equilibrium curve. The two set of loci intersect at point RA which corresponds to a composition of about (0.14, 0.47). This point has been referred as the reactive azeotrope by Doherty *et al.[1][2]*..

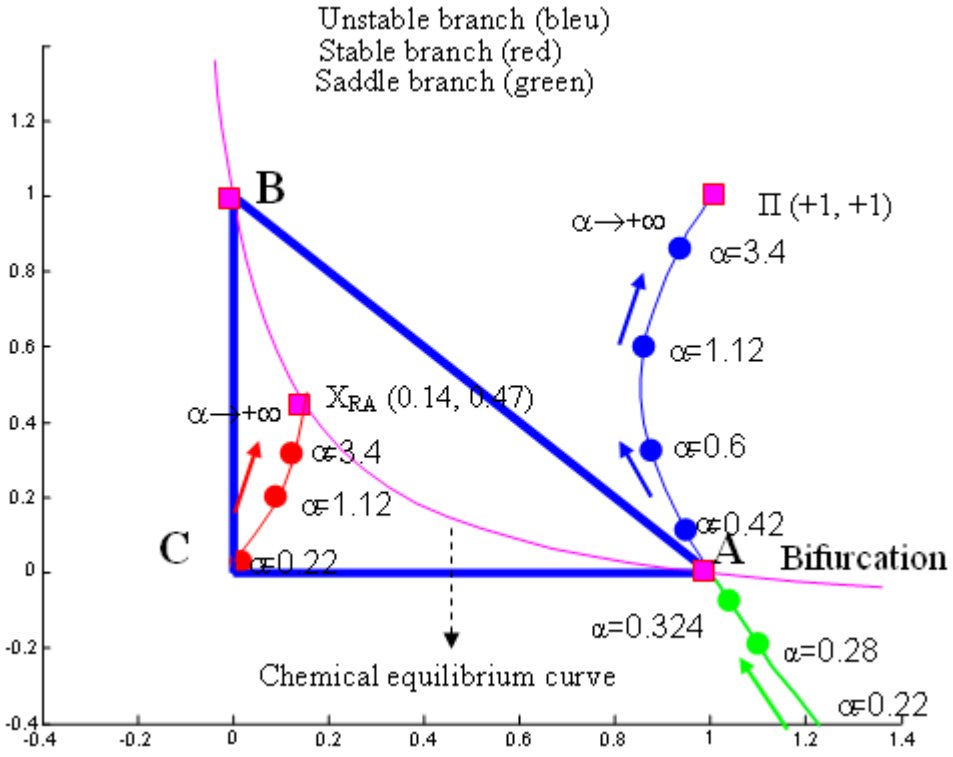


Figure 5.2: Singular point curve and singular point bifurcation behaviour for different values of parameter α in the range -∞≤α ≤0

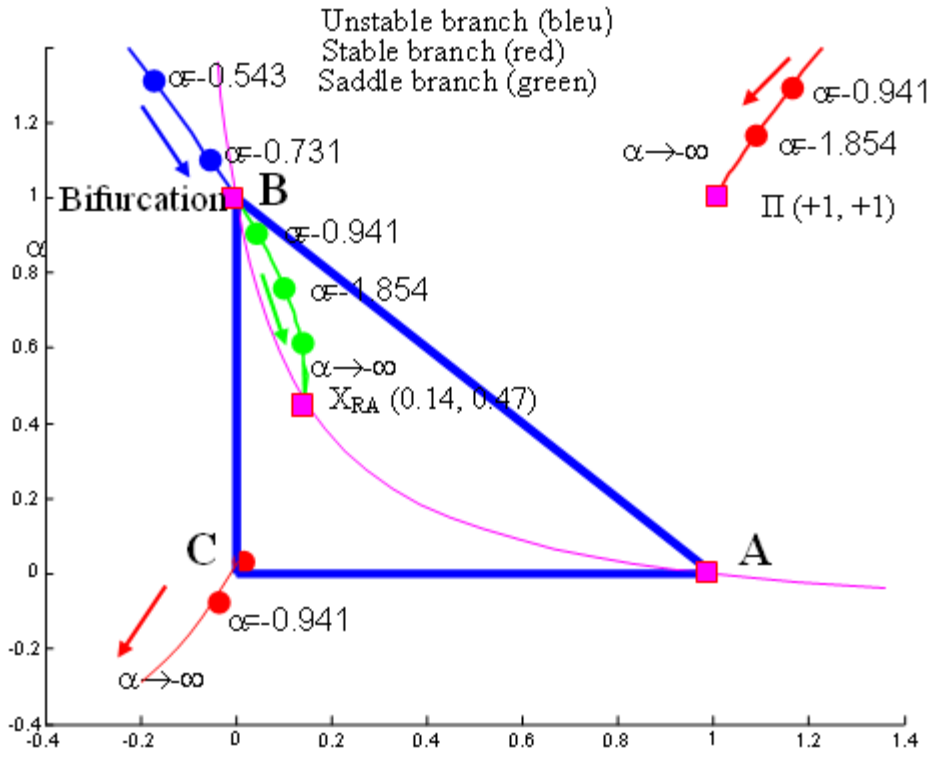


Figure 5.3: Singular point curve and singular point bifurcation behaviour for different values of parameter α in the range $-\infty \leq \alpha \leq 0$

Different behaviors emerge for either $0 \leq \alpha \leq \infty$ or $-\infty \leq \alpha \leq 0$. We will look separately at each of the two cases:

Case I **$\underline{0<\alpha<+\infty}$**

1. The pure component B is a fixed singular point. No matter what transformation occurs, this point remains in the same location. We also see that if the volatilities of components A and B relative to C are kept constants, this point is always a saddle point. This result occurs specifically in this system (as opposed to

dstillation, mebrane separation systems or reactive distillation systems with irreversible kinetics) as the separation vector field and reaction vector field are both zero at this point. This has a profound effect on the resulting topological transformations of the process vector field which results in very different behaviour to that found in other systems previously examined.

2. As the parameter α increases the stable node moves from the pure component C towards inside the MBT forming what we call the positive stable branch of the singular point curve and represented in red in Figure 5.2. One can see also that the stable node eventually reaches the chemical equilibrium locus for $\alpha \to +\infty$ which the point that Doherty and co-workers referred to as a reactive azeotrope.

3. There is another branch of the singular points curve that passes through pure component A. The pure component A is an unstable node in the $\underline{S}$ field. As the parameter α increases the saddle point moves along the singular points curve and at a value of about $\alpha = 0.35$, the pure component A exchanges stability from an unstable node to a saddle point. In reality the pure component A is a fixed singular point (as for point B) as the separation vector field and reaction vector field are both zero at this point. Therefore this point does not move in the space but changes its nature. For $\alpha > 0.35$, the unstable node moves along the singular point curve towards the pole point Π for $\alpha \to +\infty$. One can see that the nature of the node located at point A is quite complicated in the $\underline{p}$ field and is affected by the singular point curve that passes through point A. The behaviour of the singular points occurring at the points A and B at a finite value of α is again the result of the $\underline{S}$ and $\underline{r}$ vector fields both being zero at the pure component A and B vertices. In other systems the pure component would typically be a node only when the value of the scalar parameter (equivalent to α) is zero.

In summary the overall topology for this case when $0 \le \alpha \le \infty$ reduces to 3 different scenarios corresponding to:

- $0 < \alpha < 0.35$,the topology is shown in Figure 5.4
- $0.35 < \alpha < +\infty$, the topology is shown in Figure 5.5
- $\alpha = 0.35$, the topology is shown in Figure 5.6

We will firstly discuss the number of singular points in the process vector field and the impact on these nodes on the topology.

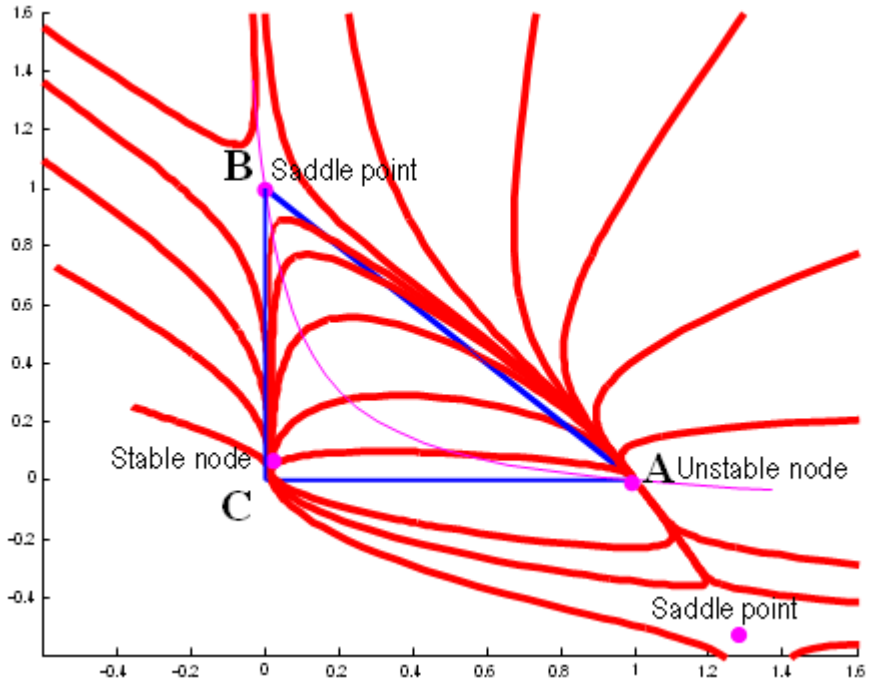


Figure 5.4: Reactive Residue Curve Map for α=0.22

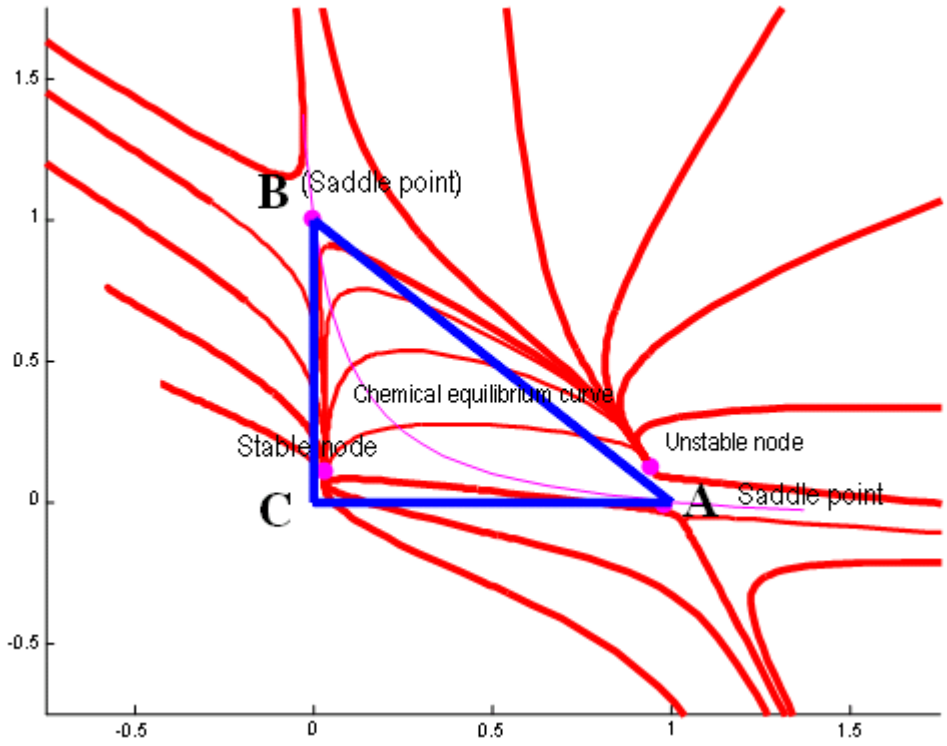


Figure 5.5: Reactive Residue Curve Map for α=0.42

At about $\alpha = 0.35$ a bifurcation happens when the saddle point meets the unstable node. In Figure 5.6 we have plot the reactive residue curve map at the bifurcation point and we have superimposed on this map the eigenvalue map.

We can see that:

- The bifurcation reduces the number of distinct and real singularities.
- The bifurcation also introduces new types of singularities. In Figure 5.6 the singular point located at the pure component A is indeed a unstable half node saddle as it lies at the limit of the unstable node region (blue) and the saddle point region (green) .

- We also see that by examining the eigenvalue map that potential bifurcation exists where different nodes types regions meet. However all the regions where different nodes types regions meet do not necessarily create bifurcation. For example the stable node region (red) and the saddle point region (green) meet inside the mass balance triangle without introducing any bifurcation.

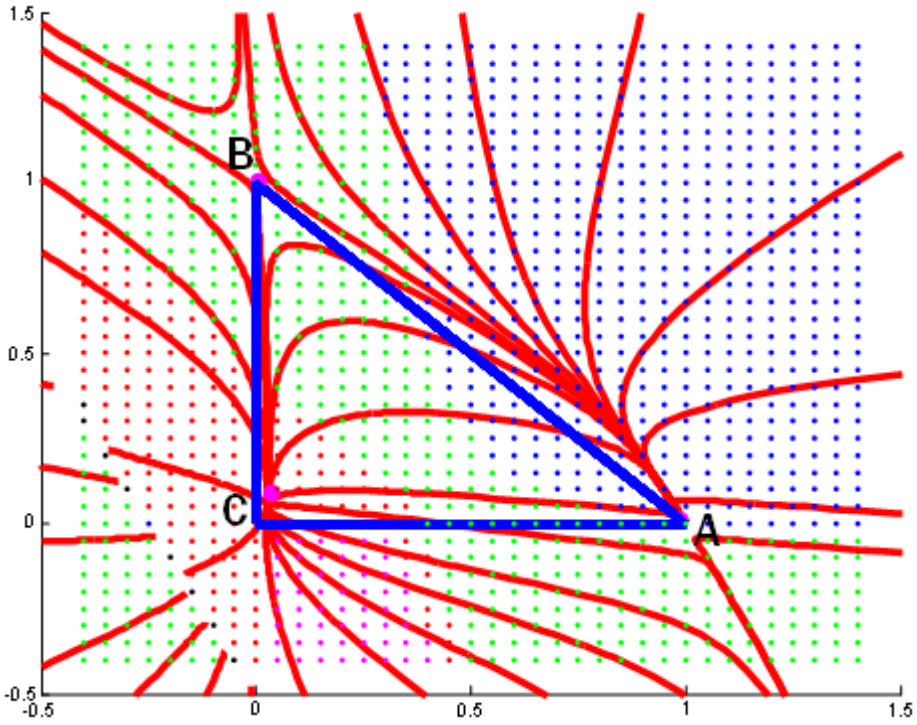


Figure 5.6: Residue Curve Map for reactive distillation at the bifurcation point (α~0.355) with the eigenvalue map where unstable region (blue), stable region (red) and saddle region (green)

We had previously seen that the S vector field **had 3 nodes**, corresponding to pure A , B and C. In addition there was a curve of discontinuity in the RCM map. If we now

examine the p maps (see Figure 5.4,5.5,5.6) we notice **4 nodes** in the diagram. Thus we can see that the reversible reaction vector introduces extra nodes to the p field. For the case of positive values of the parameter α, the solution of the process equation $\underline{p} = 0$ always leads to seven solutions except for the case of bifurcation where the number of solutions reduces to five. For example for the value of $\alpha = 0{,}22$ the solutions are [0; 1], [1; 0], [1.2306; -0.4043], [-0.04-1.622i; -0.2478-2.3436i], [-0.04+1.622i; -0.2478+2.3436i], [0.015; 0.03031], [-3.6651; 6.3692].
We can see that two of the solutions are complex and this will be the case for all values of α in the range $[0; +\infty[$. We enlarge the map represented in Figure 5.4 and we also see that one of the solution lies on the other side of the discontinuity line that is the point [-3.665; 6.369]. This solution will never move inside the MBT and furthermore it does not affect composition trajectories inside the MBT. This is the reason why we have chosen to consider only the four real remaining singular points in Figures 5.4, 5.5 and 5.6.
The implications of the above behaviour is that in the RRCMs as shown in Figures 5.4 and 5.5, the stable node moves inside the MBT. This is very interesting behaviour.Let us consider what this means from the experimental point of view: as the experiment proceeds, the still material will reach a steady state composition inside the MBT. Although this might not be all that suprising from an intuitive point of vue, previous work on other linear combination of vector fields often resulted in no stable nodes in the MBT.

Case II $-\infty<\alpha<0$

We extend the same previous analysis and we see from Figure 5.7 that:

1. the pure component A is now a fixed singular point and it is always an unstable node.

2.The stable node moves from the pure component C towards outside the positive space forming a negative stable branch. At the same time we can see that a stable node moves on the top right branch towards the pole node Π and eventually will reach that point for $\alpha \to -\infty$ in Figure 5.7.

3.An unstable node moves from outside the MBT for $\alpha > -0.89$ and at about $\alpha = -0.89$ the pure component B exchanges stability from saddle point to unstable node. For $\alpha < -0.89$, the saddle point moves inside the MBT until it reaches the chemical equilibrium curve as $\alpha \to -\infty$. Similarly we deduce again 3 different scenarios for $\alpha > -0.89$, $\alpha < -0.89$ and $\alpha = -0.89$

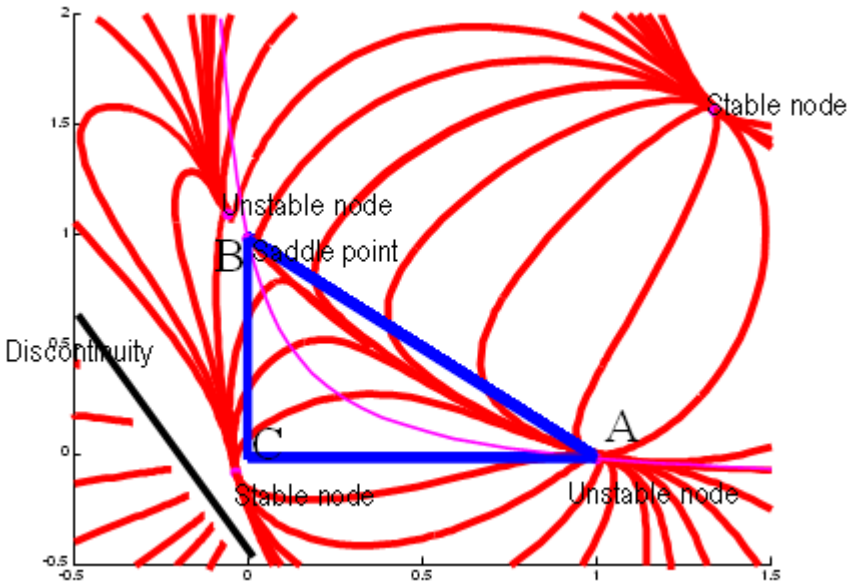


Figure 5.7: Residue Curve Map for reactive distillation; A + B ↔C, Ke=4 for α=-0.721

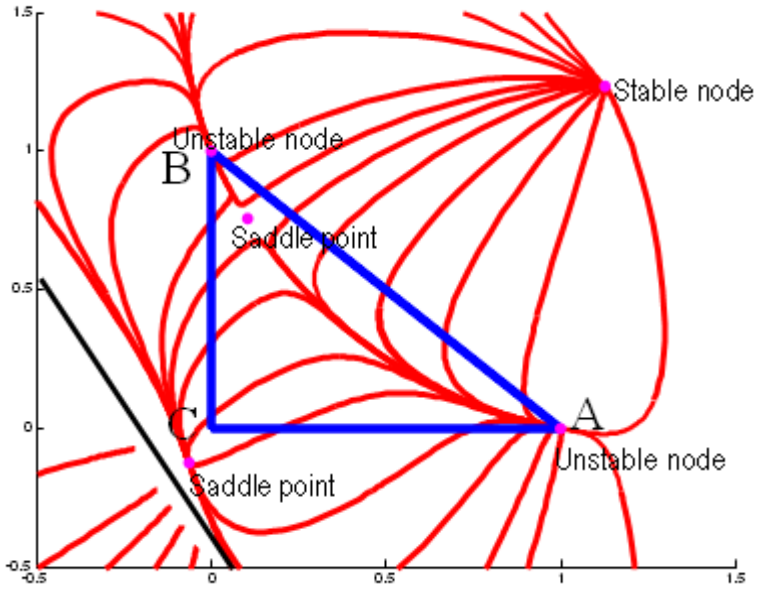


Figure 5.8: Residue Curve Map for reactive distillation; A + B ↔C, Ke=4 for α=-1.9

The numerical approach shows that for the case of negative values of the parameter α, the solution of the process equation again leads to seven solutions except for the case of bifurcation where the number of solutions again reduces to five. For example for the value of $\alpha = -0.721$ the solutions are [0; 1], [1; 0], [-1.2173; -1.8766], [-0.034; -0.0672], [-0.057; 1.109], [1.34; 1.5776], [-2.5308; 4.757].We enlarge the map represented in Figure 5.7 (see Figure 5.9) and we also see that two of the solutions lie on the other side of the discontinuity line that is the points [-2.5308; 4.757] and [-1.2173; -1.8766]. Again the movement of these singular points is limited by the discontinuity line. This is the reason why we consider the five remaining singular points in the maps represented in Figures (5.7 and 5.8).

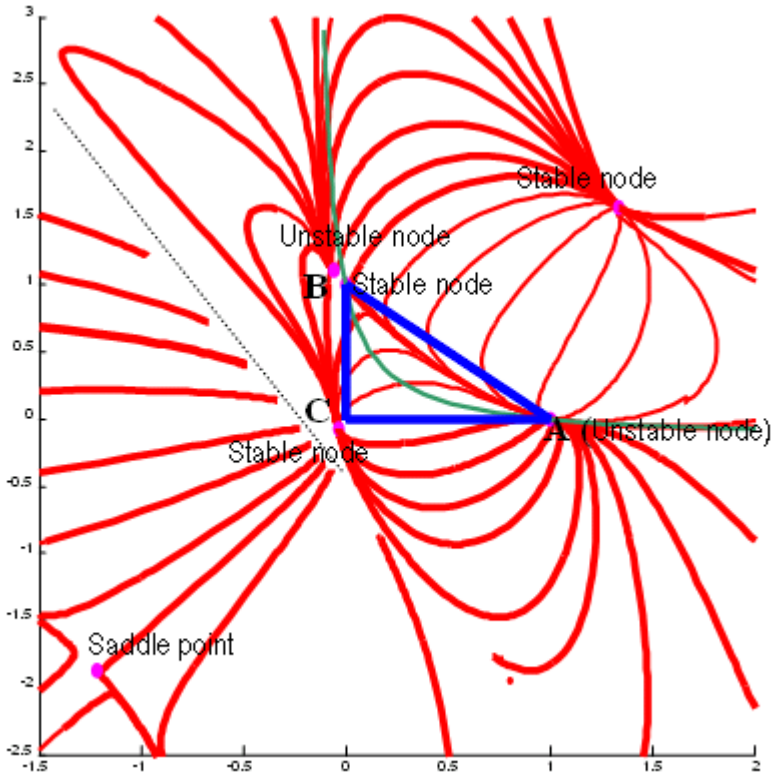


Figure 5.9: Enlarged Residue Curve Map for reactive distillation; A + B ↔C, Ke=4 for α=-0.721

The analysis further reveals the behavior of composition profiles inside the MBT is more complicated for negative value of α than positive α. For negative value of α one can see that the reaction vector $\underline{r}$ introduces a bifurcation region inside the MBT. One of the implications of the above behavior is that depending on where one starts the batch experiment one might end up with AB, BC or CA binary mixtures in Figure 5.4b. Furthermore the saddle point moves inside the mass balance triangle. This

would be interesting as a batch reactive condensing experiment. We will discuss later this case when we consider the meaning of the negative parameter α.

Discussion

In all cases we deduce that the superimposition of the reaction field on the separation vector field has two implications namely locking and movement of singular points. We will look at each case separately:

- Locking of singular points

The simultaneous batch process vector $\underline{p}$ is a linear combination of the separation vector $\underline{S}$ and the reaction vector $\underline{r}$. We call S_s the solutions of the equation $\underline{S} = \underline{0}$, r_s the solutions of the equation $\underline{r} = \underline{0}$ and p_s the solutions of the equation $\underline{p} = \underline{0}$. We see that the solutions of the equation $\underline{p} = \underline{0}$ necessarily contain solutions of the equation $\underline{S} = \underline{0}$; and that in cases where the reaction is reversible, there will always be points where $\underline{r} = \underline{0}$. We call "locked" singular points, singularities that are common to r_s and p_s.

This mathematical result affects the topology of reactive residue curve map as locked nodes do not move in the composition space and are fixed points in both the untransformed and transformed maps. We also observe that as some other singular points move in the composition space, the potential exists for these "locked" singular points to change their topological behavior. It is immediately apparent and to some extent obvious that this fact has significant implications on the resultant topology and feasibility.

In Figures (5.4), (5.5), (5.6), (5.7) and (5.8) the points A and B are locked singular points but the pure component C does not exhibit this behaviour. The locus of points that satisfy the condition $\underline{p} = \underline{0}$ depends on the orientation of the reaction vector and its magnitude.

If the magnitude of the reaction vector is changed the number of branches does not change i.e. this locus still has two branches such that one goes through the pure components B and C and the other branch passes through the unstable node A, but the curvature of the locus will change. As a result of the coexisting null points in the separation and reaction vector fields, there are always locked singular points at the pure components A and B but the nature of the singularities at those points change for some net magnitude of the reaction vector.

- Movement of singular points

All the other singular points or the net process nodes that are not locked move in the mole fraction composition space. The position of singular points on the locus of $\underline{p} = \underline{0}$ depends on the scaled size of the reaction vector via the parameter α.

5.4.4 Analytical Analysis

According to the Liapounov theorem, the linearized form of the combined process vector $\underline{\mathrm{p}}$ around the singular point $\underline{\mathrm{x}}_s$ is defined by:

$$\underline{p} = J(\underline{x}_s).(\underline{x} - \underline{x}_s) \qquad (5.7)$$

$$J(x_S)=\left[\begin{array}{ccc} & \vdots & \\ \cdots & \left(\frac{\partial p_i}{\partial x_i}\right)_{P,x=const} & \cdots \\ & \vdots & \end{array}\right]_{x=x_S} = Jacobian\ Matrix \qquad (5.8)$$

For our case the process occurring in the batch still and represented by equation 5.1a can also be rewritten generally as:

$$p_i = x_i(1-h_i)+\alpha(\upsilon_i - x_i)(x_i x_j - \frac{1 - x_i - x_j}{K_e})\ i=1,2 \qquad (5.9)$$

and

$$h_i = \frac{alpha_i}{\sum_j alpha_j x_j}\ ;\ \alpha \text{ is a scaling factor} \qquad (5.10)$$

$alpha_i$ is the relative volatility of component i

The matrix $J(\underline{x}_s)$ becomes:

$$J(\underline{x}_s)=\begin{bmatrix} J_{ii} & J_{ij} \\ J_{ji} & J_{jj} \end{bmatrix} \qquad (5.11)$$

Where

$$J_{ii} = -x_i\frac{\partial h_i}{\partial x_i}+\alpha(\upsilon_i - x_i)(x_i + \frac{1}{K_e}) \qquad (5.12)$$

$$J_{ij} = -x_i\frac{\partial h_i}{\partial x_j}+(1-h_i)+\alpha(\upsilon_i - x_i)(x_i + \frac{1}{K_e})-\alpha(x_i x_j - \frac{1-x_i-x_j}{K_e}) \qquad (5.13)$$

By assuming that the 2*x2* matrix $J(\underline{x}_s) = [a_{jk}]$ is constant, we are left with an eigenvalue problem:

$$J(\underline{x}_s)(\underline{x} - \underline{x}_s) = \lambda(\underline{x} - \underline{x}_s) \qquad (5.14)$$

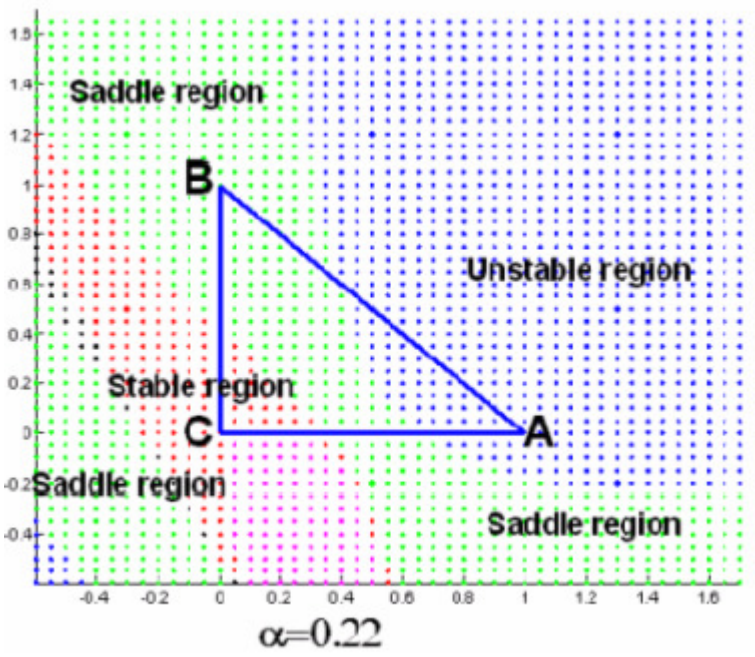


Figure 5.10: Eigenvalue Map for reactive distillation; A + B ↔C, Ke=4 for α=0.22

For different values of the parameter α we can now analyze the properties of the jacobian matrix $J(\underline{x}_s)$ at discrete points in the entire composition space. The nature of any singular point is determined by the eigenvalues of the jacobian matrix at this point. Using this approach and for different values of the parameter α, we can

calculate the eigenvalues at various points and when we plot them as shown in Figure 5.10 and 5.11. We can clearly see disparate regions of similar behaviors. In each of these regions the nature of the singularities when considered from an eigenvalue perspective are identical.

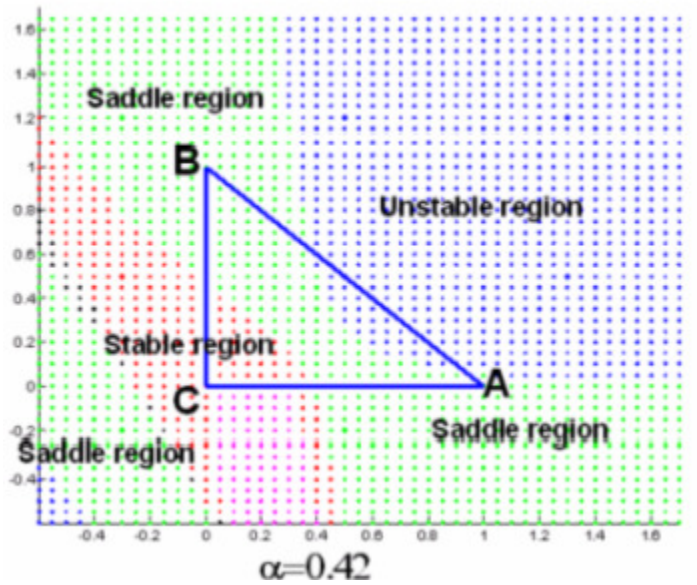


Figure 5.11: Eigenvalue Map for reactive distillation; A + B ↔C, Ke=4 for α=0.42

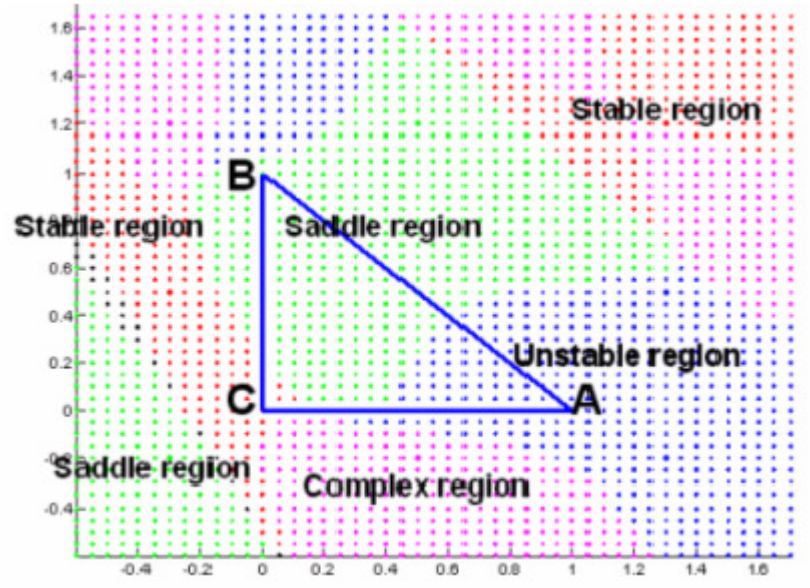


Figure 5.12: Eigenvalue Map for reactive distillation; A + B ↔C, Ke=4 for α=-0.72

For every value of the parameter α, and hence every linear combination of the separation and reaction vector fields, there is a unique eigenvalue map. We also determine (numerically) the number and position of singularities. The singular points are defined by $\underline{p} = \underline{0}$ The nature and positions of these singular points depends on the choice of the parameter α in the process vector equation.

The Figures 5.10 ,5.11 and 5.12 show discrete regions of singular points types in the composition space for particular values of α. These maps are consistent with the reactive residue curve maps described in Figures 5.4, 5.5., and 5.7 respectively with regard to the nature of singularities occurring in specific regions of the composition space. One can see that the parameter α determines the size of the different regions in the eigenvalue maps and hence will only change the details of the shape of RRCMs and not the topology.

The manipulation of this parameter by the selection of the appropriate design parameters offers an opportunity to modify the behavior of a system as by varying the parameter α, we can shift the eigenvalues map of the system independently of the reaction vector direction.This parameter is a direct reflection of the relative amount of separation to reaction permitted at any specific stage of a process.

We also see that as the regions of the eigenvalue map change, the location of the locked singular points both inside and outside the MBT does not change. We think that this is the explanation of the occurrence of bifurcations.For example in Figure 5.10 a singularity occurring at $x_1 = 1$ and $x_2 = 0$ would be unstable in nature while a singularity at $x_1 = 0$ and $x_2 = 1$ would demonstrate the characteristics of a saddle point. The region indicated in magenta corresponds to complex eigenvalues. Tapp *et al.[8]* were able to show that, for the case of the separation and mixing vectors, these complex regions of eigenvalues can not be shifted inside the MBT due to mass balance constraints. This is effectively also the case for reaction and separation and we could not find a case where for a particular parameter α the complex region lies inside the MBT.

The black region of eigenvalues in Figure 5.10 correspond to the border of stable and saddle singular points on the eigenvalues map. This region also does not move. In Figures 5.4, 5.5 and 5.6 one can see the existence of a discontinuity locus that limits composition trajectories in the reactive residue curve maps. Tapp *et al.[8][9]* showed that this locus always exists and is an artifact of the thermodynamic model. In most of the figures presented in the paper this locus is not visible as we have chosen to limit the size of the composition space. But this locus will be visible by a simple extension of the map.

The discontinuity locus is a straight line only for ideal mixtures but for non ideal mixtures this locus can be a curve and it always lies outside the MBT. In the

reactive residue curve maps represented above, we were able to see that this locus lies at the border of the stable and saddle regions of the eigenvalues map.

5.4.5 Summary of results for example 1

The eigenvalue maps provide a strong complementary tool for analyzing singular points outside the MBT. The use of these maps can help us to understand how singular points move in the composition space when one superimposes a reaction vector field on the separation vector field. This is effectively realized in the design of any item of equipment that combines the phenomenon of reaction and vapor liquid separation in the same unit.

5.5 Example 2

We now apply our analysis to a more realistic example of the metathesis of 2-pentene to 2-butene and 2-hexene where there is no net change in the total number of moles due to reaction:

$2C_5H_{10} \longleftrightarrow C_4H_8+C_6H_{14}$ (5.15)

The reaction equilibrium constant is Ke=0.25 at 298 K and the following law describes the kinetics of this reversible reaction as described by Okasinski *et al.[12]*:

$$R(x) = 0.5k_f(x^2_{c5} - \frac{x_{c4}x_{c6}}{K_e}) \quad (5.16)$$

where x_{C4} is the mole fraction of 2-butene ; x_{C5} is the mole fraction 2-pentene and x_{C6} is the mole fraction of 2-hexene.

The system is modelled using the NRTL property package, with default parameters, from ASPEN PLUS® (Table 2).

The overall process batch reactive-separation system is defined by:

$$\frac{d\underline{x}}{d\xi} = \underline{p} = \underline{S} + \alpha\underline{r} \qquad (5.17)$$

Where $\underline{S} = (\underline{x} - \underline{y}^{*})$ and $\underline{r} = \underline{\upsilon}R$

In the composition space of mole fraction x_{C4} and x_{C6}, the direction of the reaction vector is the same as that of the stoichiometric vector. The chemical equilibrium locus, defined by the equation $R = 0$, is a curve running through the pure product components Butene (x_{C4}) and Hexene (x_{C6}). The interesting behaviour of this system and in fact the difference with the previous case we have considered lies in the position of the singular points.The singular point curve is constituted of one locus branch running through all the pure component products (Figure 5.13) and never lies inside the Mass Balance Triangle.

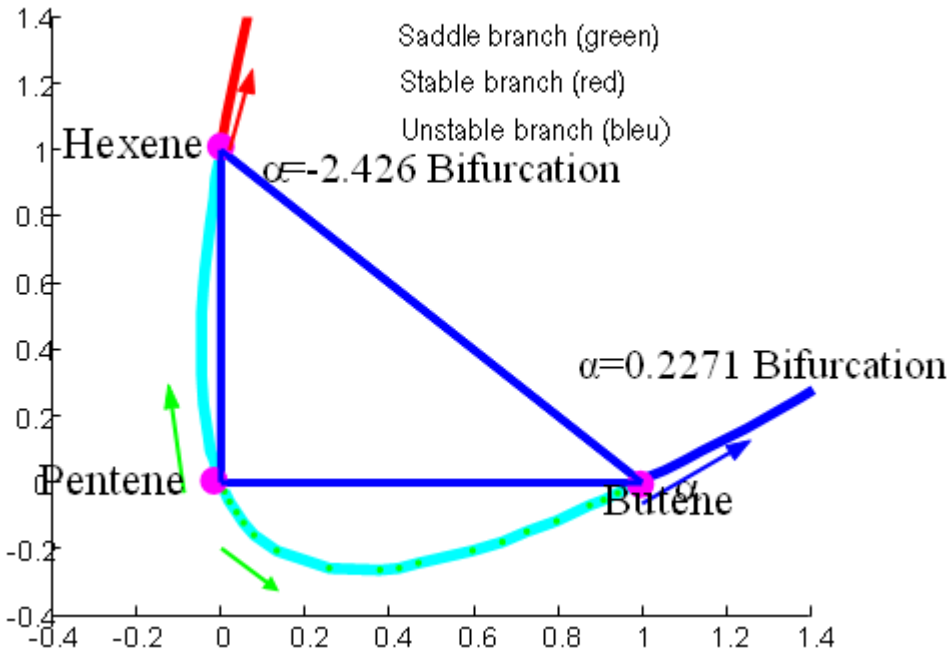


Figure 5.13: Singular points curve and bifurcation behavior for different parameter α in the range -∞≤α≤+∞ for the Butene-Hexene-Pentene System

Antoine equation	*A*	*B*	*C*
1	*8.08*	*1582.27*	*239.73*
2	*8.11*	*1592.86*	*226.18*
3	*8.38*	*1788.02*	*227.44*
NRTL	b_{ij} *(cal/mol)*	b_{ji} *(cal/mol)*	$c_{ij}=c_{ji}$
1—2	*67.29*	*-70.51*	*0.3*
1—3	*144.48*	*-12.74*	*0.31*
2—3	-2.56	56.24	0.3

Table 2: Thermodynamic Data for the Butene (1)-Hexene (2)-Pentene (3) System from ASPEN PLUS

- For positive value of the parameter α , there are 2 locked nodes: Hexene which is always a stable node while Butene is initially an unstable node. There is a branch of the singular point curve which comes from the Pentene node and runs through the Butene node. As the parameter α increases, the saddle point node initially located at the Pentene node moves along the singular point curve and at about α =0.22 it exchanges stability with the pure component Butene. At value of α above this critical value, pure component Butene is a saddle point node. Thus the Butene node switches stability from an unstable node to a saddle point node.

- For negative values of the parameter α , all the singular points are again located on the singular point curve as for positive values. There are again 2 locked nodes: Butene is always an unstable node while Hexene is initially a stable node. As the parameter α decreases the saddle point node initially located at the pure component Pentene moves along the singular point curve and at about α =-2.42 it exchanges stability with the pure component Hexene. At value of α below this critical value, pure component Hexene is a saddle point. Thus Hexene switches stability from a stable node to a saddle point node.For illustration purpose in Figures 14 and 15 we plot the composition trajectories for two different negative values of the parameter *α,* below and above the critical value.

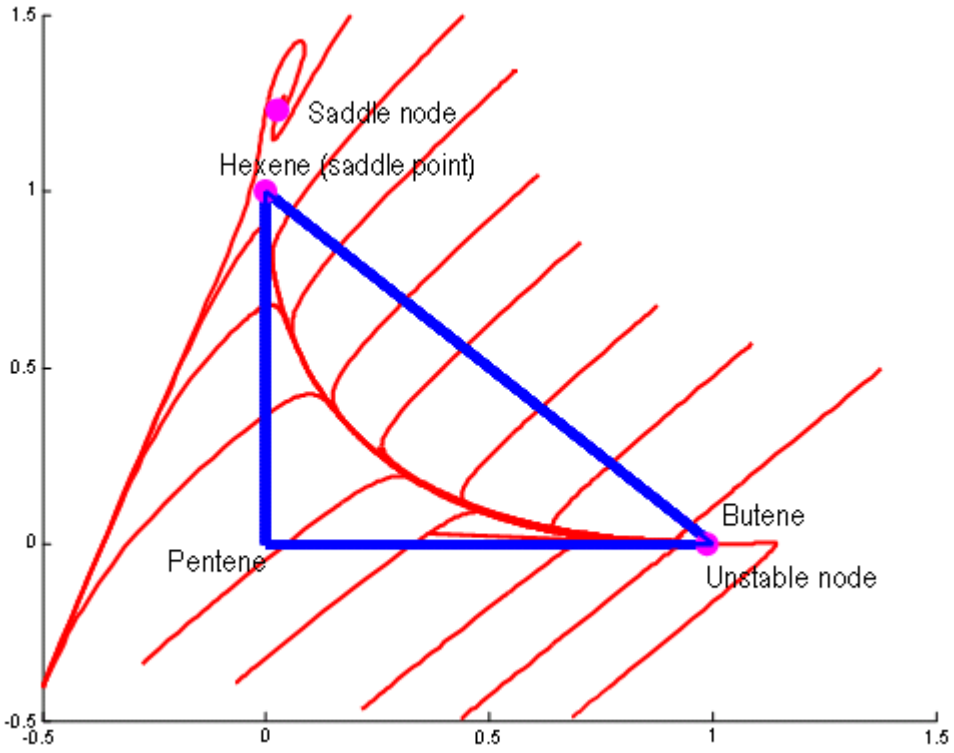


Figure 5.15: Residue Curve Map for reactive distillation;
$2C5H10 \leftrightarrow C4H8+C6H14$, Ke=0.25 for α=-5.1

These nodes occur at the intersection of the reaction and separation vector fields. Although the nodes do not move, they can change their stability which leads to fairly complex topology of the combined vector fields. In summary we have shown that a linear combination of vector fields where one of the vector fields has a continuity of nodes rather than discrete nodes, has a profound impact on the resultant topology of the combined vector field. The simple concept of "moving triangles" that holds in column profiles map,batch reaction with irreversible kinetics no longer looks as simple in this case. This leads to interesting consequences in terms of behaviour and synthesis of these systems.

For example the analysis of Figures 14 and 15 shows that for negative value of the parameter α , no nodes could be moved inside the MBT. In an experimental point of view this means that in a batch experiment for the reactive distillation of the Pentene-Butene-Hexene system, there will not be steady state compositions inside the MBT as the topology shows and that there will not be reactive azeotropes inside the MBT. The batch mixture will tend to a binary mixture on the boundary of the Mass Balance Triangle (MBT). In Figure 14 for example, if we do a batch reactive condensing experiment the batch mixture will tend towards the bifurcation curve and then will move along this curve towards the Butene node (the unstable node). It is very interesting that there is a bifurcation line inside the MBT, thus the batch mixture will be very sensitive to initial conditions.

5.6 Batch Reactive Condensation Experiment

To explain the meaning of a negative parameter α , let us consider the reverse of a boiling experiment, namely a batch reactive condensation experiment. We initially fill a still with V moles of vapor of composition y^* We allow the mixture to react, the rate of formation being given by $\underline{r}(y^*)$ We also set the conditions such that the mixture is at its dew point P. We remove at a rate $\dot{L}$ liquid of composition x from the still where x is the liquid composition in equilibrium with vapor of composition y^*. The mole balance describing this system, assuming that the number of moles does not change with reaction is:

$$\frac{-dy^*}{d\varepsilon} = (x - y^*) - \alpha \underline{r}(y) \qquad (5.18)$$

if we compare this equation to the equation describing the batch boiling experiment we see that geometrically this would be similar to a negative α and following the

batch boiling curves in the opposite direction(i.e from stable node to unstable node for example).

The position of the nodes would be fairly similar and in difficult separation(i.e $x - y^*$ small), the similarity would be greater. For example Figure 5.16 would be interesting as a batch reactive condensing experiment: in this case the batch mixture will tend towards the bifurcation curve and then will move along this curve towards the pure components B or C (unstable nodes). It is very interesting that there is a bifurcation line inside the MBT, thus the batch mixture will be very sensitive to initial conditions (Figure 5.16).

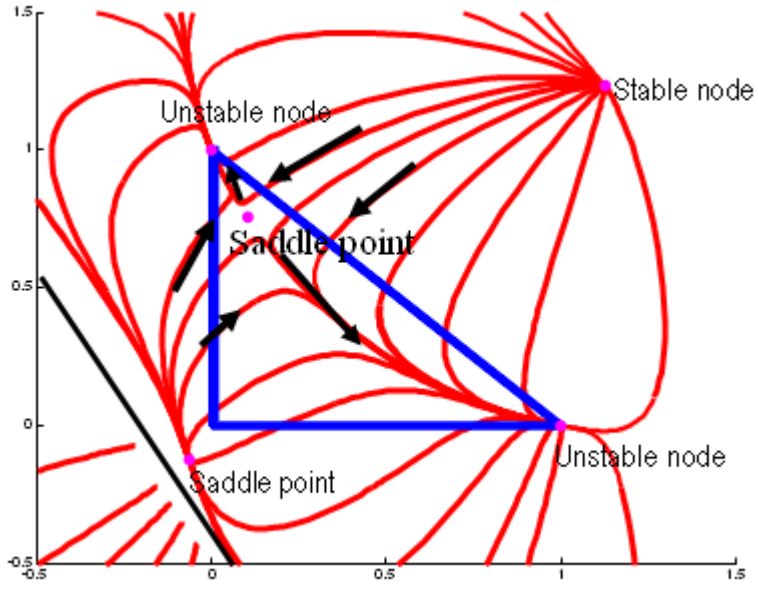


Figure 5.16: Residue Curve Map for reactive condensation;
A + B↔ C, Ke=4 for α=-1.9

5.7 Conclusion

We have analysed the positions of singularities in the transformed phase diagram when one superimposes a single chemical reaction with nodes corresponding to a reversible chemical reaction on a separation vector field. The analysis of the diagram phases and eigenvalues maps provides evidence that the topology of the reactive residue curve maps depends on the direction of the reaction vector. The analysis further reveals that by adding a vector field with a continuous curve of nodes as found in reversible chemical reaction,one would increase the number of nodes (singular points) in the separation vector field S. This leads to vector maps that are much more complex than for other systems such as linear combination of separation and mixing or separation and irreversible chemical reactions. Another feature that arises from the curve of nodes in the reversible chemical reactions map is the occurrence of locked nodes.This analysis is far from complete. However we believe this work introduces elements to ease the analysis of behaviors observed by previous researchers.

Bibliography

1. Ung, S., Doherty.M.F," Vapor-liquid phase equilibrium in systems with chemical reactions" Chemical Engineering Science, 1995, 50, pp.23-48

2. Barbosa, D., Doherty.M.F,"The simple distillation of homogeneous reacting mixtures" Chemical Engineering Science, 1988, 43, pp.541-550

3. Hauan, S., Westerberg, A., Kristian, L.,"Phenomena-based analysis of fixed points in reactive separation systems" Chemical Engineering Science, 2000, 55, pp. 1053-1075

4. Hauan, S. and K.M.Lien,"A phenomena based design approach to reactive distillation"Trans.I.Chem.E, 1998, 76(A), pp.396-407

5. Hoffmaster, W., Hauan, S.," Difference points in reactive and extractive cascades. III-Properties of column section profiles with arbitrary reaction distribution" Chemical Engineering Science, 2004, 59, pp. 3671-3693

6. Huang, Y-S., Qi, Z., Schlunder, E-U., Sundmacher, K," Residue curve maps for reactive membrane separation" Chemical Engineering Science, 2004, 59 (14), pp.2863-2879

7. Venimadhavan, G., G.Buzad and M.F.Doherty,"Effects of kinetics on residue curve maps for reactive distillation."AICHE Journal, 1994, 40(11), pp. 1814-1824

8. Tapp, M., Holland, S., Glasser, D. & Hildebrandt, D.,"Column Profile Maps 2. singular points and phase diagram behaviour in ideal and nonideal systems " Industrial and Engineering Chemistry Research, 2004, 43 (14), pp 3590-3603

9. Tapp, M., Holland, S. T., Hildebrandt, D., Glasser, D.,"Column Profile Maps Part A: Derivation and interpretation" Industrial and Engineering Chemistry Research, 2004, **43**(2), pp 364-374

10. Holland, S.T., Tapp, M., Glasser, D., Hildebrandt, D., Hausberger, D.,"Novel separation system design using "moving triangles" Computers and chemical engineering, 2004, **29** (1), pp.181-189

11. Doherty, M.F. and Malone, J.D.," Conceptual Design of Distillation Systems" McGraw Hill, New York, 2001

12. Okasinski, M.J., Doherty, M. F.," Design method for kinetically controlled staged reactive distillation columns" Industrial and Engineering Chemistry Research, 1998, 37 (7), pp 2821-2834

6 Chapter 6 Reactive Column Profile Map Topology: Continuous Column with non Reversible Kinetics

This chapter has been presented at AICHE annual meeting 2006 under the title:Reactive Residue curve map:analysis of the topology for a continuous reactive distillation column. It has been submitted to the Computers & Chemical Engineering Journal and is currently under review

6.1 Abstract

In this chapter we present a topologically based approach to the analysis and synthesis of reactive distillation columns. We extend the definition of Tapp et al. [2] of a Column Section in non reactive distillation column to a Reactive Column Section (RCS) in a reactive distillation column. A RCS is defined as a section of a reactive distillation column in which there is no addition or removal of material or energy. We introduce the concept of a Reactive Column Profile Map (RCPM) in which the profiles in the RCPM correspond to the liquid composition profiles in the RCS. By looking at the singular points in the RCPM, it is demonstrated that for a single chemical reaction with no net change in the total number of moles, the bifurcation of the singular points depends on both the difference point as introduced by Hauan et al. [1] as well as the direction of the stoichiometric vector. These two vectors combine to define what we call the Reactive Difference Point Composition. We show that there only certain feasible topologies of the RCPM and these depend only on the position of the Reactive Difference Point Composition. We look at a simple example where the Vapour Liquid Equilibrium (VLE) is ideal and show that we can classify regions of

Reactive Difference Point Compositions that result in similar topology of the RCPM. Thus by understanding the feasible topologies of the RCPM, one is able to identify profiles in the RCPM that are desirable and hence one is able to synthesize a reactive distillation column by combining RCS that correspond to the desired profile in the RCPM.

We believe that this tool will help understand how and when reaction could introduce unexpected behaviors and this can be used as a complementary tool to existing methods used for synthesis of reactive distillation columns.

6.2 Introduction

Doherty et al. [5][6][7][8][9][10][11][12][15][16] applied the well known concept of Residue Curve Mapping technique to systems undergoing equilibrium reactions. For example they were able to show that for kinetically controlled reactions and for constant heating policy input, one could derive an autonomous formulation of the Reactive Residue Curve Map (RRCM) in term of the Damkohler number.

On the other hand the behavior of fixed points has been used as design tools for reactive distillation columns. Buzad et al [7] were able to show that fixed points change the position when the Damkohler number changes. They use the continuation method in order to relate the composition of the fixed points to the Damkohler number. They conclude that in the case of staged columns for example, stripping and rectifying profiles intersect only for some relative position of the fixed points via the Damkohler number Da.

Hauan [4] consider a reactive distillation column as the sum of three independent vector phenomena: mixing, separation and reaction. A kinetic fixed point happens when the vector contribution of the non-zero phenomena cancel each other. He suggests further that by altering the mixing or reaction vector length via reflux ratio or

external feeds for example, one could avoid fixed points in a reactive distillation column.

Later Hauan, Ciric, Westerberg and Lien [1] [15] introduce the concept of scalar/vector difference point in reactive cascades. The reactive cascade difference points are defined as points resulting from the combination of the stoichiometric vector and product compositions. In the case of a single chemical reaction, for example, the difference points move in the direction of the chemical reaction. By using this approach, they were able to determine the number and location of reactive and non reactive stages.

This chapter reintroduces the concept of the difference point and many of the conclusions of Hauan et al.[1] and Hoffmaster et al.[13][14] are revisited from the perspective of CPM and RCPM theory. The essence of this paper is about synthesis of reactive distillation columns via RCPM and Column Profile Map (CPM). In particular we show when reaction could introduce unexpected behavior.

6.3 Review of CPM's for systems described by ideal thermodynamic

The Residue Curve Map (RCM) extended to the entire space (positive and negative space) has been plotted by Tapp et al. [2] as it is shown in Figure 6.1 below. They were able to distinguish 7 different regions of similar composition profile behavior in the RCM and these regions are indicated on Figure 6.1.

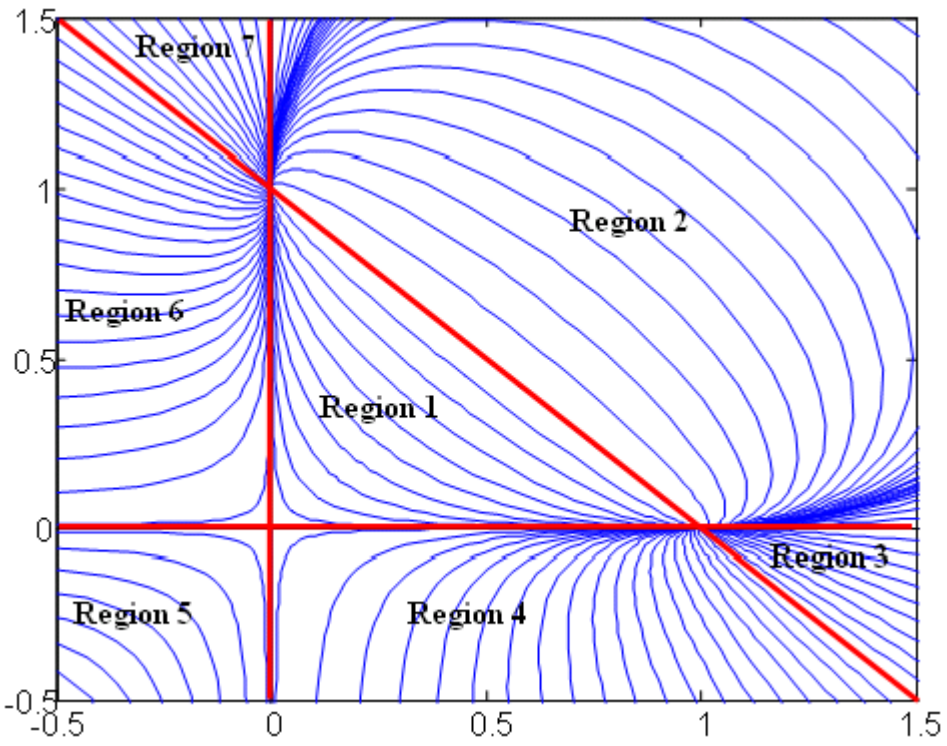


Figure 6.1: Extended Residue Curve Map (RCM) for ideal system

Tapp et al. [2] consider the case when one adds a mixing vector with parameters XΔ (difference composition point) and R (reflux ratio) to the separation vector. These parameters define the length and the direction of the mixing vector. They were able to draw a full profiles map as in the case of the Residue Curve Map (RCM) which they referred to as the Column Profile Maps (CPM).By looking at the behaviors of the CPM, Tapp et al. [2] were able to highlight a very interesting fact: namely that the CPM solutions have the same topology as the RCM. However all the original singular points although presents have been shifted in the composition space of mole fractions or Mass Balance Triangle (MBT). This shifting of nodes depends primarily on the location of the difference composition XΔ. Tapp et al. [2] studied different cases

where the difference point XΔ lies in each of the seven regions of the extended composition shown as shown in Figure 6.1. To illustrate the concept we present some of the main results of Tapp et al. [2] :

- X_Δ in Region I

When the difference point X_Δ is located in Region I, One can see that region 4 previously lying outside the MBT for the RCM can be moved inside the MBT. The stable node as well moves inside the MBT. The topology of this CPM is most familiar as it corresponds to conventional rectifying (stripping) profiles.

- X_Δ in Region II

The difference point X_Δ is located in Region II on the extended map. In this case the regions 2 and 4 previously lying outside the MBT moved inside the MBT. All the singular points of the separation vector (unstable node, stable node, saddle point) moved outside the MBT. This is very interesting behavior as it implies that there are no singular points in the mass balance space, i.e. in the region of positive mole fractions.

- X_Δ in Region I

Two of the singular points; namely the stable node and the saddle point, move inside the MBT. The shifting of the saddle point inside the MBT is indeed an interesting behavior. Two separatrix lines near the light–intermediate axis and the heavy-intermediate axis are moved inside the MBT.
However for the heavy-intermediate separatrix all the profiles move towards the stable node and so these profiles are not sensitive to the initial condition. But profiles

starting around the light-intermediate separatrix axis would however still be sensitive to initial point.

- X_{Δ} in Region V

Again all the singular points move outside the MBT. However a separatrix boundary appears in the region close to the intermediate-low boiling axis. This means that a region of instability near the light-intermediate axis is moved into the MBT. Thus the liquid composition would be very sensitive to initial conditions in this region. For example in this case one could find a profile that move into the intermediate corner. Hence the intermediate component, which was an unstable node in the RCM, now has profiles moving directly into it. One might therefore be able to produce pure intermediate component by using a profile that runs into the intermediate corner.

6.4 Preliminary Definitions

We extend the definition of Tapp et al. [2] and we define *a* Reactive *Column Section (RCS) as section of the countercurrent reactive column in which no feed or energy is added or removed between the inputs and outputs of the column*. Thus for example the column shown in Figure 6.2 has 4 column sections and any (or indeed all) of these sections could have reaction occurring in them and thus be a RCS. We now consider that the column section expanded in Figure 6.2 is a RCS and in order to develop a model describing the equipment we assume:

- The chemical reaction only takes place in the liquid phase
- The liquid and vapor molar overflow are constant in the equipment
- Constant heat of reaction
- For simplicity we will assume that there is no change in the number of moles with reaction. This assumption can be relaxed if necessary and the

discussion below would still apply with minor changes to the direction of movement of the difference point.

6.5 Mathematical model of a Reactive Column Section

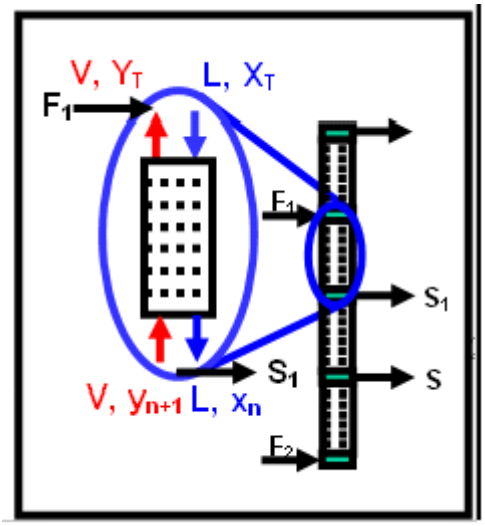


Figure 6.2: Reactive distillation column with 4 column sections

If we consider the occurrence of only one chemical reaction, the total and components balances in the liquid phase over the column section in Figure 6.2 are given by:
If we consider the occurrence of only one chemical reaction, the total and components balances in the liquid phase over the column section in Figure 6.2 are given by:

$$0 = -L_T - V_{n+1} + L_n + V_T - \xi \sum \upsilon_i \tag{6.1}$$

and

$$0 = -L_T X_T - V_{n+1} y_{n+1} + L_n x_n + V_T Y_T - \xi \upsilon \tag{6.2}$$

ξ is the total turnover of the reaction, υ is the stoichiometric coefficient , $\sum \upsilon_i$ is the sum of the stoichiometric coefficients. From (6.1) we know that if $\sum \upsilon_i = 0$ then:

$$L_{n+1} = L_T + V_{n+2} - V_T \tag{6.3}$$

We also set that:

$$\Delta x_\Delta = VY_T - L\ X_T \tag{6.4}$$

and

$$\Delta = V - L \tag{6.5}$$

In (6.4) the term $\underline{x}_{\Delta}$ is the composition difference point and Δ is the flow rate difference point introduced by Hauan et al.[1] and adapted by Tapp et al. [2]. Note that the compositions at the ends of the column section are related via equation (6.4) when the total number of moles due to the chemical does not change or in the case of extractive cascades without reaction. We put (6.3) and (6.4) in (6.2) under the assumption that the vapour and liquid flow rates V and L are constant and we get:

$$0 = L(x_{n+1} - x_n) - V(x_{n+1} - y_{n+1}) - \Delta x_{n+1} + \Delta x_{\Delta} - \xi \upsilon \tag{6.6}$$

Writing (6.6) in vector differential form leads to:

$$\frac{d\underline{x}}{dn} = \frac{V}{L}(\underline{x} - \underline{y}) + \frac{\Delta}{L}(\underline{x}_{\Delta} - \underline{x}) - \frac{\xi}{L}\underline{\upsilon} \tag{6.7}$$

We can rearrange (6.7) to give:

$$\frac{d\underline{x}}{dn} = \frac{V}{L}(\underline{x} - \underline{y}) + \frac{\Delta}{L}(\underline{x}_{\Delta R} - \underline{x}) \tag{6.8}$$

Where

$$\underline{x}_{\Delta R} = (\underline{x}_{\Delta} - \frac{\xi \underline{\upsilon}}{\Delta}) \tag{6.9}$$

The term $\underline{x}_{\Delta R}$ is a reactive composition difference point and it is a linear combination of the mixing difference point $\underline{x}_{\Delta}$ and the term $\frac{\xi \underline{\upsilon}}{\Delta}$, i.e. $\frac{\Delta}{L}\underline{x}_{\Delta} - \frac{\xi}{L}\underline{\upsilon}$

Unlike the non reactive column section where the composition difference point $\underline{x}_{\Delta}$ was constant but could change from one section to another via feed streams addition or streams removal, the reactive composition difference point $\underline{x}_{\Delta R}$ is not constant in the reactive column section but changes its magnitude in the direction of the stoichiometric vector as found by Hauan et al.[1]. For example the difference point would move from the point at the top of the reactive column section in the direction of the stoichiometric vector. The distance the difference point moves would depend on how much reaction occurs. Hauan et al. [1] showed that the use of the difference point composition could increase vastly design flexibility as well as effective modelling of complex systems (distillation column sections, absorption or stripping units) as the difference point was not restricted to product compositions or values within the Gibbs or mass balance triangle (MBT). Hoffmaster et al. [13] [14] further

demonstrated how the theory of difference points may be applied to practical design of complex separation cascades with reaction. However in this paper we will try to link the difference point theory and the Column Profile Maps (CPM) concept. To simplify the approach we have assumed that the reaction happens on one tray i.e. the difference point moves suddenly and then stays fixed for the reactive column section. This assumption cancels the need of the reaction extent computation along the reactive column section as this would require defining the kinetics and the change in the liquid holdup inside the RCS. We assume discrete value of the total extent of reaction so that we might be able to assess the impact of the difference points on Reactive Column Profiles by releasing all other constraints. Although the incrementally computation of the extent of reaction will provide a vast sequence of topologies, it will be not necessary at the early stages of Process Synthesis as there is only a limited number of possible different topology for a given stoichiometric vector direction and top compositions to the column section. The amount of reaction in a given stage will determine when bifurcations occur for a particular system for example but will not affect the type of bifurcations occurring as this is fixed by the direction of the reaction. In this regard the above assumption will provide the same set of qualitative results as a computer modelling. One notices as well that in an analogous manner to Hauan et al. [1] and Tapp et al. [2] we define the difference point flowrate of a reactive column section (RCS) as Δ=V-L which under our assumptions is also constant. We will particularly consider the topological implications of the movement of the reactive difference point $\underline{x}_{\Delta R}$. By looking at the change of the maps one is able to scan many options and relate the topologies of RCS to those of non- reactive column sections.

6.6 Reactive Difference Point Composition and Application

6.6.1 Stoichiometric vector

To understand how the difference point composition is helpful in understanding the topology of the Reactive Column Section (RCS), one need to consider the behaviour of the reactive difference point $\underline{x}_{\Delta R}$ .Because the extent of the chemical reaction changes as the chemical reaction proceeds, the reactive difference point $\underline{x}_{\Delta R}$ will move in the direction of the stoichiometric vector $\underline{\upsilon}$. For the chemical reaction A+B→2C, one can plot the stoichiometric line SL and find out that different cases emerge as the reactive difference point $\underline{x}_{\Delta R}$ crosses in different regions of the extended composition space of mole fractions.

In this chapter we are dealing only with irreversible kinetics as the reaction vector field map in this case has the same topology as the mixing vector field for non reactive case. For this reason the Column Profile Map (CPM) concept can be extended to reactive distillation column without any further complexity. This is not the case for reversible kinetics where we found very complex behaviors as shown in chapter 5.

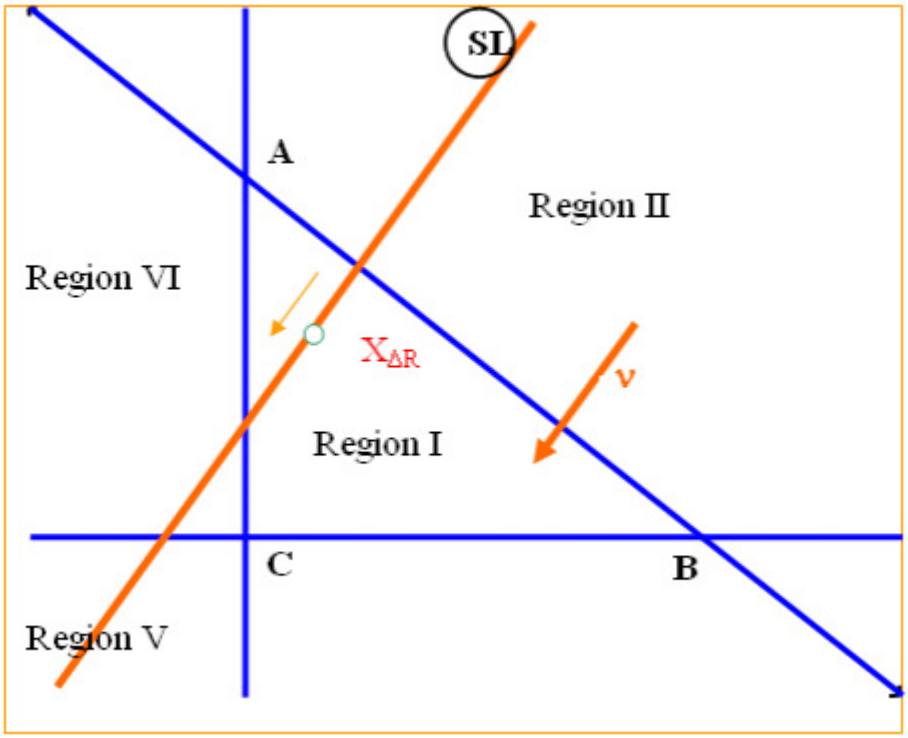


Figure 6.3: Location of the reactive difference point as the chemical reaction proceeds for reaction A+B→2C

We consider the line SL in Figure 6.3 and we analyze the topological implications as the chemical reaction occurs in the RCS. We note that initially $\underline{x}_{\Delta R}$ is located in region I. The topology of the RCPM with $\underline{x}_{\Delta R}$ in region I would move the stable node inside the MBT. As $\underline{x}_{\Delta R}$ crosses into region VI for example the topology of the RCPM would change, shifting the saddle point inside the MBT and introducing at the same time a bifurcation region into the positive space. In this case one might find that the column profile bifurcates under certain operating conditions. Further reaction will moves $\underline{x}_{\Delta R}$ into region V. When $\underline{x}_{\Delta R}$ is in this region the major factors that will change is that the column will not have a pinch point in the MBT. Furthermore the

bifurcation that could occur for profiles along the intermediate-high boiling axis in region VI will no longer occur in region V. This will possibly simplify the behaviour, design and control of these RCS in this region.

6.6.2 Relationship between CPM and RCPM

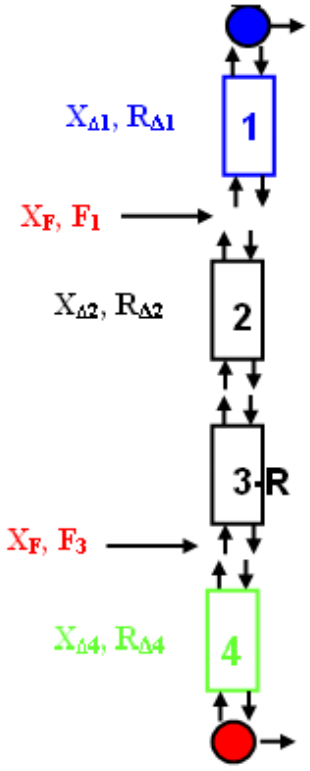


Figure 6.4: Figure 4: Distillation Column with 4 Column Sections (CS)

We have seen that the equation for a RCS is the same form as that for a non-reactive column section apart from the fact that the reactive difference point $X_{\Delta 1}$ changes along the stoichiometric vector for the RCS. We can thus visualize that as the reaction

proceeds in the RCS, the reactive difference point moves along the stoichiometric vector. Hence the map that describes the possible column profiles will also change and the resultant topology at a fixed reactive difference point and Δ will correspond to the CPM with the difference point equal to the reactive difference point and the same value of Δ.Hence the CPM of Tapp et al. [2] can be used to understand the shifting of topology with reaction. This arises from the fact that both equipments can be described as a linear combination of a separation vector field S and a vector field described by the difference vector $\underline{X}_{\Delta}$. The Reactive Column Section on the other hand is described by a linear combination of the separation vector field S and a reactive difference point $\underline{X}_{\Delta R}$ which we can consider to be variable in this case. When the mixing vector field is the same as the reaction vector field, we can see that the resultant field resulting from the linear combination must be the same. Hence the interesting result is that the two maps are identical: the CPM with the difference point equal to the reactive difference point of the RCPM and the same value of Δ.

6.7 Application

What implication does that have on the synthesis?

Let us consider a first column section with a $X_{\Delta 1}$= [0.01 0.7] and $R_{\Delta 1}$ as shown in Figure 6.4. This first column section needs to operate as a rectifying section with $X_{\Delta 1}$ = X_D thus the profile has to start at the difference point composition and this is represented as the dashed black line in Figure 6.5.

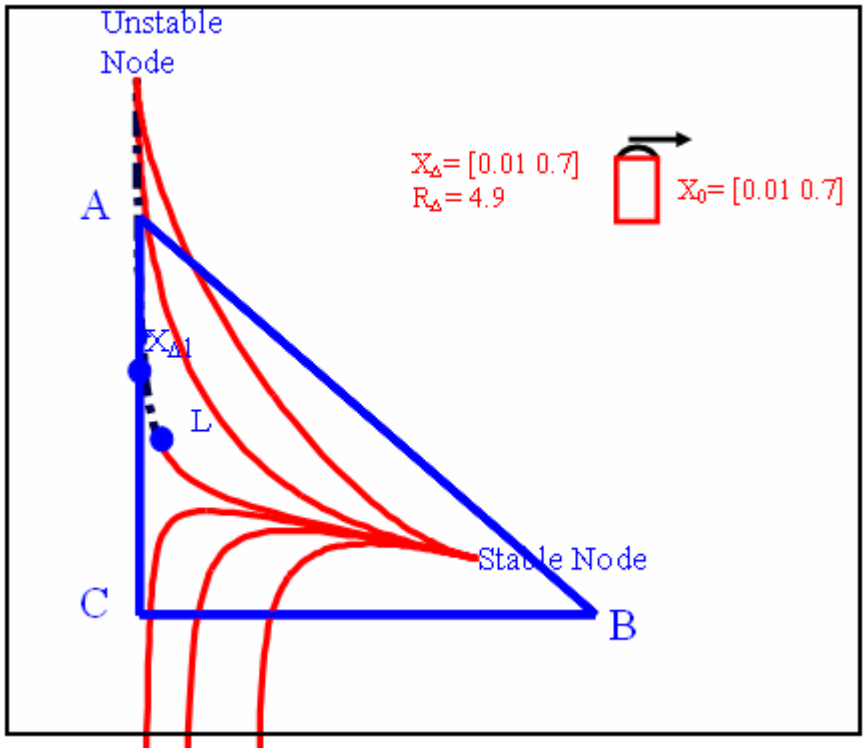


Figure 6.5: Column profile for the first column section for XΔ1 = [0.01; 0.7]

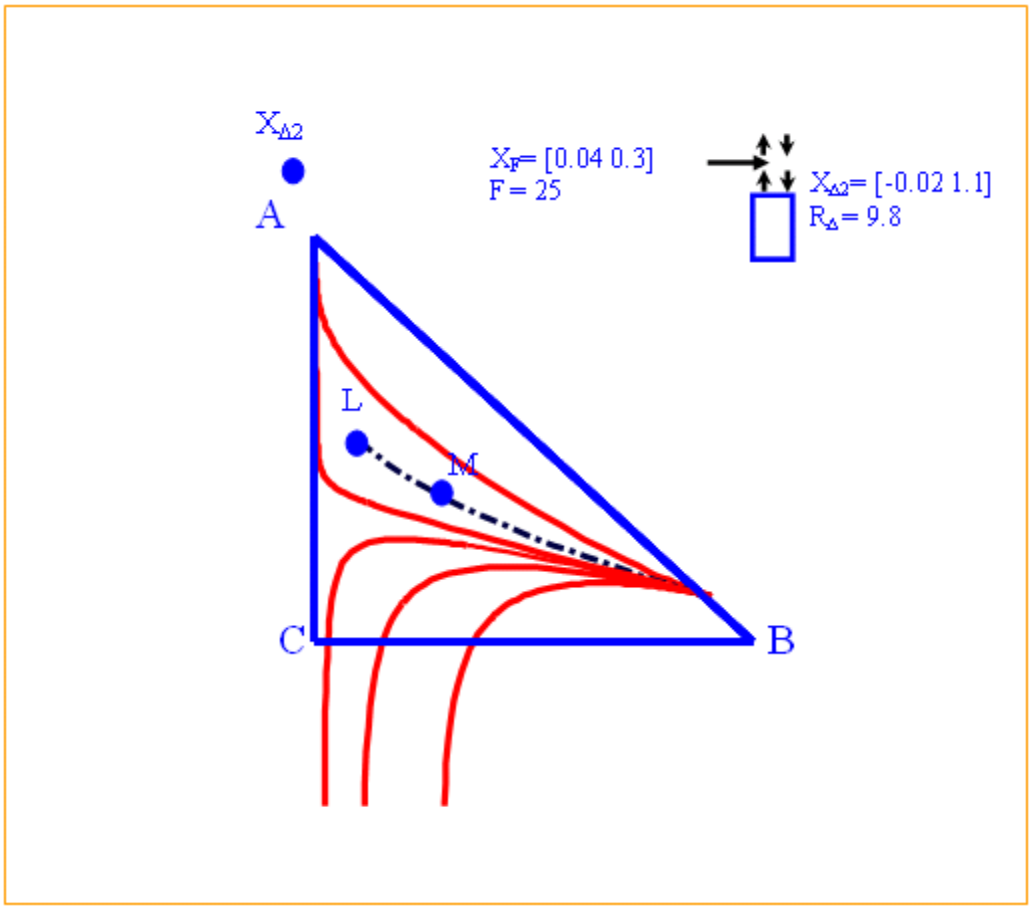


Figure 6.6: Column profile for the second column section for XΔ2 = [-0.021; 1.1]

Let us suppose that we add feed material of composition X_F= [0.04; 0.3] at point L. This results in a new difference composition $X_{\Delta 2}$ and $R_{\Delta 2}$ as shown in Figure 6.6 and calculated using:

$$X_{\Delta 2} = \frac{\Delta_1 X_{\Delta 1} - F X_F}{\Delta_2} \quad and \quad \Delta_2 = \Delta_1 - F \tag{6.10}$$

Tapp et al. [2] were able to show that the term $\Delta X_{\Delta i}$, is the net molar flowrate of a component i in a column section. This molar flowrate remains constant throughout a non reactive column section under the assumption that the liquid and vapour flowrate are constant. However by feed addition and sidestream withdrawal we can manipulate the sign of $\Delta X_{\Delta i}$ for the individual components so that some are positive while others are negative. From Equation 6.10 One can see that $X_{\Delta 1}$, X_F and $X_{\Delta 2}$ lie on a straight line and that the difference composition $X_{\Delta 2}$ lies in region VII. The second column section needs to have a profile that runs at point L on the first profile starting at the composition $X_{\Delta 1}$.

This can be realized by using a difference point $X_{\Delta 2}$ in region VII with a high reflux ratio of R_Δ = 9.8. This results in a CPM shown in Figure 6.6. The dashed black line in Figure 6 represents the second column section profile.

Let us now suppose that at point M we add reaction in a third reactive column section (RCS): the difference point $X_{\Delta 2}$ will move from region VII to region VI along the stoichiometric line as the chemical reaction proceeds inside the RCS. If we suppose that the reactive difference point is equal to $X_{\Delta 3}$= [-0.6 0.52] after adding a certain amount of reaction, then the resultant composition profile inside the RCS is shown as the black dashed line in Figure 6.7.One notice that we have chosen the difference point $X_{\Delta 3}$ along the stoichiometric vector (-1, -1, 2) so that the column could converge. But we could have stopped $X_{\Delta 3}$ anywhere along this line. It is basically the designer choice as to where to place $X_{\Delta 3}$ within the constraints that the column converge i.e. how much reaction occurs. The reactive column profile runs towards the

highest boiling component and at point N we can add feed material as shown in Figure 6.8 to achieve the desired separation.

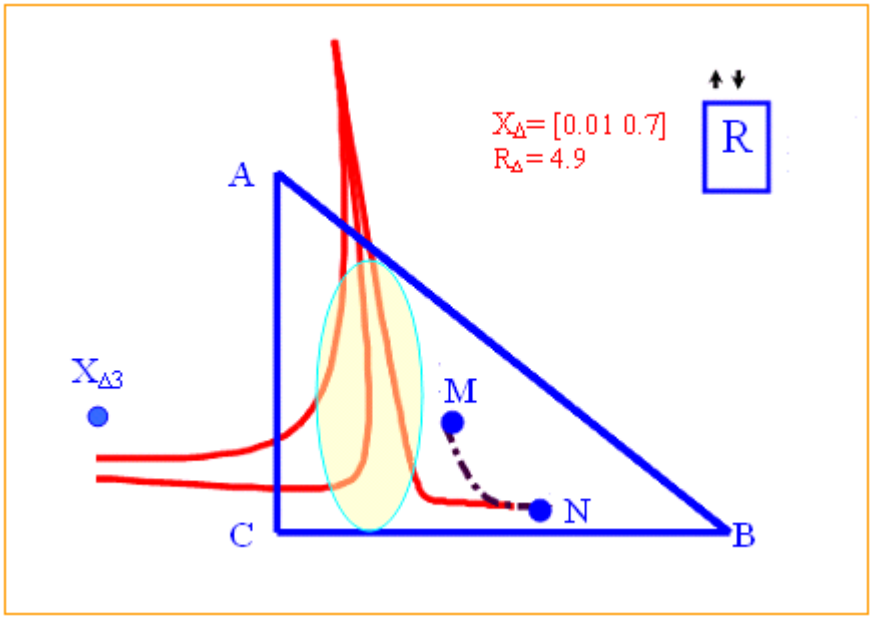


Figure 6.7: Reactive column profile for the third column section for XΔ3 = [-0.6 0.52]

The last column section needs to operate as a stripping section with $X_{\Delta 4} = X_B$ thus the profile has to end up at the difference point composition. This is achieved by adding an appropriate amount of feed material and the column profile is represented as the dashed black line in Figure 6.8.

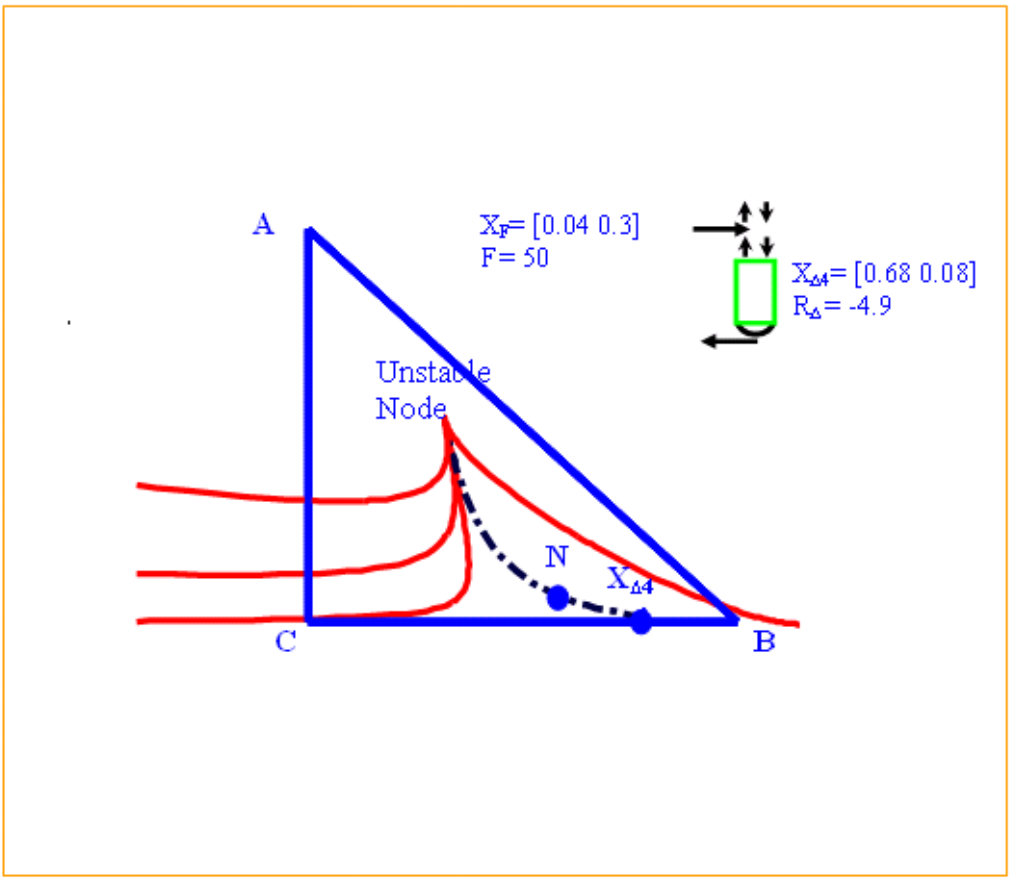


Figure 6.8: Column profile for the fourth column section for XΔ4 =XB= [0.68;0.08]

However if we have added a little more reaction at point M such that the resultant reactive difference point in the RCS was $X_{\Delta 3}$= [-1.1 0.02], the composition profile inside the reactive column section would have looked like in Figure 6.9. One can see that dashed black profile runs towards the intermediate boiler and that the simulation will not converge. This is the case of bifurcation we mentioned earlier due to the fact that the difference point $X_{\Delta 3}$ lies in region VI and as we said earlier there is a light-intermediate separatrix axis inside the MBT.

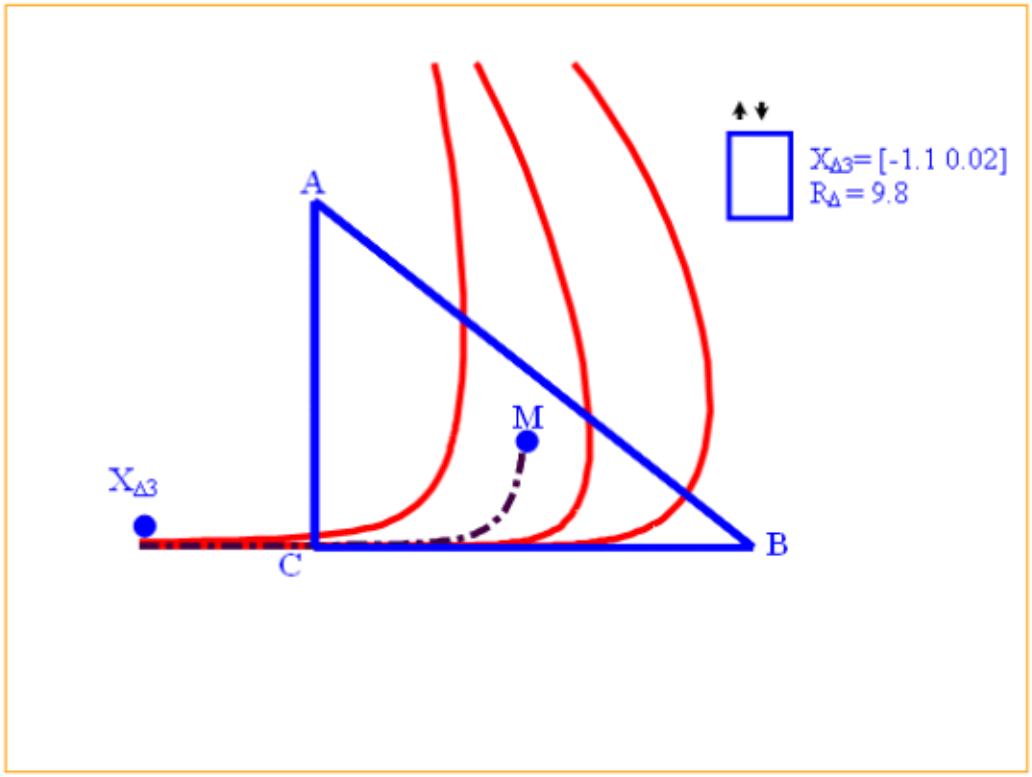


Figure 6.9: Reactive column profile for the third column section for XΔ3 = [-1.1 0.02]

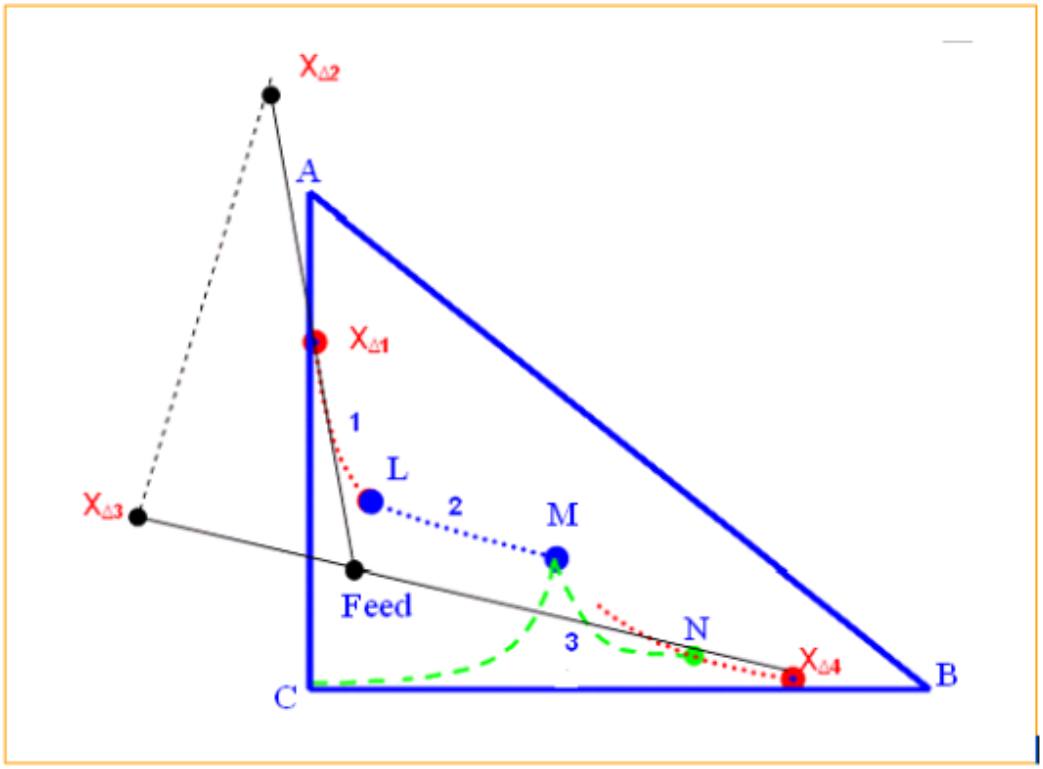


Figure 6.10: Sequence of column section profiles for the entire distillation column

6.8 Discussion

It has been shown that the close interaction of reaction and separation in reactive distillation systems may display a complex effect on the singular points of the system (nodes and saddle points) Venimadhavan et al. [8][19].When different control parameter change (liquid hold up, catalyst level, production rate etc…), the topological texture of column profiles change and new structures appear which we refer to as Reactive Column Profiles. The main consequence being that the feasibility changes when the topology changes. Our analysis of Reactive Column Profile Map

(RCPM) shows that as new patterns appear separatrix line(s) can be moved inside the MBT introducing instability regions in the composition space (bifurcation regions). Different methods have been used to represent these changes among other the continuation methods. However in this paper we have coupled the difference point analysis of Hauan et al. [1] and the graphical generation of Column Profile Map (CPM) [2] and show that:

1. Reactive Column Profile Map can be used to understand column behavior in terms of the operability and stability criterion. In fact an important role in successfully designing reactive distillation columns lies in avoiding areas of instability where a small change in the composition of the initial condition could result in profiles running in the "wrong" direction (bifurcation regions). By handling carefully the reactive difference point through the use of RCPM one can achieve profiles that avoid these regions of instability. But more generally the shifting of singularities of the RCPM can be used to introduce any desirable system behavior in the MBT space. One might even be able to sample the pure "saddle" composition. One can also use this technique to identify what conditions will avoid the possibility of stationary points in the MBT.
2. One has the possibility to subdivide creatively the entire distillation column in column sections with difference points as shown by Hauan et al. [1]. Each difference point corresponds to a particular topology of the Reactive Column Profile Map. One is then able to generate a whole range of difference points within the limitations of the mass balance and achieves a vast range of profiles. These difference points, however, must be generated within the column section as shown by Hoffmaster et al.[13] [14].By capturing all different topologies, the Reactive Column Profile Map approach eliminates a significant portion of the trial-and-error typically associated with column design. This characteristic makes it an obvious

complementary tool for existing techniques by providing visual insights into solutions.

6.9 Conclusion

The behavior of a Column Section (CS) is described by a Column Profile Map (CPM). The topology of the CPM depends on the position of the difference point and that there are regions of the composition space where the topology of the CPM is similar. A Reactive Column Section (RCS) can be regarded as a column section where the difference point moves in the direction of the stoichiometric vector. The topology of the Reactive Column Profile Map (RCPM) changes as the reactive difference point crosses into different regions of the extended composition space of mole fractions (positive and negative space). By understanding how the location of the nodes of the RCPM changes, one can be able to manipulate the movement of the difference points to achieve profiles that avoids regions of potential instability (close to bifurcation).

Bibliography

[1] Hauan, S., Ciric, A.R., Westerberg, A.W., Lien, K.M.," Difference points in extractive and reactive cascades I-Basic properties and analysis" Chem Eng Sci, 2000, 55, pp 3145-3159

[2] Tapp, M., Holland, S., Glasser, D. & Hildebrandt, D.,"Column Profile Maps Part A: Derivation and interpretation" Ind Eng Chem Res, 2004, 43, pp 364-374

[3] Qi, Z., Sundmacher, K.," The impact of interfacial mass transfer on the feasible products of countercurrent reactive separation processes " Separation and purification technology, 2004, 34, pp 201-211

[4] Hauan, S.,” On the behaviour of reactive distillation systems” PhD. Thesis, 1998, Norwegian University of Science and Technology, Trondheim

[5] Ung, S., Doherty, M.F,” Vapor-liquid phase equilibrium in systems with chemical reactions” ” Chem Eng Sci, 1995, 50 (1), pp.23-48

[6] Ung, S., Doherty, M.F,” Synthesis of reactive distillation systems with multiple equilibrium chemical reactions” Ind Eng Chem Res, 1995, 34, pp 2555-2565

[7] Buzad, G., Doherty.M.F,” Design of three-component kinetically controlled reactive distillation column using fixed-point methods” ” Chem Eng Sci, 1994, 49 (3), pp.1947-1963

[8] Venimadhavan, G., Buzad, G., and Doherty, M.F.,”Effects of kinetics on residue curve maps for reactive distillation.” AICHE Journal, 1994, 40 (11), pp. 1814-1824

[9] Okasinski, M.J., Doherty, M.F,” Design method for kinetically controlled staged reactive distillation columns”, Ind Eng Chem Res, 1998, 37, pp 2821-2834

[10] Chadda, N., Malone, M., Doherty, M.F., “Feasible products for kinetically controlled reactive distillation of ternary mixtures”, A.I.Ch.E. Journal, 2000, 46(5), pp. 923–93

[11] Gadewar, Malone, M., Doherty, M.F., “, Feasible region for a countercurrent cascade of vapor–liquid CSTRs”, A.I.Ch.E. Journal, 2000, 48(4), pp. 800–814.

[12] Groemping, M., Dragomir, R., Jobson, M., “Conceptual design of reactive distillation columns using stage composition lines”, Chemical Engineering Proceedings, 2004, 43, pp. 369–382.

[13] Hoffmaster, W., Hauan, S.,”Sectional and overall reachability for systems with S-shaped distillation lines”, A.I.ChE. Journal, 2002, 48 (11), pp. 2545–2556

[14] Hoffmaster, W., Hauan, S.,” Difference points in extractive and reactive cascades. III—Properties of column section profiles with arbitrary reaction distribution” Chem Eng Sci, 2004, 59 (17), pp. 3671–3693.

[15]. Lee, J., Hauan, S., Lien, K., Westerberg, A., “Difference points in extractive and reactive cascades. II—Generating design alternatives by the lever rule for reacting systems”, Chem Eng Sci, 2000, 55 (16), pp. 3161–3174.

[16]. Malone, M., Doherty, M.F., “Reactive distillation”, Ind Eng Chem Res, 2000. 39, pp. 3953–3957.

[17] Taylor, R., and Krishna, R., “Modelling reactive distillation”, Chem Eng Sci, 2000, 55(22), pp. 5183–5229

.

[18] Zheng Y., & Xu,” Study on catalytic distillation processes, Part II: Simulation of catalytic distillation processes, Quasi homogeneous and rate based model” Trans. I. Chem. E., Part A, 1992, 70, pp 465-470.

[19] Venimadhavan, G., Doherty, M.F., Malone, M.F.,”Bifurcation study of kinetic effects in reactive distillation”, AICHE Journal, 1999, 45(3), pp. 546-556

[20] Jimenez, L., Wanhschafft, O.M., Julka, V.,” Analysis of residue curve maps of reactive and extractive distillation units”, Chem Eng Sci, 2000, 34, pp. 1401-1414

7 Chapter 7 Conclusion

In the development of Process Synthesis, there has been a need for simple tools that look at new ways of process evaluation and design (modelling).These tools need to be able to provide a basis for assessment of comparative process options with less rigourous data.

This thesis has attempted to demonstrate some of Process Synthesis applications from simple experimental techniques, to tools for the understanding and analysis of distillation processes (separation with reaction, separation with mixing) using vector formulations.

The research in this thesis contributes to the area of chemical process synthesis, adopting the physical task-based approach to synthesis. i.e., the optimal arrangement of fundamental (physical/chemical) transformation tasks to achieve the processing objective will define the design of the process and equipement, rather than the other way around. The key principle used in the study is the exploitation of the generic vectorial representation of three physical phenomena,separation , mixing and reaction in the process models as used for process synthesis and analysis. The demonstrated power of the approach is that it allows one to exploit the formal mathematical similarities between the different processing modes(batch/continuous). In practical terms it means that results from batch experiments can be translated and interpreted for the continuous mode.It has been experimentally demonstrated that the stripping operations in batch mode comply with the vector representation and hence can be interpreted for continuous cases. Concerning reactive separation systems an extensive analysis has been made of the impact of the presence of a single reaction in a two

phase separation system on the behaviour of the system, using the concept of reactive residue curve map (reactive column profile map) . The studies are restricted to ternary systems with a single reaction. Extensive topological reactive residue curve map (reactive column profile map) have been generated and analysed, offering new insights for manipulation for process behaviour in process synthesis and design. This is demonstrated by means of an example of the synthesis of a counter-current reactive distillation column.

The significance of the contribution of this research is in offering extended fundamental insights in creating process synthesis options for reactive-separation systems, creating the essential structural basis for subsequent mathematical optimization of the performance of process designs. This is an opportunity for new processing schemes and new ways of increasing efficiency in traditional chemical process design.This work has laid the basis for future work (experimental and theoretical) to validate the techniques introduced here. For example the control and instability of batch and continuous reactive distillation should be much more predictable from the work presented in this thesis. In the table below we present different formulae derived from each of the genericf vectorial terms ($\underline{S}$, $\underline{M}$, $\underline{r}$) and on the basis of the table we recommend some future works

S	**M**	**r**	**p**	**Conclusions & Recommendations**
S	φM	-	S+ φM	1. The length and direction of the vector field M affects the location of nodes and the mapping of the vector field 2.Different arrangement (parameter φ/ direction of M) of fundamental transformation to achieve processing objectives 3.Future study if S is replaced by λS where λ is a matrix function of the local value of x (for instance mass transfer effects)
S	φM		S + φM	1. Looked at the case where S negative 2.Replaced –S with variable M

$\underline{S}$	-	$\alpha\underline{r}$	$\underline{S} + \alpha\underline{r}$ ($\underline{r}$=irreversible)	1. Related the topology of $\underline{p}$ with the parameter α 2.Related the topology of $\underline{p}$ with the stoichiometry 3.Predicted unstable regimes in reactive distillation (bifurcations) 4.Future experimental validations needed
$\underline{S}$	-	$\alpha\underline{r}$	$\underline{S} + \alpha\underline{r}$ ($\underline{r}$=reversible)	1. considered $\underline{r}$ reversible with nodes 2.Future simulations needed to construct a coherent link with Column Profile maps theory
$\underline{S}$	$\varphi\underline{M}$	$\alpha\underline{r}$	$\underline{S} + \varphi\underline{M} + \alpha\underline{r}$	1. considered $\underline{r}$ irreversible without nodes 2. Future study where $\underline{r}$ is exothermic reversible and/ or multiple reactions

Table 3: General overview of generic vectorial formulae derived and analysed in the thesis

List of Notation

$\underline{x}$	Vector of the liquid mixture composition
$\underline{y}^*$	Vapour phase composition in equilibrium with $\underline{x}$
$\underline{x}_d$	Vector of feed material composition (batch)
$\underline{x}_D$	Distillate material in continuous column
L	Liquid flow rate
V	Vapour flow rate
D	Distillate flow rate
r	Reflux ratio
s	Reboil ratio
$\underline{S}$	Separation vector
$\underline{M}$	Mixing vector
$\underline{X}_\Delta$	Difference composition in column section
$\underline{X}_T$	Top liquid composition in column section
$\underline{Y}_T$	Top vapour composition in column section
$\underline{x}_b$	Vector of bottom material composition
$\underline{x}_B$	Bottom composition in continuous column
$\underline{x}_P$	Pinch point composition
$\dot{d}$	Material addition flow rate
$\dot{b}$	Removed material flow rate
$\dot{v}$	Amount of vapour formed
l	Amount of residue in the batch still
h	Tray position
q	Feed state
Da	Damkholer number
k_0	Reaction rate constant at standard temperature
R	Reaction rate

$\underline{r}$	Reaction vector
R_{Δ}	Reflux ration in column section
k_f	Forward reaction rate constant
K_e	Chemical equilibrium constant
$\underline{p}$	Process vector
$X_{\Delta R}$	Reactive difference point composition

Greek letters

ξ	Scalar quantity non-linearly related to time
η	Scalar quantity non linearly related to stage number
φ	Scalar quantity
$\underline{\rho}$	Resultant distillation vector
α	Scaling parameter
Δ	Difference flow rate in a column section
λ	Amount of residue in the still
υ_i	Stoichiometric coefficient of component i
υ_T	Sum of stoichiometric coefficients of species involved in a chemical reaction
$\underline{\upsilon}$	Stoichiometric vector
ρ	Molar density
ζ	Total turnover for the chemical reaction

Abbreviations

MBT	Mass Balance Triangle
RCM	Residue Curve Map
RRCM	Reactive Residue Curve Map
RCPM	Reactive Column Profile Map

Appendix A. Process Synthesis of Reactive Distillation Systems

This appendix has been presented at the Distillation and Absorption conference in September 2006 in London, UK under the title : when and how much to use reactive distillation

A.1 Abstract

Process design deals with synthesis and optimization tasks, where process synthesis means to conceive a set of processing units and the interconnections between these units which will fulfill the performance target of a process, and optimization means the evaluation of the best set of parameter values of the system. The intensive use of modular simulators, e.g. ASPEN PLUS® or numerical solver tools as gPROMS has hugely increased our ability of optimizing process structures; thus finding the set of alternatives solutions structures has become the key factor in the process design task.

Frey et al. [1] showed how knowledge of reactive distillations lines and potential reactive azeotropes can be used for the systematic design of reactive distillation processes. Hauan et al. [2] demonstrates how phenomena vectors may be used in the early stage of the design of reactive distillation columns for graphical determination of stationary points (reactive azeotropy) as possible boundaries of the feasible regions. They further showed how to use the length of phenomena vectors for preliminary design of complex hybrid process.

However in this paper we use simple thermodynamics features given VLE data and preliminary kinetics considerations to show on practical ground the power of thermodynamics insights for the determination of the structure(s) in the early stage of process synthesis. Our interest in this paper is a quick and systematic geometric procedure for establishing whether reactive distillation is advantageous or not with regard to a

particular system. The aim of the presented approach is to reduce the complexity of the combined process in order to enable simple structure solutions to be recognized quickly. We consider a case study to illustrate the approach.

A.2 Introduction

Let us suppose that we have a process in which reaction and separation occur simultaneously. Let us suppose also that one has the possibility to switch on and off the reaction by introducing the catalyst. We consider the resultant process as a combination of the separation process and chemical reaction process. The global process occurring can be represented as:

$$\underline{p} = \alpha \underline{S} + \lambda \underline{r} \qquad \text{(A.1)}$$

where $\underline{r}$ is the reaction vector, $\underline{S}$ is the separation vector , λ and α are scaling factors and $\underline{p}$ is the combined process vector.The normal classic optimization tries to optimize by choosing the parameter λ and α but the difficulty is that $\underline{S}$ and $\underline{r}$ can bifurcate. In the present paper we introduce a simple graphical technique using thermodynamic features.

The framework of the approach consists of the following steps:

- Determination of the topology of the separation vector field

At infinite separation efficiency the trajectories of the distillation process for different initial compositions coincide with the residue curve map (RCM) which has been considered as a powerful tool for flowsheet (structures) development and feasibility analysis of conventional multi-component separation processes[3]. We first consider the location of the singular points of the system and then derive the possible distillation boundaries in the mass balance triangle (MBT). We then draw in the different separation

regions defined by these boundaries the average directions of separation vectors. We will illustrate later this concept when dealing with a practical case.

- Determination of the chemical equilibrium line (surface)

The chemical equilibrium curve represents the maximum degree of conversion of reagents for chemical systems and as such help to discern the forward reaction zone and to estimate when the chemical equilibrium conditions occur.

- Determination of optimum structure(s) for achievement of target objectives for the combined process.

A.3 Example 1: Butene-Pentene-Hexene System

In this example let us suppose that we want to make Pentene from Butene and Hexene and that we have the reaction:

BUTENE + HEXENE ↔2PENTENE (A.1)

One notices that there is no change in the number of moles and we assume that the reaction takes place via a catalyst in the liquid phase.

In this case the Residue Curve Map is very simple as the system is essentially ideal and it is shown in Figure A.1. On the same graph we have shown the chemical equilibrium curve and this divides the space into two parts, namely R1 where Pentene is produced by reaction and R2 where pentene is decomposed by reaction.

.

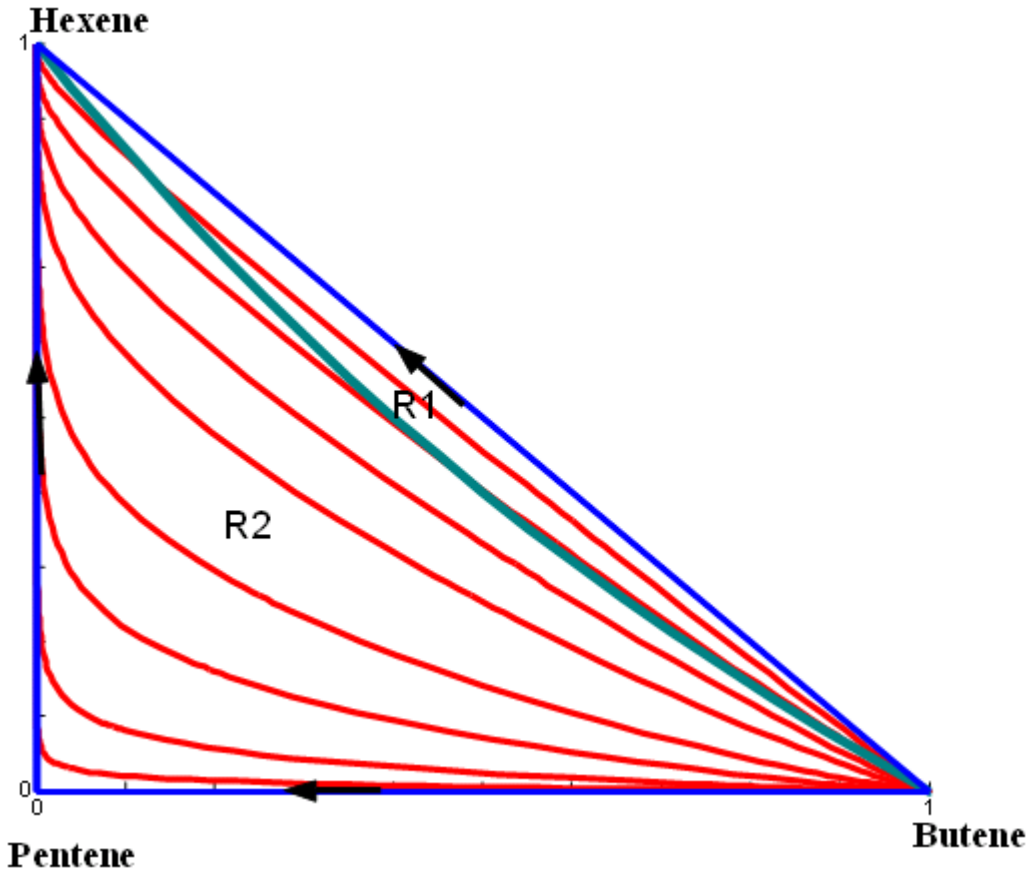


Figure A.1 Residue Curve Map for Hexene-Pentene-Butene System @1 bar with chemical equilibrium curve superimposed(green). R1 is region where Pentene production occurs and R2 is region where Pentene is decomposed.

The question is how one can use this information for choosing a structure.Clearly if we feed an equimolar mixture of Hexene and Butene we need to perform some reaction while in region R1. If we try to do simultaneously separation we will be taking a reactant out of the liquid (Butene) rather than a product (Pentene) and this will not be an advantage. This suggests we do the reaction on its own in a separate reactor. The exit from the reactor from region R2 will not have much pentene in it as the Region R1 is quite small. This product will need to be fed to a pair of columns in order to separate the unreacted Hexene and Butene and this will be recycled to the reactor. Once we are in

Region R2 there is no point doing simultaneous reaction and separation as we will be destroying the product. Therefore we come up with the structure (flowsheet) in Figure A.2. Notice we have shown that we have separated the mixture first into the pair Pentene and Hexene with Butene as the alter stream. But we could just as easily done it first into Butene and Pentene with Hexene the alter stream.The important result we have come up with is that in this case there is no good reason for doing reactive distillation. In fact this could make it worse. We have chosen in this case to separate reaction and separation.

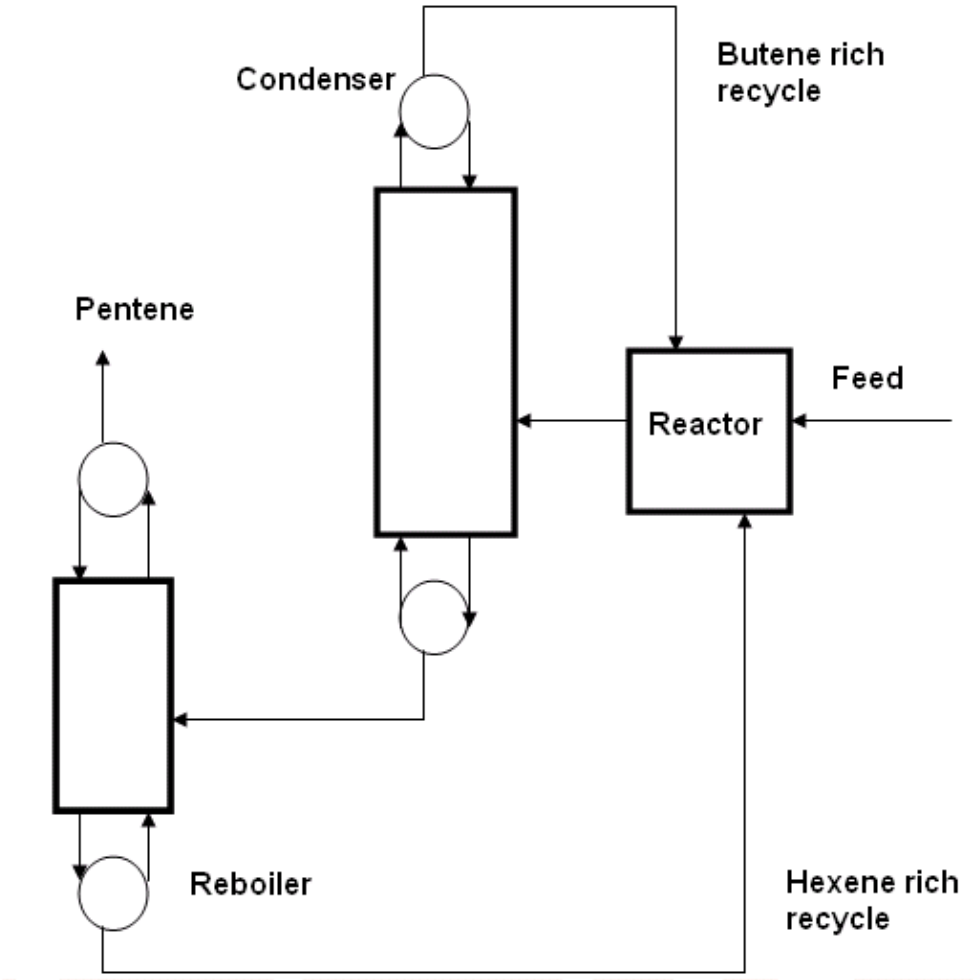


Figure A.2: Proposed Process flowsheet for Pentene manufacture from Butene and Hexene.

Another interesting possibility that could be examined would be the divided wall column shown in Figure A.3. This however is merely a comparison between two different distillation systems and so does not fall within the ambition of this paper.

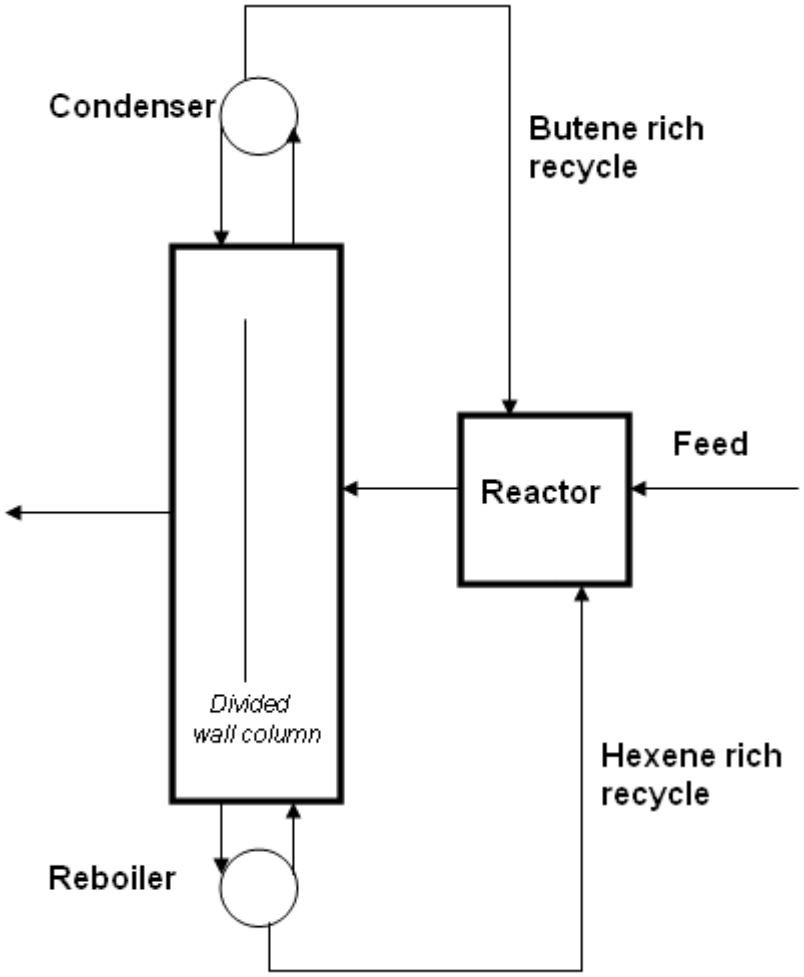


Figure A.3: Proposed Divided wall column process for Pentene manufacture

A.4 Example 2: MTBE Process Synthesis

MTBE (Methyl tertiary butyl ether) was once seen as a replacement for lead additives in car fuel. It is produced from the reaction of methanol (MeOH) and isobutene (IBUT) with a catalyst in the liquid phase. This system has a complex separation sequence due to the high non-ideality of the system due to the polarity of the methanol compared with the

non-polar MTBE product. The principal reaction is equilibrium limited and has the following stoichiometry:

IBUT + MEOH ↔MTBE (A.2)

A.4.1 The Topology of the separation vector field

The topology of the separation vector field is determined by the number and position of singular points. In this situation there are 3 pure components and 2 azeotropes. These 5 singular points divide the mole fraction composition space in 2 regions defining a distillation boundary inside the mass balance triangle (MBT).Thus the essential topology of the separation vector field can be represented by the mass balance triangle and the boundary between the two regions as shown in Figure A.4.

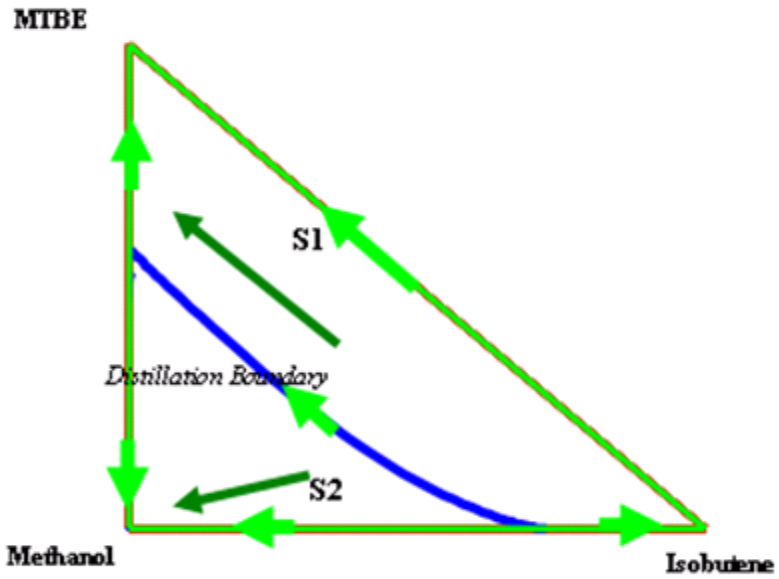


Figure A.4 Distillation Regions for the MTBE system@8bar

$$\gamma_i = \exp\left(\frac{\sum_j x_j \tau_{ji} G_{ji}}{\sum_k x_k G_{ki}} + \sum_j \frac{x_j G_{ij}}{\sum_k x_k G_{kj}}\left(\tau_{ij} - \frac{\sum_m x_m \tau_{mj} G_{mj}}{\sum_k x_k G_{kj}}\right)\right)$$

The total pressure P_{tot} of the system was set to 8 bars. The vapour pressure P_{vap} for each pure component has been calculated using the Antoine equation. The NRTL (Non Random Two Liquid) model has been used to determine the liquid activity coefficient γ

Where $G_{ij} = \exp(-c_{ij} + d_{ij}(T - 273.15K)\tau_{ij})$ and $\tau_{ij} = a_{ij} + \frac{b_{ij}}{T} + e_{ij} \ln T + f_{ij} T$

The MTBE System binary parameters a_{ij}, b_{ij}, c_{ij}, d_{ij}, e_{ij} and f_{ij} for the NRTL model are taken from the ASPEN PLUS® Databank. All figures for the MTBE system are generated with these binary parameters at P_{tot} = 8 bar

From Figure A.4, two separation regions may be schematically identified:

1. Separation Region S1

   Movement in this region is mainly such that the liquid composition becomes richer in MTBE as shown by the arrow.

2. Separation Region S2:

   Movement in this region will mainly be such that the methanol mole fraction in the liquid phase increases as shown by the arrow

   In each of the separation regions we represent the direction of the residue curves by average directions. The average direction represents the average change in the liquid composition during the boiling process.

A.4.2 The Chemical Equilibrium Line

The equilibrium constant is evaluated as a function of temperature from thermodynamics. Both the chemical equilibrium and rate equations with activities offer simple models with less parameters to fit. The kinetics are taken from Venimadhavan et al. [4]:

$$ln(Ke) = \frac{6820}{T} - 16.33 \qquad \text{(A.3)}$$

where K_e is the chemical equilibrium constant and T is the temperature in Kelvin

The chemical equilibrium that we consider describes both the thermodynamic (when the chemical affinity is null) and kinetic equilibrium compositions (when the rates of the forward and reverse reactions are equal). In Figures (A.5) we distinguish the reverse chemical zone (R1) and the forward chemical reaction zone (R2).

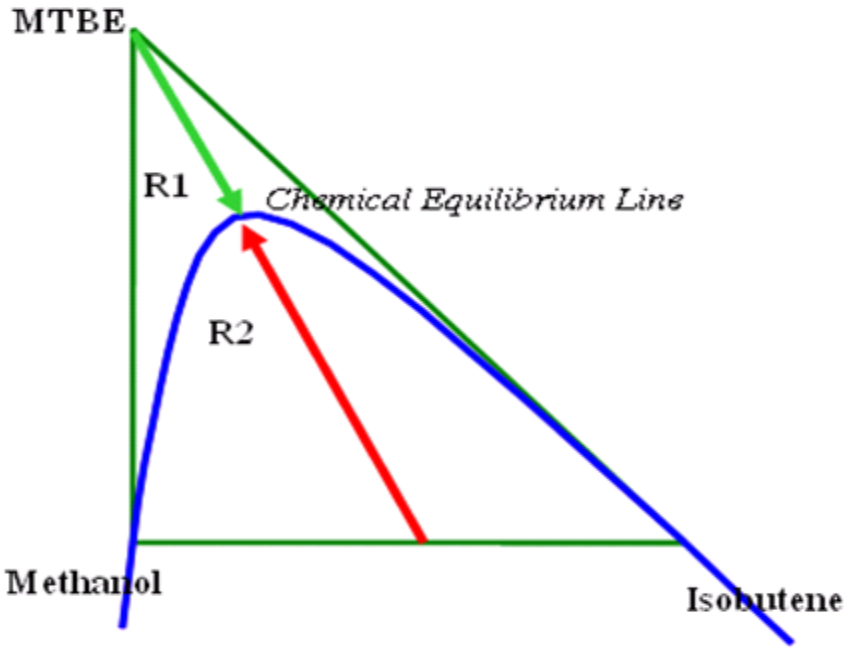


Figure A.5 Forward and Reverse chemical reaction zones for the MTBE system @ 8bar

A.4.3 Combination of Separation and Reaction

In order to design a reactive distillation system we need to look at the way we combine the separation and reaction vector fields. Let us plot all the important features of the reaction and separation mass balance triangles on the same graph. We notice that we have four separate regions in Figure A.6. In any of the four regions one will have qualitatively different behaviour.

We suppose that the objective is that we would like to make as pure as possible MTBE in a process as simple as possible and we would also like to ensure we make significant

quantities of the MTBE. Let us look at each of the four regions separately and evaluate what is happening. Let us also suppose that one starts with an equimolar mixture of Methanol and Isobutene.

We evaluate the properties of the different regions in shown in Figure A.6:

- Region 1 is such that reaction and separation are mainly toward component Methanol
- Region 2 is such that reaction is toward MTBE and separation to Methanol
- Region 3 is such that reaction and separation are mainly toward component MTBE
- Region 4 is such that reaction moves away from MTBE and separation to MTBE

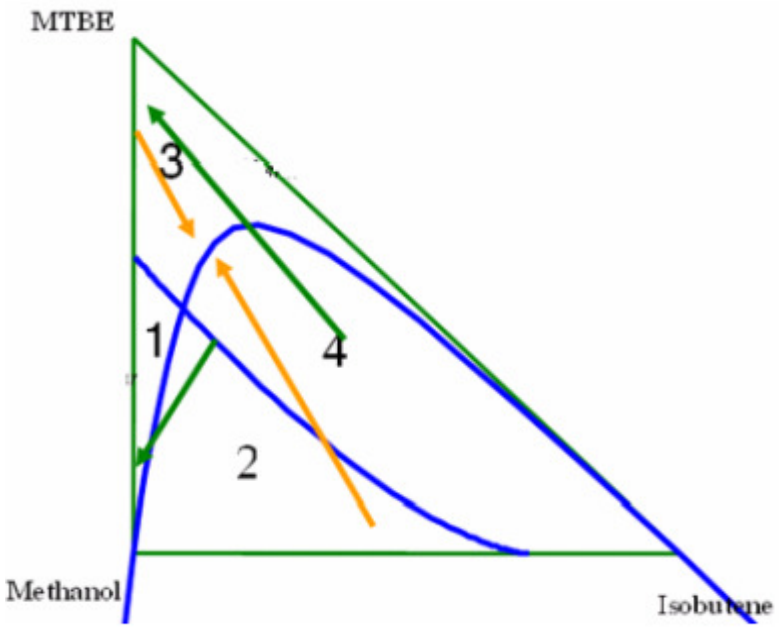


Figure A.6 Properties of Regions of qualitatively different behaviour by superimposing the separation and reaction mass balance triangle for the MTBE system @ 8bar

We suppose that the initial material composition is an equimolar mixture of Methanol and Isobutene in region 2 as shown in Figure A.4; one can see that the separation will take us towards pure Methanol corner while reaction will take us to MTBE. So by using reaction only one can cross into region 4.

In region 4 both reaction and separation will move us towards region 3. Once we cross into region 3, reaction will take us back to reactants while separation will move us towards MTBE corner.The strategy is to start with reaction alone (region 2) – in region 4 have simultaneous reaction and separation – in region 3 have separation alone. By using this simple analysis we have obtained the sequences of the solution

A.4.4 Possible practical implications

It is interesting to see what a reactive distillation column might look like that incorporates these ideas from above. A possible system that incorporate these ideas is shown in Figure A.7.

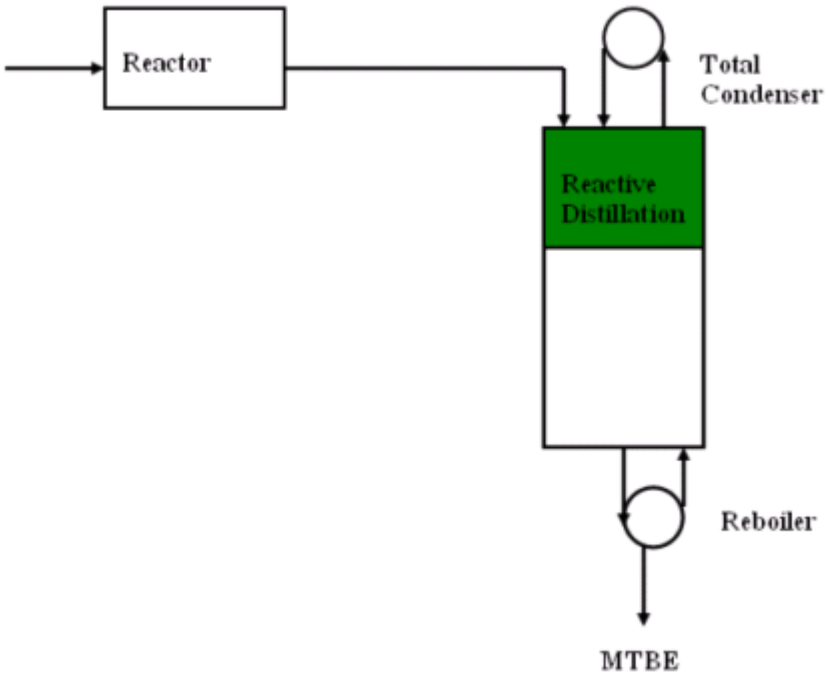


Figure A.7 Properties of Regions of qualitatively different behaviour by superimposing the separation and reaction mass balance triangle for the MTBE system @ 8bar

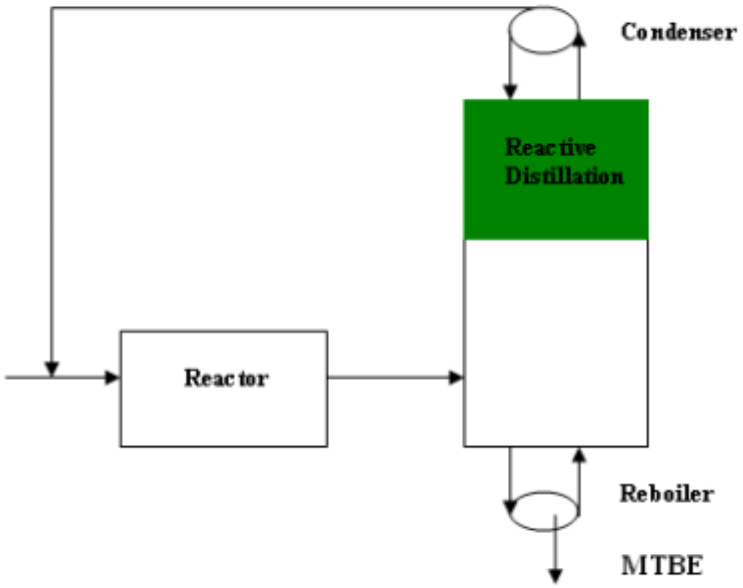


Figure A.8 Properties of Regions of qualitatively different behaviour by superimposing the separation and reaction mass balance triangle for the MTBE system @ 8bar

Interestingly this is not the same as the system usually used in industry as illustrated in Figure A.8. It would be of interest to do simulations and optimizations to see how the two systems compare each other.

A.4.5 Discussion

This analysis has been done entirely using very simple thermodynamics data and so could be done at a very early stage of the analysis of a proposed process. The important result is that one is able to synthesize a structure for the system based only on this simple topological information. Once this has been done one is in a position to do a more detailed optimization using more standard simulation techniques.

Interestingly the proposed solution in this instance is one that in principle agrees with what one might expect if one used more sophisticated methods of analysis such as Pontryagin's maximum principle. In this case the process vector is an affine combination of two vectors. In this case one often finds that the solution has first the one process followed by a mixture of the two processes followed by the other process on its own [5] . Again in this case we would not find solutions which have parallel structures or recycles such as found in Figure A.8. It would be therefore of further interest to compare the results of Figures A.7 and A.8.

A.5 Conclusion

In this paper we produce simple diagrams based only on a minimum of thermodynamic information and using only topological information arrive at proposals for a structure that includes where to do separation and reaction either alone or together. Many current simulations can both simulate and optimise proposed structures. The part that is currently missing are methods to choose the structures. This paper suggests some initials ideas on how this might be done.

Bibliography

[1] Stichlmair, J., Frey, T., "Reactive distillation processes", Chem. Eng. Technol. **22** (1999) 95-103

[2] Hauan, S., Lien, K.L.,"A phenomena based design approach to reactive distillation", Chem. Eng. Res. Des., Trans. Inst. Chem. Eng., **76**(1998) 396-407

[3] Fien, G., Liu, Y., "Heuristic synthesis and shortcut design of separation processes using residue curve maps", Ind. Eng. Chem. Res., 33 (1994) 2505-2522

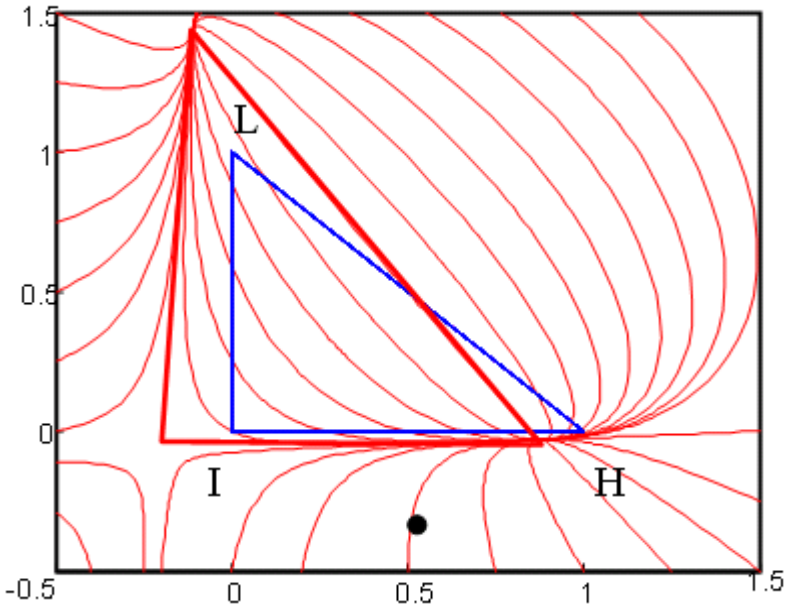
[4] Venimadhavan, G., Malone, M. F., Doherty, M. F., "Effects of kinetics on residue curve maps for reactive distillation" AIChE J., 40(1994) 1814-1824

[5] King, R.P., Glasser, D., Stone, S. L., "Optimal catalyst concentration profile for bifunctional catalysts", Journal of optimization theory and applications, 10(1972) 94-108

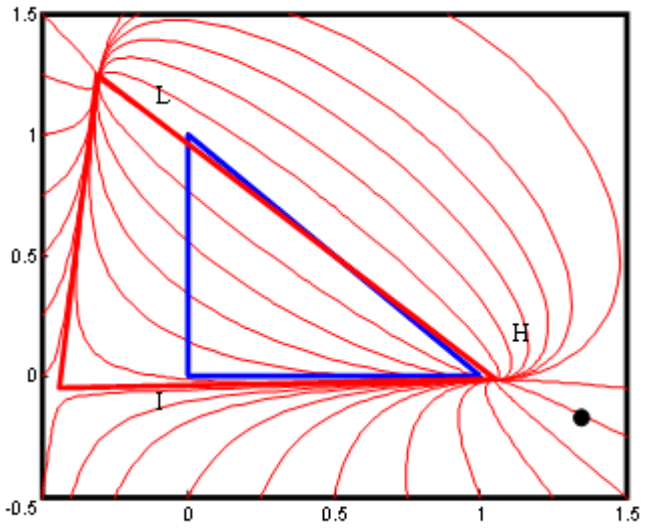
Appendix B. Behaviors of Column Profile Maps (CPM) For X_Δ in Different Regions

Behaviors of Column Profile Maps (CPM) for the difference composition X_Δ in different regions of the composition space of mole fractions as llustrated by Tapp, M., Holland, S., Glasser, D. & Hildebrandt, D.,"Column Profile Maps Part A: Derivation and interpretation" Ind Eng Chem Res, 2004, 43, pp 364-374 as explained in section 6.3. All these figures have the parameter R_Δ=9.

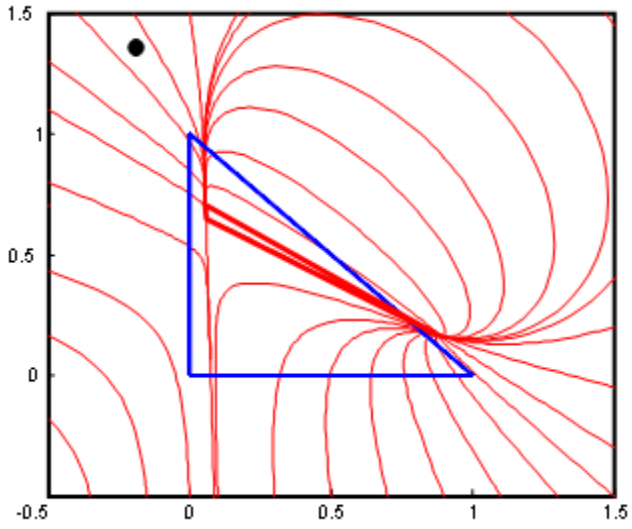
1. *X_Δ = [-0.3; 0.5; -0.4] in Region IV*



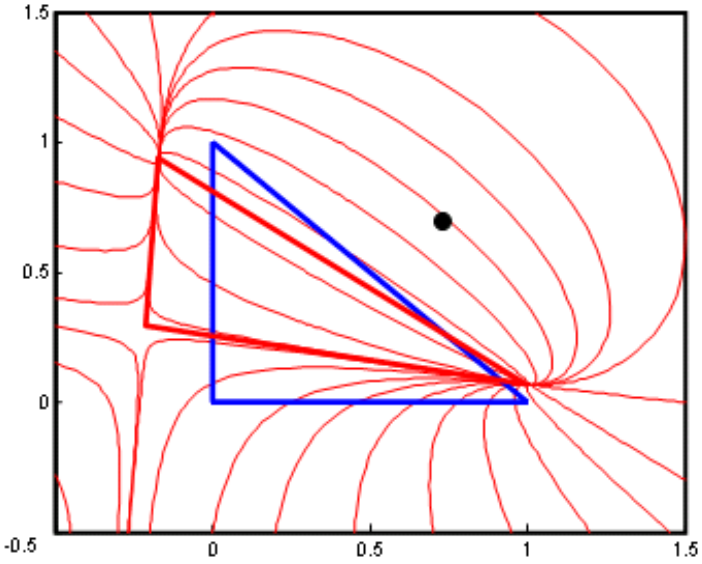
2. X_{Δ} = [-0.2; 1.4; -0.2] *in Region III*



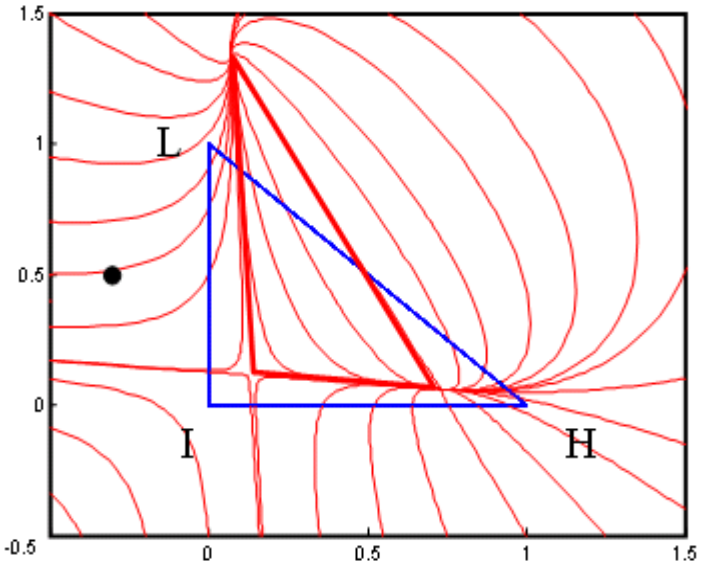
3. X_{Δ} *= [1.4;-0.2; -0.2]* in *Region VII*



4. $X_\Delta = [0.7; 0.7; -0.4]$ *in Region II*



5.$X_\Delta = [0.5; -0.3; 0.8]$ *in Region VI*



6. $X_{\Delta} = [-0.3; -0.3; 1.6]$ *in Region V*

